

Pore Water Constituents of Deeply Buried Gulf Coast Muds as
Indicators of Diagenetic Alteration

A THESIS

Presented to

The Faculty of the Division of Graduate Studies

by

Gary Andrew Cooke

In Partial Fulfillment
of the Requirements for the Degree
Master of Science
in the School of Geophysical Sciences

Georgia Institute of Technology

August, 1977

Pore Water Constituents of Deeply Buried Gulf Coast Muds as
Indicators of Diagenetic Alteration

Approved:

Kevin C. Beck, Chairman

Charles E. Weaver

J. Marion Wampler

Date approved by Chairman: 8/12/77

ACKNOWLEDGMENTS

I would like to thank Dr. K. C. Beck, my committee chairman, for his help with and criticism of this work. I am grateful to Dr. C. E. Weaver and Dr. J. M. Wampler who, as the other members of my committee, provided much information and help over the last four years. Dr. J. H. Reuter's assistance with both personal and professional problems of mine is greatly appreciated. Dr. C. O. Pollard has provided me with some first rate instruction and information during my stay here. Dr. John Hower also helped me with his discussion and suggestions.

A number of people have provided help at various stages of this work and I am particularly grateful to them all. W. Scott Parks was invaluable to me in his assistance with the care and feeding of the computer. Dr. Lin Pollard was helpful in tracking down some of the references. Dianne Clark has helped me in ways too numerous to mention and deserves special thanks. Annette Plunkett deserves mention for her excellent job of typing this thesis. Individuals in the Engineering Experiment Station, the Aerospace Engineering School and Sanitary Engineering provided instruction and access to their instruments which is greatly appreciated. It would be difficult for me to catalogue all of the individuals who have befriended me during my sojourn at Tech as a lot of people have come and gone these last four years. However, Bob Dooley

and Derrold Holcomb must be specially mentioned here for their enormous contributions to my sanity.

Special thanks are reserved for Cynthia Miller for performing the tedious task of drafting the figures for this thesis as well as marrying me and providing much of my financial support. Drs. Weaver and Beck have also helped supplement my stipend with consulting work at various times. The thesis work itself was funded by NSF Grant #DES-72-0711-A01 and the samples and well log data were provided by Continental Oil Company.

This work is dedicated to my mother, who along with my father (whom I'll dedicate my Ph. D. to) is responsible for it all.

TABLE OF CONTENTS

	Page
ACKNOWLEDGMENTS	ii
LIST OF TABLES	vi
LIST OF ILLUSTRATIONS	viii
SUMMARY	xi
Chapter	
I. INTRODUCTION	1
II. METHODS AND PROCEDURE	5
III. DATA	17
IV. DISCUSSION A	46
The Validity of and Corrections to Pore Water Water Analyses	
1. The Extent of Drill Mud Contamination	
2. Effects of Squeeze Temperature and Pressure on Pore Water Chemistry	
a. Variation in Pressure of Squeezing	
b. Effects of Temperature of Squeezing	
3. Effects of and Correction for Evaporation Prior to Squeezing	
4. Comparison of Squeezing and Leaching Methods of Pore Water Recovery	
V. DISCUSSION B	79
Mineralogic and Chemical Variations During Gulf Coast Burial Diagenesis	
1. The Occurrence and Recognition of Non- Diagenetic, Mineralogic Variations	
2. Mineralogy of the Sidewall Cores and Relation to Burial Diagenesis	
3. Solid Chemical Changes in Gulf Coast Sediments with Depth	
4. Variation of Interstitial Waters During Pelitic Sediment Burial	
5. The Nature of Boron/Silica Variation in Pore Waters and Solids	

	Page
6. Metals During Burial Diagenesis	
VI. CONCLUSIONS	173
BIBLIOGRAPHY	177

LIST OF TABLES

Table	Page
1. Pore Water Chemistry (Squeeze Data)	18
2. Pore Water Variations with Squeeze Pressure	19
3. Trace Elements in Pore Waters (Squeeze Data)	20
4. Chemistry of Drill Mud Liquids	21
5. Pore Water Chemistry (Leach Data)	25
6. Pore Water Leach Chemistry of a Sequentially Trimmed Sample	26
7. Weight Percent (110°C Dry) in Size Fractions	27
8. Clay Mineralogy of <44 μm Size Fractions	30
9. Major Element Chemistry of the <0.1 μm Fraction (110°C Dry)	32
10. Major Element Chemistry of the 0.1-2 μm Fraction (110°C Dry)	33
11. Major Element Chemistry of the 2-44 μm Fraction (110°C Dry)	34
12. Major Element Chemistry of the >44 μm Fraction (110°C Dry)	35
13. Boron Content of <0.1 μm and Bulk Samples	36
14. Na_2CO_3 Soluble Silica of <0.1 μm and Bulk Samples Samples	37
15. Exchange Ion Chemistry, <0.1 and 0.1-2 μm Fractions	38
16. Manganese in Solid Samples (110°C Dry)	40
17. Iron and Zinc in Solid Samples (110°C Dry)	41
18. Cu, Co, and Cr in Solid Samples (110°C Dry)	42

Table	Page
19. Temperature Corrections for K and Mg in Squeeze Pore Waters	63
20. Extent of Evaporation During Transportation and Storage	72
21. Pore Water Chemistry of Squeezed Cores, Corrected for Evaporation	73
22. Ratio of Squeeze/Leach Determined Pore Water Chemistries	77
23a. Bulk Chemistry of Gulf Coast Pelitic Sediments (Avg. of Sample Sets)	93
23b. Bulk Oxide/ Al_2O_3 Ratios of Gulf Coast Pelitic Sediments	94
24. Major Element Chemistry of the $<0.1 \mu m$ Fraction (Ignited)	108
25. Trace Metal Contents of Natural Waters	154

LIST OF ILLUSTRATIONS

Figure	Page
1. Qualitative Estimation of Shale Distribution in Wells 2 and A4	29
2. Well Log Temperature Variation with Depth for High Island Block 110 Wells	43
3. Variation in Fluid Pressure with Depth in Wells 2 and A4 from Acoustic Logs	45
4. Variations in Na, Cl and Br Determined by Leaching Trimmed Sections of Sample 538	49
5. Ratio of Ca, Mg and K to Na for Interstitial Waters Extracted at Different Pressures	53
6. Cumulative Composition of Intersitital Waters Expelled with Increasing Pressure	55
7. Deviation of Squeezed Pore Water Chemistry with Changes in Extraction Temperature	60
8. Uncorrected Chloride Content of Squeezed Pore Waters	64
9. Variation of the Ca to Cl Ratio with Depth for Squeezed Samples	67
10. Porosity vs. Acoustic Travel Time for Cores Studied, Relative to <u>In Situ</u> Relationship of Magara (1968)	71
11. Illite/Montmorillonite Ratio in Gulf of Mexico <2 μ m Surface Sediments	81
12. Variation of the 0.1-2 μ m Clay Minerals with Depth	85
13. Variation of the <0.1 μ m Clay Minerals with Depth	87
14. Variation of the Percent 10A Layers in the Illite/Smectite Mixed Layer Clay with Depth	89

Figure	Page
15. Bulk Sample Oxide/ Al_2O_3 Ratio Variations with Depth for Gulf Coast Pelitic Sediments	95
16. SiO_2 Variation in $<44 \mu\text{m}$ Size Fractions (110°C Dry) with Depth	98
17. Al_2O_3 Variation in $<44 \mu\text{m}$ Size Fractions (110°C Dry) with Depth	99
18. Fe (as Fe_2O_3) Variation in $<44 \mu\text{m}$ Size Fraction (110°C Dry) with Depth	100
19. CaO Variation in $<44 \mu\text{m}$ Size Fraction (110°C Dry) with Depth	101
20. MgO Variation in $<44 \mu\text{m}$ Size Fraction (110°C Dry) with Depth	102
21. K_2O Variation in $<44 \mu\text{m}$ Size Fraction (110°C Dry) with Depth	103
22. Na_2O Variation in $<44 \mu\text{m}$ Size Fraction (110°C Dry) with Depth	104
23. TiO_2 Variation in $<44 \mu\text{m}$ Size Fraction (110°C Dry) with Depth	105
24. Sr Variation in $<44 \mu\text{m}$ Size Fraction (110°C Dry) with Depth	106
25a. SiO_2 and Al_2O_3 Variation in $<0.1 \mu\text{m}$ Gulf Coast Samples (Ignited Basis) with Depth	109
25b. K_2O , MgO and Fe_2O_3 Variation in $<0.1 \mu\text{m}$ Gulf Coast Samples (Ignited Basis) with Depth	110
26. Variation in the Exchange Ion Chemistry of the $<0.1 \mu\text{m}$ Fraction with Depth	113
27. Total Exchange Ions (as Meq/100 gm) vs. % 17A Layers in $<0.1 \mu\text{m}$ Fraction	115
28a. Interstitial Chloride Variations with Depth in Pelitic Sediments and Gulf Coast Tertiary Sands.	126

Figure	Page
28b. Interstitial Na/Cl Variations with Depth in Pelitic Sediments and Gulf Coast Tertiary Sands	130
28c. Interstitial K/Cl Variations with Depth in Pelitic Sediments and Gulf Coast Tertiary Sands	133
28d. Interstitial Mg/Cl Variations with Depth in Pelitic Sediments and Gulf Coast Tertiary Sands	135
28e. Interstitial Ca/Cl Variations with Depth in Pelitic Sediments and Gulf Coast Tertiary Sands	137
28f. Interstitial SO ₄ /Cl Variations with Depth in Pelitic Sediments and Gulf Coast Tertiary Sands	140
29. Variation in the Si/B Aqueous Molar Ratio with Depth, Squeezed and Leached Samples	150
30. Variation in Na ₂ CO ₃ Soluble Silica with Depth	152
31. Variation in the Bulk Sample Metal Contents with Depth	158
32. Variation in the <0.1 μm Metal Contents with Depth	160
33. Variation in the 0.1-2 μm Metal Contents with Depth	161
34. Variation in the >2 μm Metal Contents with Depth	163
35. Variation in the >2 μm/<2 μm Metal Ratios with Depth	164

SUMMARY

A series of sidewall cores from pelitic sediments in the Gulf of Mexico (High Island Block 110), covering depth ranges of 390-1289 meters and 2851-3242 meters, were analyzed for interstitial water and solid chemical and mineralogic constituents in order to examine the effects of burial diagenesis. Previous reports suggest that burial diagenesis of Gulf Coast clays involves a reaction whereby smectite in the finer size fractions incorporates K and Al and releases silica to produce 10A layers in a mixed layer illite/smectite. The data of this study suggest that Fe and perhaps Mg are also lost from the smectite in this reaction. Only a slight decrease in fine fraction silica is seen. However an increase in Na_2CO_3 leachable silica in the samples immediately above the high pressure zone may be the result of silica, released from the clays at this depth, forming poorly crystalline compounds. The primary source of K for the formation of 10A layers in the illite/smectite is discrete illite, which is present in all size fractions and decreases with increasing depth to the top of the high pressure zone. The depletion of iron in the fine fractions is balanced by an increase in coarse fraction iron, indicating the occurrence of a reaction involving removal of iron from clays and subsequent precipitation as large crystals or micro-concretions of pyrite at depth. Other heavy metals

show the same movement from fine fractions, where acid reducing and oxidizing leaches show they are associated with clays, to coarse fractions with increasing depth. Zn and Cu appear to be associated with the sulfide phase in the coarse fractions, while Mn and Co may occur in coarse grained carbonates.

Analysis of interstitial waters by pressure extraction, although limited by errors involving pressure and temperature changes after core recovery, is shown to be superior to leaching techniques for the accurate determination of interstitial constituents. Leaching causes alteration of clay-water exchange equilibria and dissolution of solids, resulting in errors in leach determined water chemistries as well as exchange ion chemistries determined on washed samples.

The interstitial water chemistry of shallow samples (<700 m) shows some evidence for expulsion, during initial compaction, of more saline water than that which remains in the pores. This is probably due to the association of less saline waters with clay surfaces where it is less readily expelled. At greater depths some effects of membrane filtration concentration can be seen, but these are not nearly as dramatic as those reported in sands. At depths below 3070 meters the salinity of the pore fluids again decreases due to the release of low salinity interlayer water from 17A clay collapse. It is this dewatering that is primarily responsible for the deep high pressure zone observed in Gulf Coast sediments. Diagenetic reactions in the sediments which can be

postulated on the basis of interstitial water analysis include:

- 1) Absorption of ~70% of the interstitial K and Mg by clay minerals during the initial 1000 meters of burial.
- 2) Release of Na to the interstitial waters below 1000 meters by the decomposition of Na-feldspar or replacement of Na with Ca in clay exchange positions.
- 3) Release of K, SO_4 and perhaps HCO_3 and organic carbon into interstitial waters during the release of interlayer water during clay collapse.
- 4) The association of boron and silica, in a readily soluble solid as well as in solution; with a 2:1 boron:silica molar ratio remaining constant in both interstitial water and water soluble solid below 600 meters.
- 5) The loss of minor amounts of trace metals from shales undergoing deep burial through increased solubilities and diffusion.

CHAPTER I

INTRODUCTION

The chemical and mineralogic changes accompanying the deposition and burial of land-derived aluminosilicate detritus in marine basins have received considerable attention in recent years. Much of this work has focused on the observed temperature dependent collapse of hydrated clays due to the fixation of ions (primarily potassium) in interlayer positions (Burst, 1969; Dunoyer De Segonzac, 1969; Perry and Hower, 1970; Weaver and Beck, 1971). Frequently occurring at roughly the same depth as this reaction is an increase in formation fluid pressure above hydrostatic which may be due in part to the release of interlayer water (Powers, 1967) and other causes (Chapman, 1972a; Barker, 1972; Magara, 1974b; 1975a, b). The presence of high pressure shales with associated higher fluid contents has been cited as a possible factor in deep petroleum migration (Powers, 1967; Cordell, 1972; Chapman, 1972b). Additional reactions which may accompany deposition and burial of pelitic sediments have also been proposed. Most of these can be encompassed in the reaction: K-Feldspar + K-Mica + Smectite => Illite + Chlorite + SiO₂.

The primary difficulty in interpretation of the nature of diagenetic reactions using mineralogic and chemical analysis of natural systems involves the additional complications provided

by changes in source area or depositional regimes (Parnham, 1966; Hower, et al., 1976). This is particularly true in the Gulf of Mexico where progradational trends can provide a transition from nearshore to open Gulf sediments with depth (Perry and Hower, 1970; Weaver and Beck, 1971) and the proportions of eastern and western source materials can vary causing a concomitant variation in composition (Holmes and Hern, 1942). The determination of sediment constituents other than minerals and major elements would aid in interpretation of complex natural systems.

Analysis of pore water ion concentrations may provide a sensitive indicator of reactions between aqueous and solid components (Weaver and Beck, 1971; Sayles and Manheim, 1975). The concentrations of ions in pore waters of deep sediments will reflect original water chemistry at deposition modified by diagenesis, ion diffusion and subsurface fluid flow (Berner, 1971; Rieke and Chilingarian, 1974; Manheim and Sayles, 1974). The squeezing procedure for extracting pore waters from semi-consolidated sediments has been examined with respect to temperature (Mangelsdorf, et al., 1969; Bischoff, et al., 1970; Russell and Fallgatter, 1972) and pressure (Manheim, 1966; Shishkina, 1968) of squeezing. Despite modifying effects controlled by these factors, a reliable measure of variations in pore water chemistry is believed obtainable (Manheim and Sayles, 1974; Manheim, 1974; Sayles and Manheim, 1975). A large portion of the pore water data obtained by squeezing is from cores

obtained from pelagic and deep ocean sediments and from a few samples of shallowly buried pelitic sediments (Manheim, et al., 1968; Chan and Manheim, 1970; Sayles, et al., 1970; Manheim, et al., 1970; Manheim, et al., 1973; Sayles, et al., 1972; Waterman, et al., 1973; Manheim, et al., 1974; Gieskies, 1974; White, 1975; Siever, Beck and Berner, 1965; Sholkovitz, 1973; Manheim and Bischoff, 1969). In contrast to this, little work has been done on the squeezing of deeply buried (>1000 meters) pelitic material.

To date the only comprehensive data on Gulf Coast pelitic sediment pore waters were obtained using leaching techniques (Weaver and Beck, 1971; Schmidt, 1973). The leaching technique involves addition of known amounts of distilled water (or other liquid) to known amounts of sample whose pore water content has been determined, and correction of the resultant aqueous concentrations to original pore water concentrations through multiplication by the dilution factor. However, in employing this method it is necessary to take into account dissolution of solid species and alteration of clay equilibria, which may vary according to length and temperature of treatment as well as dilution factor used (Manheim, 1974). Therefore leaching data will reflect the original pore water chemistry modified by absorption/desorption reactions induced by alteration of the original pore solution.

In addition to the analysis of pore water and water soluble chemistry of samples, further data which can supplement

major element chemistry and mineralogic studies in the interpretation of pelitic sediment burial diagenesis include analysis of exchange ion chemistry (Russell, 1970; Drever, 1971a; Weaver and Beck, 1971; Berner, 1971; Spears, 1973) and analysis of trace elements, including data obtained on the reducible and oxidizable trace metals of sediments (Chester and Hughes, 1967; Presley, 1969).

The purpose of the present study is to analyze suitable samples of deeply buried Gulf Coast pelitic sediments for major element abundances and clay mineralogy of the solid, and to supplement these data with analyses of interstitial water obtained by squeezing and by leaching, and exchange ion and trace metal analyses of the solids. These data can help provide a basis for interpretation of events occurring during transportation, deposition and burial of aluminosilicate detritus.

Samples involved in this study are sidewall cores from two nearby Gulf Coast wells, offshore from the Texas-Louisiana state line in the High Island block 110. Core depths are from 390 to 1289 meters (7 samples) and 2851 to 3064 meters (6 samples) in well 2, and 3390 to 3588 meters (3 samples) in well A4. The shallower samples are mostly within the depth range of the deeper Deep Sea Drilling Project (DSDP) pelitic sediment cores while the deeper samples enter the main high pressure zone and are Upper Miocene in age.

CHAPTER II

METHODS AND PROCEDURE

Sidewall cores of clay rich layers of well 2 were recovered, wrapped in plastic film and aluminum foil, sealed tightly in Schlumberger jars and transferred to the lab at ambient temperature. Samples from the three levels of well A4 were not wrapped but only placed in jars. Multiple cores were taken at some depths. Prior to analysis all samples (except one core at 538 m, discussed below) were trimmed to remove outer layers of drill mud and expose material which showed no visible evidence of contamination. Several of the cores (from 844 m and 1289 m) showed signs of gypsum precipitation at the surface only. This material was removed during trimming. The trimmed core was then cut up into pea-sized pieces for analysis.

All labware was acid washed and rinsed with distilled water prior to use. Plastic ware (Polypropylene or Teflon) was used in most analyses, always for SiO_2 and boron determinations. Reagent and sample liquid aliquots of less than 2 ml were made using Eppendorf micro-pipettes which show reproducibility within 0.1% for aliquots greater than 200 μl and within 0.5% if less than 200 μl . All reagents and dilutions were prepared using distilled, deionized (Corning 3508A demineralizer) water (DDH20) which was boiled before leach analyses and carbon

determinations. The 70% HNO_3 and 6N HCL were routinely distilled in a small fused quartz still to remove trace impurities.

Approximately 2 grams of each trimmed, divided sample was set aside for the determination of weight loss upon air drying at room temperature and at 110°C . From the trimmed, divided core material of five samples, about 10 grams of each sample was accurately weighed and a measured amount (approximately 25 ml) of DDH₂O (boiled) was added. The sample and water were then stirred overnight and transferred to a 50 ml polypropylene centrifuge tube. Centrifugation at 12,000 RPM for 1/2 hour using a Sorvall SS-3 centrifuge with an SS-34 rotor was sufficient to separate the solid from the leaching solution. The supernate was then analyzed for major and minor constituents as the H_2O leachable fraction.

For assessment of drill mud contamination one fresh core was trimmed into five separate samples with the outermost layer, coated with drill mud, identified as sample 538A and the central portion of the core as sample 538E. These samples were leached as described above to provide solutions for determination of chemical constituents.

The squeeze procedure utilized as much core material as was available (≤ 80 g). Immediately after trimming, the cut up sample was placed in a stainless steel squeezer and squeezed on a hydraulic press to a maximum pressure not exceeding 5000 lbs/sq. in. (352 Kg/cm^2). The effluent was

collected in 0.75 ml plastic vials (preweighed and sealed from the atmosphere). If more than 0.7 ml was collected, additional vials were used and the maximum pressure used in obtaining each vial of fluid was recorded. If a second vial was collected, 5 μ l of 70% HNO₃ was added to stabilize metals in solution. In two cases (390 and 1150 II) additional liquid was collected after the second vial and used to study the effects of squeeze pressure. All vials collected were capped and placed in a closed plastic box with wet tissues to prevent evaporation losses. The squeezed sample at 538 m consisted of three cores which were trimmed and cut up and then divided into two samples (538 I and II). The squeezed sample at 1150 m consisted of two cores, one appearing slightly more firm than the other. The less firm one was cut up, major sand lenses were removed, and the remainder was squeezed as sample 1150 I. The second core was trimmed and squeezed without the removal of sand lenses as 1150 II.

After squeezing a portion of the solid sample was washed and fractionated as follows: Approximately 10 grams (110°C. dry) of the squeezed sample was broken up and distributed evenly among four centrifuge tubes (50 ml polypropylene) and filled halfway with water. The sample was suspended using a Biosonic ultrasonifier with a titanium microprobe tip. Sonification of samples promotes the dis-aggregation of aggregates of smaller grains and thus would provide a true grain size distribution. However, this technique may also act to break

up larger grains. After sonification water was added to within 5 cm of the top of the centrifuge tube. Centrifugation at 15,000 RPM for 30 min. resulted in all of the solid settling out. This washing procedure was repeated with additional water until the supernate showed no sign of Cl^- (no precipitate when HNO_3 and silver nitrate were added). The sample was resuspended and washed through a 44 μm sieve with water. The material on the sieve was then dried at 110°C, weighed and labeled the >44 μm fraction. Some of the <44 μm slurry was transferred to centrifuge tubes and centrifuged at 500 RPM for 12 min. using an International centrifuge (model UV with a #240 rotor) to settle out the >2 μm fraction. The suspension was removed and saved and the settled solid was resuspended by sonification using any additional <44 μm slurry. This process was repeated until all of the <44 μm suspension was centrifuged. The settled solid was resuspended in water and centrifuged to separate the <2 μm material which had been carried down with the >2 μm fraction. This process was continued until the supernate was clear. The solid was then removed and dried at 110°C, weighed, and labeled as the 2-44 μm fraction. The <2 μm suspension was then centrifuged on the Sorvall high speed centrifuge (SS3 with SS34 head) at 7000 RPM for 24 min. to settle out the >0.1 μm fraction. The suspension was removed and saved and resuspension of the settled solid and centrifugation was continued until the <2 μm slurry was exhausted and the <0.1 μm material was washed from the settled solid. The

solid was dried at 110°C, weighed, and labeled the 0.1-2 μm fraction. The $<0.1 \mu\text{m}$ suspension was then centrifuged at 15,000 RPM for 60 min. to collect most of the remaining solid ($\geq 0.03 \mu\text{m}$). Solid material collected at this stage was not resuspended with each new addition of $<0.1 \mu\text{m}$ suspension, thus allowing much of the $<0.03 \mu\text{m}$ material to remain in the settled solid. When all of the liquid generated by previous stages had been centrifuged at this rate the solid was dried at 110°C, weighed and labeled the $<0.1 \mu\text{m}$ fraction. All of the squeezed samples were fractionated in this manner. Sample 1000 was finely divided and split into two samples prior to washing and fractionation.

Constituents analyzed in the solutions generated by squeezing and leaching were Na, Ca, Mg, K, Cl, SO_4 , HCO_3 , organic carbon, Br, F, SiO_2 , B, Fe, Cu, Cr, Mn, Sr, and Zn. The pH was also determined on a few samples. Due to the small amounts of liquid obtained from most samples it was not possible to obtain data on all of the above components from each sample. Standard techniques were employed, with sample and reagent aliquots scaled down to obtain maximum data from minimum sample.

Immediately after squeezing, 0.1 ml of the sample was taken into a Corning flow-thru pH meter (#46100) which was standardized with a pH 8.0 buffer and then rinsed thoroughly with DDH₂O. After the sample was read, a few drops were ejected from the bottom of the capillary, the tip was rinsed

and the remainder of the sample was ejected into a small, pre-weighed glass vial. This vial was reweighed and the liquid was diluted approximately 1:10 with DDH₂O (boiled). Inorganic and organic carbon were determined on this liquid using a Beckman infrared spectrophotometer. The leach samples were also analyzed for inorganic and organic carbon in this manner.

For the major cations (Na, Ca, Mg, K), 0.1 ml of the squeeze liquid was placed in a 15 ml glass vial, 0.5 ml of 6000 ppm LiCl was added and the solution diluted to 12.5 grams total weight with DDH₂O. This gave a 1:125 dilution with 240 ppm LiCl. Leach solutions were diluted 1:3 and given the same LiCl matrix. For analysis of sodium, 1 ml of the diluted samples was further diluted to 5 ml (for a total 1:625 dilution of the squeeze liquids and 1:15 dilution of the leach liquids). Standard analytical techniques using a Perkin-Elmer 301 atomic absorption spectrophotometer (AAS) and stock standard solutions were employed. Sodium was determined using a perpendicular one-slot burner to provide a useful range of 0-60 ppm. 150 ppm Na (as NaCl) was added to the standards for Ca, Mg and K analyses to help match the sample matrix.

Chloride and sulfate were determined on a second 0.1 to 12.5 ml dilution (without LiCl) of the squeeze liquid, while a 1:4 dilution of the leach liquid was used for these analyses. The chloride determination was performed using the method of Belcher and Wilson (1964), a titration with Hg(NO₃)₂, in the presence of diphenyl carbazone, 1-nitroso-2-naphthol, and

ethanol. Aqueous Cl standards were made from stock NaCl solution.

Sulfate, bromide, boron and silica analyses were all performed spectrophotometrically using a Gilford model 222 photometer, model 2443 rapid sampler with a 1.0 cm cell with vacuum attachments and a model 2411 adapter linking all this to a Beckman model DU lamp and optical system. Sulfate was determined using the method of Klipp and Barney (1959) which involves the release of chloranilate from barium chloranilate through the precipitation of BaSO_4 . The resultant solution was filtered and absorbance of the chloranilate in solution was read at 330 nm.

The bromide analysis employed an oxidation of Br^- with chloramine T in the presence of phenol red, an acetate buffer and sodium thiosulfate as described by Presley (1971). The resultant color is measured at 595 nm. For this analysis 0.05 ml of the squeeze liquid was employed.

The boron analysis of squeeze and leach liquids involved development of a boron-curcumin complex in a sulfuric acid-acetic acid-ammonium acetate medium using the method described by Presley (1971). The analysis was scaled to use 0.05 ml of the squeeze liquid and absorbance was measured at 550 nm.

The silica analysis employed the method of Strickland and Parsons (1968), which involves the formation of silicomolybdic acid using a dilute, acidified ammonium molybdate solution with subsequent reduction of the complex with an acid

reducing solution. Absorbance was read at 812 nm, and 0.1 ml of squeeze sample was utilized.

Fluoride was measured using a specific fluoride electrode (Orion 96-09) and an Orion pH meter (model 801). The spike technique of Warner (1971) was modified to use 0.05 ml of the sample and 0.05 ml of a total ionic strength buffer (TISAB IV, made with CDTA). The fluoride electrode was mounted in an inverted position and a salt bridge was employed to make contact between the solution placed on the electrode and a reference electrode. Standards and samples spiked with 1.0 ppm F^- were also prepared and run.

Sr, Cu, Cr, Zn, Fe, and Mn were determined in the pore fluids using the Heated Graphite Atomizer (HGA) technique of Segar and Gonzales (1972) using ammonium nitrate to eliminate NaCl interferences when char temperatures are below 1400°C (Ediger, et al., 1974). A Perkin-Elmer model 2100 HGA attachment to the atomic absorption unit and a deuterium arc background corrector were employed in the analysis.

The ions Mg^{+2} , Ca^{+2} , Na^+ and K^+ in exchange positions were determined on 0.2 g samples of the 110°C dry <0.1 μm and 0.1-2 μm size fractions. The samples were suspended in 8 ml 0.1N Ba^{++} (from $BaCl_2$) with the sonifier in 18 ml polypropylene centrifuge tubes. This slurry was allowed to stand for one hour and then centrifuged for one hour at 12,000 RPM. The supernate was poured into plastic bottles and the solid was washed twice by suspending and centrifuging in 0.1N Ba^{++}

solution. One ml of 6000 ppm LiCl was added and the solution was made up to 25 ml with 0.1N Ba⁺⁺ solution. Mixed standards of Na, Ca, Mg, and K were prepared with 240 ppm LiCl in 0.1N Ba⁺⁺ solution. Samples were analyzed by standard atomic absorption techniques.

Major element abundances in the solid samples were determined by fusion of a 0.1 g sample (110°C dry) with 0.7 g LiBO₂ (G. F. Smith) in a graphite crucible by heating at 930°C for 1/2 hour, followed by dissolution of the molten bead in 100 ml of 5% HNO₃. This solution was filtered (Whatman #42) to remove graphite and plastic and analyzed by AAS using USGS rock standards dissolved in the same manner.

Trace metals abundances in the <0.1 μm and 0.1-2 μm samples were determined by analysis of solutions obtained by an acid digestion technique. To a 0.1 gram (110°C dry) sample in a teflon beaker two drops of DDH₂O were added. Then 5 ml of a 6:2:1 mixture of 48% HF:70% HNO₃:70% HClO₄ was added and the solution allowed to stand overnight at about 70°C. Solutions were then evaporated down until dense fumes of perchloric acid evolved, and an additional 5 ml of 48% HF was added. Samples were fumed down to near dryness, redissolved in 5 ml 6N HCl, transferred with DDH₂O to 25 ml volumetrics, diluted to the mark and transferred to 30 ml plastic bottles. Standards were prepared from stock 1000 ppm solutions and diluted in the same manner as the solid samples, using 1.0 ml of the mixed standards to a final volume of 25 ml in 1.2N HCl. Cu, Cr, and

Co were analyzed by heated graphite atomizer, while Mn, Zn, and Fe were analyzed by standard AAS flame techniques.

The concentrations metals released into solution by sequential reducing and oxidizing leaches were determined by the method of Presley (1969). Samples and blanks were shaken for four hours in 10 grams of 0.25 M hydroxylamine hydrochloride in 25% acetic acid and then centrifuged to clear the solution. The liquids were transferred to teflon beakers and the solid was washed twice with DDH₂O. This wash liquid was also added to the teflon beakers. To this liquid was added 0.5 ml 70% HNO₃ and the solution was evaporated. The residue was dissolved and taken up to 25 ml with 10% HNO₃, and analyzed as the reducible fraction for Cu, Cr, and Co by HGA and for Mn, Zn, and Fe by flame AAS. Standards were given identical matrices by evaporating 10 ml of the reducing solution for each 25 ml of 10% HNO₃ in the final solution. Solid material remaining from the reducing leach was further treated with a total of 5 ml of 30% H₂O₂ added at intervals over three days. The resulting solid residue was separated and rinsed 3 times using suspension and centrifugation procedures, and the supernate for each sample was combined in a teflon beaker. These liquids were evaporated to dryness and the residue redissolved in 1N HCl and labeled the oxidizable fraction. Analyses were carried out using AAS as outlined above, with standards having identical matrices. Clay carryover during decanting of the oxidized material was a problem and was shown to create positive

errors in the metal concentrations determined. Therefore, oxidizable metal values obtained can only be reported as less than or equal to the amount determined in this analysis. Filtration of the oxidized material as described in Presley (1969) should eliminate this problem.

Na_2CO_3 leachable silica was determined on selected $<0.1 \mu\text{m}$ fractions and on bulk samples, using the method described by Hurd (1973). Due to low concentrations of leachable silica the undiluted solution was analyzed spectrophotometrically as above, necessitating HCl neutralization and vacuum degassing of samples prior to analysis.

Analysis of boron in the bulk samples and the $<0.1 \mu\text{m}$ fractions was carried out on an ARL 1.5 meter Quantograph (Arc Emission Spectrograph) using a 10 amp, 250 volt arc with a 30 second burn time. Samples and standards (NBS SRM 93a and USGS std. GSP1) are mixed 1:2 with graphite containing 250 ppm Be (as beryl) (Reynolds, 1965). The line densities on the film negatives were read on a Joyce double beam recording microdensitometer using the boron line at 2497.7A and the Be line at 2650A for an internal standard.

Mineralogic analyses were performed using a Norelco X-ray diffractometer. Oriented samples were prepared for clay analyses of the $<0.1 \mu\text{m}$, $0.1-2 \mu\text{m}$ and $2-44 \mu\text{m}$ fractions by sedimentation of 25 mg of each sample in one ml DDH₂O onto a 1.5 sq. in. (9.7 cm^2) glass slide. These slides were run from 2° to $40^\circ 2\theta$ glycolated and from $2-25^\circ 2\theta$ after heating at

300°C for 2 hours. The 001 illite and kaolinite (002 chlorite) reflections from these patterns were used to calculate percent mixed layer clay, percent illite and percent 1:1(2:2) clay while the 002/004 kaolinite/chlorite peaks were used to distinguish chlorite from kaolinite. The intensity of the 001 kaolinite peak was divided by an experimentally determined value of 2.5 to equate with 10 A intensities. The percentage of 10 A and 17 A layers in the mixed layer clay was calculated using the shift in 002/003 reflection occurring between 5.0 and 5.7 A (Reynolds and Hower, 1970). The percent 17 A layers in the mixed layer clay of the >2 μm material could not be determined using this method as the 002/003 peaks were too small. The non-clay mineralogy of the 2-44 μm and >44 μm fractions was examined using random powder packs.

CHAPTER III

DATA

From 1 to 4 cylindrical sidewall cores (1" (2.54 cm) diameter, 2" (5.08 cm) length) were obtained from each of 16 depths in the two wells studied. Well #2, from which 13 of the samples were obtained, was drilled vertically and thus the true vertical depth below sea level corresponds to the well depth for these samples. However, well A4, a short distance from well #2, was drilled at a slight angle. Correction of the reported depths (3390, 3480, 3588 m) from which sidewalls were taken to the true vertical depths (3074, 3164, 3242 m) is necessary in order to permit comparison of the two wells. A comparison of well logs indicates that, stratigraphically, the true vertical depth 3074 m layer in well A4 correlates with a depth of ~3103 m in well #2. Therefore, the samples from well A4 lie below the deepest sample from well #2 (3063 m) both vertically and stratigraphically. For the purpose of data presentation all samples will be identified by their true vertical depth in meters.

The analyses of waters obtained by squeezing, as well as the weight loss of the bulk samples on room temperature (P. W.) and 110°C (I. W.) drying, are reported in Tables 1-3. Aqueous chemistries of two drill muds from well #2 (DM 1, shallow; DM 2, deep) are presented in Table 4. Squeeze liquid

Table 1. Pore Water Chemistry (Squeeze Data).

Depth Meters	P. W. (%) *	I. W. (%) **	pH	Cl (ppt)	SO4 (ppm)	HCO3 (ppm)	OC (ppm)	Na (ppt)	K (ppm)	Mg (ppm)	Ca (ppm)	B (ppm)	SiO2 (ppm)	Br (ppm)	F (ppm)
390	17.7	4.0	6.45	21.1	4500.	200.	30.	12.7	102.	840.	1230.	.32	7.3	11.0	.26
538 I	13.4	3.2	*****	23.1	2250.	*****	*****	14.2	130.	415.	832.	.52	2.5	57.0	1.10
538 II	13.2	3.4	7.60	22.1	2200.	*****	*****	13.6	110.	397.	800.	.42	2.5	57.8	.88
692	8.0	6.5	*****	40.2	4080.	*****	*****	22.5	198.	1625.	1880.	.96	3.3	10.0	*****
844	17.9	5.4	*****	32.9	6550.	*****	*****	20.1	180.	1490.	1190.	2.08	*****	8.5	*****
1000	11.5	5.8	7.13	32.2	1100.	110.	54.	19.5	128.	662.	1100.	1.09	2.2	37.5	.87
1150 I	14.8	5.8	6.78	21.6	3890.	115.	60.	15.1	110.	275.	590.	.95	2.7	17.3	.86
1150 II	*****	*****	7.31	18.0	5310.	95.	52.	14.4	139.	353.	490.	.78	2.2	61.8	.63
1289	9.1	6.0	*****	41.6	7300.	*****	*****	38.4	135.	594.	388.	*****	*****	*****	*****
2851	*****	*****	*****	19.6	6190.	*****	*****	15.9	183.	*****	728.	*****	*****	*****	*****
2906	7.2	4.6	8.04	20.1	5500.	695.	732.	15.7	87.	38.	525.	.95	2.5	14.0	*****
2961	12.2	3.4	7.24	19.5	5530.	450.	700.	15.6	102.	45.	579.	.95	3.1	12.5	1.34
3007	9.5	4.6	*****	24.1	4940.	*****	*****	18.0	98.	30.	622.	1.08	2.7	7.5	*****
3038	7.7	4.6	6.98	25.6	5720.	45.	340.	19.2	125.	69.	605.	*****	*****	*****	*****
3064	11.0	4.6	*****	25.1	5310.	*****	*****	18.8	119.	34.	509.	*****	*****	5.5	*****
3074	6.3	5.8	*****	17.1	7380.	*****	*****	12.4	78.	52.	260.	*****	*****	*****	*****
3164	9.8	5.4	*****	15.6	9750	*****	*****	13.5	65.	32.	168.	*****	2.8	*****	*****
3242	6.4	4.4	*****	18.2	*****	*****	*****	15.0	295.	59.	185.	*****	*****	*****	*****

*Bulk sample pore water content (wt % lost on room temperature drying).

**Bulk sample interlayer water content (wt % lost on room-110°C drying).

*****Not determined.

Table 2. Pore Water Variations with Squeeze Pressure.

Sample	Cl (ppt)	SO ₄ (ppm)	Br (ppm)	Na (ppt)	K (ppm)	Mg (ppm)	Ca (ppm)	Volume (ml)	P _{max} (psi)*
390 i	21.0	4460.	9.5	13.3	114.	788.	1240.	0.731	1410
390 iii	21.1	4150.	13.7	12.4	95.	838.	1220.	0.735	2550
390 iv	20.6	4750.	12.3	12.8	94.	900.	1250.	0.325	3110
390 v	21.5	5050.	8.5	12.3	92.	912.	1230.	0.613	4530
1150 i	18.1	5340.	61.5	14.8	158.	338.	480.	0.777	1410
1150 iii	18.1	5280.	62.0	14.0	122.	362.	488.	0.791	4530
1150 iv	17.4	5340.	--	14.3	125.	388.	531.	0.200	4530

*P_{max} = maximum pressure applied.

Table 3. Trace Elements in Pore Waters (Squeeze Data).

Depth (meters)	Sr (ppm)	Fe (ppm)	Cu (ppm)	Mn (ppm)	Cr (ppm)	Zn (ppm)
390	--	1.50	0.06	1.90	0.30	0.60
1150 I	--	14.20	0.07	.45	0.14	0.30
1150 II	--	0.10	0.08	.37	.0	0.20
2906	42.5*	2.25*	1.70*	.88*	--	--
2961	12.2	1.78	0.70	.14	--	--
3007	35.0*	4.00*	6.90*	.49*	--	--
3064	10.8	1.68	2.80	.22	--	--

*Evaporation prior to analysis probable.

Table 4. Chemistry of Drill Mud Liquids

	Drill Mud #1	Drill Mud #2
Cl (ppt)	15.4	19.3
SO ₄ (ppm)	3420	5850
Br (ppm)	45.0	10.9
HCO ₃ (ppm)	1040	460
Organic Carbon (ppm)	1210	4400
Na (ppt)	10.8	15.8
K (ppm)	125	162
Mg (ppm)	230	150
Ca (ppm)	800	1920
B (ppm)	2.0	2.8
SiO ₂ (ppm)	--	45
F (ppm)	0.62	--
Sr (ppm)	--	8.2
Fe (ppm)	1.9	5.5
Cu (ppm)	0	≤0.014
Mn (ppm)	0	0.30
Cr (ppm)	--	13.3
Zn (ppm)	0.92	0.82

recoveries of <0.1 ml (4 samples) allowed analysis of only Na, Ca, Mg, K and Cl and usually SO₄, while recoveries of 0.2-0.4 ml (6 samples) permitted the analysis of three or more of the following: pH, HCO₃, organic carbon, Br, boron and silica (Table 1) and the trace elements Sr, Fe, Cu, and Mn (Table 3). Recoveries of 0.7-1.3 ml (4 samples) enabled the analysis of all of the species in Table 1 and two samples with recoveries of 3.0 ml (390) and 3.3 ml (1150 II) were analyzed for major and minor constituents (Table 1) and trace elements (Table 3) and further analyses of effects of squeeze pressure were also possible (Table 2). In addition to the above analyses, samples obtained from depths 538 and 1150 consisted of enough core material to allow multiple squeezes. As mentioned previously, samples 1150 I and II represent material from different cores taken at 1150 m and 1150 I had many sand lenses removed prior to squeezing. On the other hand samples 528 I and II were an attempt at preparing duplicate squeeze samples. This attempt to obtain two identical samples was hampered by sample inhomogeneities and a desire not to break the cores up too much prior to squeezing. Despite the possible error involved in splitting samples 538 I and II, these duplicate analyses (Table 1) have an average deviation of <4% from the mean. From these data and analytical considerations, error involved in the chemical analyses of Table 1 can be estimated at about ±3% for major elements, ±5% for most other elements and perhaps as high as ±10% for some of the minor constituents.

Assuming unit activity coefficients and no ionic pairing, cation and anion total charges can be calculated for each sample. The ratio of cationic charge to anionic charge for each sample is within 10% of unity for all samples except 1289 and 3241 (both -30% anion poor). The 3241 sample is deficient in anion charge due to a lack of both HCO_3 and SO_4 analyses while the cause of the anion deficiency in 1289 pore water is unknown.

The primary sources of error in these pore water analyses include evaporation prior to squeezing, sample inhomogeneities and analytical errors. Lag time between core recovery and squeezing is an important factor in determining the extent of evaporation which may have taken place. Lag times are 60-64 days for 390-1289 (except 538), 7-11 days for 538 and 2851-3064 and 3 days for 3073-3241.

Weight loss of the core material on air drying and subsequent 110°C drying are presented in Table 1 as percent by weight P. W. (pore water) for the weight loss on air drying and percent by weight I. W. (interlayer water) for weight loss on subsequent 110°C drying. Room temperature drying was chosen as the measure of pore water content as the differential thermal analysis of clays (Grim, 1968) indicates that interlayer water loss occurs below 100°C . Weight loss from room temperature to 110°C does not represent the total absorbed water of the samples as additional absorbed water loss, up to 300°C , is observed in clays (Weaver and Beck, 1971). Duplicate

dryings of samples allow an estimate of average error at less than $\pm 5\%$.

The pore water content, determined in this manner, is used in the calculation of dilution factors for the leaching analyses. These dilution factors are in turn used to correct the leached solution chemical analyses to original pore water composition (Table 5). Table 6 presents leach data for five samples obtained by trimming first the top, bottom, and side of the core to remove the outermost rind (538 A) followed by subsequent sequentially trimmed portions into the centermost core (538 E). The correction factor used to convert these data to original pore water concentrations utilizes the total water loss up to 110°C . Error in absolute concentration induced by the use of 110°C water loss will be unimportant as the pore water concentrations of the sequentially trimmed core from 538 m will not be directly compared with any of the other pore water data.

After squeezing, samples were fractionated and the percent by weight of the solid in various size fractions was determined. These data are presented as the percentage of the bulk sample (Table 7). As discussed earlier, the $<.03\ \mu\text{m}$ fraction was determined by the weight loss on fractionation and in fact is a measure of soluble ions plus $<.03\ \mu\text{m}$ material not trapped during the maximum centrifugation plus material lost during handling. Prior to fractionation sample 1000 was homogenized and split into two samples. The average deviation

Table 5. Pore Water Chemistry (Leach Data).*

Depth (meters)	Cl (ppt)	SO ₄ (ppm)	Br (ppm)	Na (ppt)	K (ppm)	Mg (ppm)	Ca (ppm)	HCO ₃ (ppm)	Organic Carbon (ppm)
538	21.9	2810.	64.	16.7	200.	30.	64.	3840.	2930.
2906	20.1	9620.	134.	26.5	270.	52.	89.	34600.	1950.
2961B	21.5	13800.	35.	34.5	460.	111.	118.	37300.	540.
3007	17.9	4380.	57.	22.2	180.	38.	79.	28600.	1420.
3064	16.8	6970.	18.	21.5	180.	34.	66.	26000.	952.
	B (ppm)	SiO ₂ (ppm)	F (ppm)	Sr (ppm)	Cu (ppm)	Mn (ppm)	Fe (ppm)	% P.W.**	% I.W.***
538	16.	140.	16.	--	--	--	--	13.0	3.6
2906	56.	240.	--	6.3	2.5	2.70	503.	7.2	4.7
2961B	77.	350.	--	3.7	1.0	2.20	444.	5.0	3.4
3007	50.	160.	--	2.8	1.0	0.63	123.	9.5	4.6
3064	53.	140.	--	2.9	1.0	0.49	126.	11.0	4.6

*Values are reported as concentration in original pore water using wt. % loss on air drying (P. W.) to calculate dilution factors.

**% P. W. = weight loss on air drying (% pore water).

***% I. W. = weight loss on 110°C drying (% interlayer water).

Table 6. Pore Water Leach Chemistry of a Sequentially Trimmed Sample*.

Sample	Cl (ppt)	Br (ppm)	Na (ppt)	K (ppm)	Mg (ppm)	Ca (ppm)	HCO ₃ (ppm)	Organic Carbon (ppm)	B (ppm)	% T.W.**
538-A	18.0	41.8	15.6	206.	55.	92.	9900.	600	13.5	15.1
538-B	16.7	41.3	13.8	214.	47.	64.	10000.	390	11.2	15.6
538-C	15.1	38.7	13.4	210.	32.	62.	11400.	490	9.3	15.7
538-D	16.0	39.9	13.9	225.	33.	65.	--	--	--	15.2
538-E	15.0	40.0	12.5	170.	24.	51.	--	--	8.4	15.8

*Values are reported as concentration in original pore water, using % wt. loss at 110°C drying (% T.W.) to calculate dilution factors.

**% T.W. = weight loss on 110°C drying ("Total" water).

Table 7. Weight Percent (110°C Dry) in Size Fractions.

Depth	<.03 μ m	.03-.1 μ m	.1-2 μ m	2-44 μ m	>44 μ m
390	2.1	17.2	24.1	41.1	15.5
538 I	1.4	11.1	9.8	26.3	51.4
538 II	2.8	10.8	11.2	29.6	45.6
692	2.4	26.2	40.3	30.8	.3
844	4.0	27.7	34.7	33.0	.6
1000 i	2.6	26.5	41.0	28.4	1.5
1000 ii	1.8	27.5	39.5	29.6	1.6
1150 I	4.7	28.6	28.0	33.8	4.9
1150 II	2.9	20.5	24.4	27.5	24.7
1289	4.5	27.9	23.9	36.5	7.2
2851	3.9	10.4	26.0	46.2	13.5
2906	2.4	14.0	33.5	34.4	15.7
2961	2.6	9.6	32.7	37.3	17.8
3007	3.8	14.5	36.5	36.5	8.9
3038	3.0	16.7	37.2	35.2	7.9
3064	4.8	15.6	39.3	32.4	7.9
3074	5.9	15.2	45.1	32.5	1.3
3164	2.1	15.1	44.5	34.8	3.5
3242	1.5	13.6	36.6	45.8	2.5

of this duplicate size fraction analysis is 2% while the deviation for 538 is 4% (excluding the $<.03\mu\text{m}$ fractions). Thus the 538 I and II samples, as suggested earlier, may not represent a well homogenized duplicate.

A measure of the sand and shale distributions in the wells can be obtained from S. P. curves on well logs. Figure 1 is a plot of the percentage of layers of greater than average shaliness over 100 feet (30.2 m) intervals. This figure permits the determination of proximity of sidewall cores to major sand units. The wells penetrated two major sand sequences (1130-1980 m, averaging $<30\%$ shaly layers and 2255-2805 m averaging $<45\%$ shaly layers). The sequences above, between and below these sands generally contain $>80\%$ shale layers. Comparison of data in Figure 1 and Table 7 is difficult, first because Table 7 represents data from individual 2.5 cm layers in the wells while the data of Figure 1 represents averages of 30.2 m intervals, and second because sandy layers were trimmed from several samples (390, 844, 1000 and 1150 I) prior to analysis to avoid drill mud contamination. This would affect the grain size distribution by preferentially removing larger grain sizes (compare 1150 I and II, Table 7) and can be corrected for, to some degree, by recalculation of the size fraction percentages to 100% $<44\ \mu\text{m}$ material.

The clay mineralogy of the $<0.1\ \mu\text{m}$ and $0.1\text{-}2\ \mu\text{m}$ fractions (Table 8) is given in terms of percent by weight of the total clay minerals. Quartz (present in the $0.1\text{-}2\ \mu\text{m}$ and $2\text{-}44\ \mu\text{m}$ fractions)

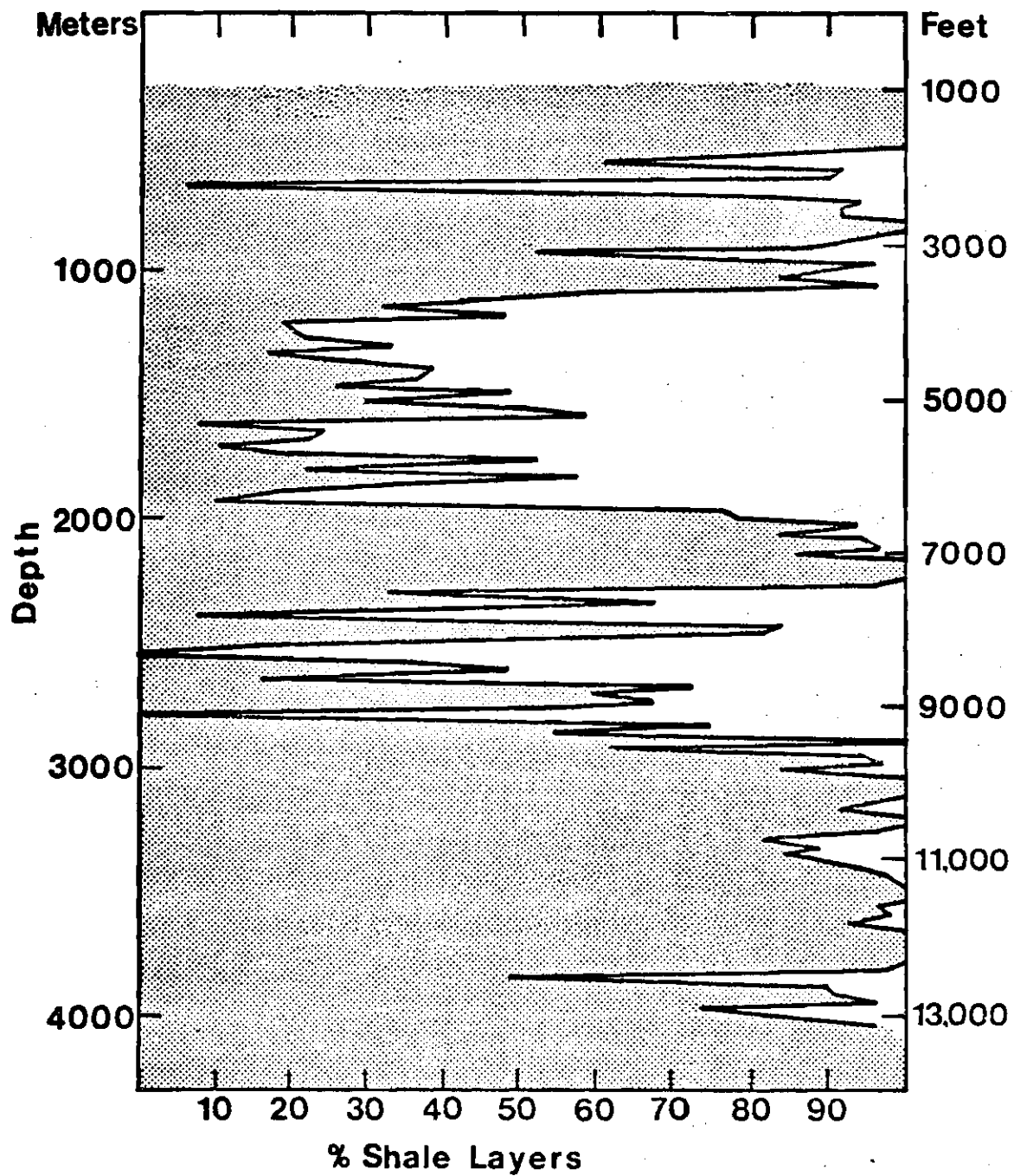


Figure 1. Qualitative Estimation of Shale Distribution in Wells 2 and A4.

Table 8. Clay Mineralogy of <44 μm Size Fractions.*

Depth (m)	<0.1 μm				0.1-2					2-44 μm				Exp. 1:1 Clay
	Illite	17A 1/S	10A 1/S	I + Ch	Illite	17A 1/S	10A 1/S	Kaolinite	Chlorite	Total 1/S	Illite	Kaolinite	Chlorite	
390	23	38	36	3	38	34	9	13	6	22	62	10	6	--
538 I	29	74	4	2	31	43	11	13	2	29	56	6	3	6
538 II	18	64	16	2	41	40	2	15	2	44	50	3	2	1
692	33	38	27	2	34	46	2	14	4	9	69	16	6	--
844	28	32	35	5	41	35	2	18	4	12	66	12	8	--
1000 I	28	36	34	2	39	36	2	20	3	24	51	20	5	--
1000 II	28	34	36	2	39	34	2	21	4	18	56	18	8	--
1150 I	19	49	27	5	27	32	10	25	6	11	64	14	11	--
1150 II	21	49	27	3	24	39	13	19	8	12	70	10	6	2
1289	31	34	31	4	40	32		23	5	19	60	13	8	--
2851	13	38	42	7	20	25	24	20	11	4	58	25	11	2
2906	18	40	37	5	28	28	25	15	4	47	31	11	7	4
2961	16	42	38	6	22	32	24	18	4	13	54	22	9	7
3007	17	35	38	10	20	31	23	20	6	45	26	12	9	8
3038	21	30	39	10	26	33	14	22	5	23	44	23	8	2
3064	18	40	37	5	28	27	24	17	4	13	56	20	11	--
3074	18	33	42	8	28	28	23	20	4	44	26	18	12	--
3164	21	33	41	5	26	27	24	19	4	33	32	26	9	--
3242	23	30	45	2	29	24	30	12	5	33	41	16	18	--

* Expressed on weight percent.

and calcite (present in 3241 in the 0.1-2 μm fraction and in most 2-44 μm fractions) are not accounted for. Kaolinite and chlorite in the <0.1 μm fraction must be grouped together due to the lack of resolution of the 002/004 peaks. The average deviation of duplicate clay analyses is 5% for samples 1000 I and II while the 538 duplicates show a particularly large deviation in the percent 10 A layers in the illite/smectite mixed layer phase due to the large expanded component of the illite/smectite.

The major element chemistry on a 110°C dry basis is presented in Tables 9-12 for the <0.1 μm , 0.1-2 μm , 2-44 μm , and >44 μm fractions. The difference between 100% and the totals represents the ignitables; organic and inorganic carbon, hydroxy groups, structural water not released at 110°C, sulfur compounds, etc.; as well as procedural errors. The average deviation of duplicate major element analyses for the size fractions of both duplicate samples is $<2\%$.

Data on the boron content of <0.1 μm fractions and bulk samples are presented in Table 13. Table 14 shows the sodium carbonate soluble silica from the same fractions. Boron analyses, performed by arc emission spectrometry, have a low degree of reliability and a deviation of $\sim 20\%$ while the soluble silica analyses are considered more precise.

Exchange ions were measured in terms of meq/100 g 110°C dry sample in the <0.1 μm and 0.1-2 μm fractions (Table 15). Totals are the sum of Na, K, Ca and Mg. The average range

Table 9. Major Element Chemistry of the <0.1 μm Fraction (110°C Dry).

Depth	SiO ₂ %	Al ₂ O ₃ %	Fe ₂ O ₃ %	MgO %	CaO %	K ₂ O %	Na ₂ O %	TiO ₂ %	Sr PPM	Mn PPM
390	55.6	20.8	7.9	2.98	.65	2.59	.34	.27	90.	725.
538I	57.3	19.4	9.6	3.06	.59	1.96	1.31	.32	150.	192.
538II	57.0	19.1	9.1	2.97	.48	1.86	1.25	.32	150.	235.
692	56.1	21.1	6.8	3.45	1.06	3.10	.54	.27	120.	412.
844	55.1	21.6	7.1	3.09	.69	3.11	.44	.30	110.	655.
1000i	55.8	20.8	7.3	3.15	1.58	3.11	.20	.27	120.	458.
1000ii	55.9	20.8	7.3	3.15	1.53	3.33	.21	.27	110.	482.
1150I	56.5	21.4	7.2	2.90	1.26	2.77	.58	.28	110.	292.
1150II	55.8	20.8	7.0	3.38	1.49	2.55	.24	.25	120.	310.
1289	54.8	22.0	5.8	2.69	.34	2.96	.98	.30	100.	338.
2851	54.2	23.2	6.0	2.49	1.67	2.49	.20	.30	240.	192.
2906	54.9	22.6	5.0	2.55	1.26	2.45	.54	.30	210.	160.
2961	54.1	22.1	5.7	2.78	1.80	2.60	.16	.25	180.	225.
3007	53.8	23.3	5.6	2.35	1.45	2.37	.42	.30	170.	155.
3038	53.7	23.6	5.2	2.44	1.49	2.52	.31	.32	160.	165.
3064	54.4	22.4	5.3	2.65	1.67	2.63	.26	.28	160.	210.
3074	54.1	22.9	5.2	2.23	1.19	2.35	.43	.28	180.	185.
3164	55.0	22.8	5.3	2.65	1.60	2.74	.24	.23	240.	190.
3242	55.1	22.1	5.9	2.80	1.67	3.32	.20	.22	200.	208.

Table 10. Major Element Chemistry of the 0.1-2 μm Fraction (110°C Dry).

Depth	SiO ₂ %	Al ₂ O ₃ %	Fe ₂ O ₃ %	MgO %	CaO %	K ₂ O %	Na ₂ O %	TiO ₂ %	Sr PPM	Mn PPM
390	54.0	22.9	6.2	2.47	.43	4.03	.40	1.18	120.	540.
538I	55.6	21.5	5.9	2.36	.39	3.69	.85	1.57	140.	215.
538II	56.3	21.4	6.0	2.44	.38	3.92	.84	1.60	150.	240.
692	55.8	21.4	5.4	2.58	.78	3.74	.49	1.12	130.	405.
844	54.5	22.9	5.5	2.34	.48	3.98	.40	1.25	110.	470.
1000i	55.6	21.2	5.6	2.47	1.17	3.72	.35	1.01	130.	478.
1000ii	54.8	21.5	5.6	2.52	1.17	3.94	.39	1.11	140.	475.
1150I	59.2	20.7	4.2	1.72	.71	2.97	.38	1.57	120.	305.
1150II	57.1	21.0	5.3	2.53	.95	3.13	.31	1.25	120.	345.
1289	57.2	21.2	4.5	1.73	.18	2.44	.54	1.97	110.	322.
2851	53.2	23.9	6.5	2.00	.97	2.51	.26	1.23	190.	170.
2906	57.5	22.5	5.0	2.14	1.04	2.87	.43	1.03	190.	162.
2961	57.3	22.3	5.7	2.26	1.40	3.00	.24	1.03	160.	230.
3007	56.3	23.1	4.6	1.71	.96	2.38	.30	1.17	150.	150.
3038	54.6	24.2	4.2	1.71	.93	2.46	.26	1.05	160.	152.
3064	55.4	22.4	4.6	2.05	1.23	2.80	.30	1.07	150.	195.
3074	56.5	23.0	4.7	1.92	.88	2.82	.39	1.03	170.	145.
3164	54.5	22.7	4.4	1.96	1.30	2.71	.26	.98	230.	158.
3242	50.1	19.4	5.5	2.25	6.90	3.06	.32	.92	350.	235.

Table 11. Major Element Chemistry of the 2-44 μm Fraction (110°C Dry).

Depth	SiO ₂ %	Al ₂ O ₃ %	Fe ₂ O ₃ %	MgO %	CaO %	K ₂ O %	Na ₂ O %	TiO ₂ %	Sr PPM	Mn PPM
390	74.5	9.2	2.8	.70	.52	2.53	1.36	1.03	120.	250.
538I	74.0	9.7	1.9	.69	.84	2.84	1.90	.91	190.	240.
538II	75.0	9.2	1.8	.62	.82	2.80	1.87	.92	170.	240.
692	66.0	9.8	5.8	1.94	2.00	2.78	1.03	.89	80.	960.
844	67.0	9.6	6.8	1.44	.80	2.71	.90	.96	80.	670.
1000i	66.5	10.2	5.6	1.32	2.56	2.60	.97	.95	110.	680.
1000ii	66.5	9.8	5.7	1.38	2.80	2.65	.98	.98	110.	680.
1150I	72.5	5.8	2.7	.41	3.54	2.10	.92	.88	100.	770.
1150II	71.5	7.2	3.0	.68	2.70	2.28	.97	.93	140.	370.
1289	74.5	6.6	4.8	.38	.11	2.14	.97	.96	100.	520.
2851	76.0	6.5	2.7	.43	1.57	1.74	.93	.77	110.	230.
2906	72.0	7.5	4.6	.60	1.31	2.16	.93	.89	150.	330.
2961	69.5	7.8	4.7	.74	3.80	1.95	.83	.75	220.	490.
3007	70.5	8.2	4.9	.75	1.46	1.70	.68	.88	120.	340.
3038	68.5	7.8	5.3	.80	1.53	1.65	.62	.86	110.	270.
3064	68.0	6.8	6.9	.80	1.51	1.62	.81	.75	160.	480.
3074	67.0	12.2	6.5	1.28	1.57	2.24	.69	.90	170.	440.
3164	58.5	10.8	7.3	1.65	3.60	1.75	.64	.75	730.	570.
3242	59.5	8.4	4.2	1.29	9.30	1.68	1.13	.63	280.	1030.

Table 12. Major Element Chemistry of the >44 μm Fraction (110°C Dry).

Depth (meters)	SiO ₂ %	Al ₂ O ₃ %	Fe ₂ O ₃ %	MgO %	CaO %	K ₂ O %	Na ₂ O %	TiO ₂ %	Sr ppm
390	78.0	5.3	0.5	0.20	0.65	1.74	1.42	0.32	150.
538 I	78.0	6.1	0.7	0.19	0.82	2.07	1.64	0.26	170.
588 II	79.5	6.0	0.5	0.15	0.70	1.82	1.58	0.26	170.
1150 II	79.0	1.4	0.3	0.08	0.70	0.98	0.38	0.20	60.
2906	79.0	3.9	1.0	0.18	0.60	1.93	0.97	0.28	80.
3038	76.5	4.1	3.9	0.26	1.72	1.40	0.61	0.22	90.
3164	43.5	10.8	12.0	1.42	14.90	0.96	0.57	0.17	770.

Table 13. Boron Content of $<0.1 \mu\text{m}$
and Bulk Samples.

Depth (meters)	$<0.1 \mu\text{m}$ (ppm)	Bulk Sample (ppm)
390	140.	65
538 I	110.	50
692	140.	80
1000 i	210.	80
1150 I	60.	80
1150 II	130.	70
2906	230.	100
2961	80.	80
3007	125	110
3038	290.	100
3064	210.	95
3164	120.	120
3242	210.	70

Table 14. Na_2CO_3 Soluble Silica of
$0.1 \mu\text{m}$ and Bulk Samples.

Depth (meters)	$0.1 \mu\text{m}$ (%)	Bulk Sample (%)
390	1.98	1.24
538 I	1.37	.66
692	1.15	.48
844	1.33	.49
1000 i	1.37	.80
1150 I	1.32	.66
1150 II	1.63	.85
1289	1.02	.73
2851	1.03	.42
2906	1.14	.63
2961	--	.74
3007	1.43	.83
3064	1.46	.87
3074	1.00	.49
3164	1.12	.70
3242	1.17	.75

Table 15. Exchange Ion Chemistry, <0.1 and 0.1-2 μm Fractions.

Depth	<0.1 μm (Meq/100 gm)					0.1-2 μm (Meq/100 gm)				
	Ca ⁺⁺	Mg ⁺⁺	K ⁺	Na ⁺	Total	Ca ⁺⁺	Mg ⁺⁺	K ⁺	Na ⁺	Total
390	21.0	20.4	4.4	6.7	52.5	12.5	11.1	3.0	2.0	28.6
538I	17.0	14.0	4.7	36.0	71.7	8.7	8.2	3.4	13.0	33.3
538II	16.0	13.5	4.2	34.0	67.7	9.4	8.6	3.2	10.9	32.1
692	32.0	13.2	5.0	10.5	60.7	16.9	8.3	2.8	1.5	29.5
844	22.0	13.5	5.3	8.9	49.7	10.6	10.5	3.7	1.3	26.1
1000i	49.0	7.9	4.4	2.2	63.5	32.0	3.2	2.7	.4	38.3
1000ii	47.0	7.3	4.4	1.5	60.2	31.0	2.9	2.7	.6	37.2
1150I	39.0	7.0	5.0	12.5	63.5	20.0	4.8	3.7	1.6	30.1
1150II	46.0	10.6	4.6	3.5	64.7	26.0	7.1	2.9	.7	36.7
1289	10.0	9.5	5.1	24.0	48.6	3.7	3.7	3.0	5.7	16.1
2851	52.0	4.8	4.3	1.7	62.8	30.0	3.6	2.8	.6	37.0
2906	44.0	3.7	4.6	12.5	64.8	32.0	3.0	3.8	5.6	44.4
2961	58.0	4.3	3.6	1.0	66.9	41.0	2.5	2.9	.5	46.9
3007	47.0	4.0	4.0	7.4	62.4	31.0	3.0	3.3	2.6	39.9
3038	47.0	3.8	3.8	4.7	59.3	31.0	2.9	3.1	1.4	38.4
3064	54.0	3.4	3.9	3.6	64.9	39.0	2.1	3.2	1.0	45.3
3074	43.0	4.6	4.0	8.7	60.3	27.0	3.4	3.5	5.0	38.9
3164	50.0	4.0	3.6	3.0	60.6	40.0	2.3	2.9	.7	45.9
3242	54.0	5.6	4.0	1.7	65.3	72.0	3.1	3.0	.5	78.6

of duplicate analyses is -10%.

Tables 16-18 list analyses of iron, manganese, zinc, copper, cobalt and chromium. Both the total amount and reducible portion of each of these metals are reported for the <0.1 μm and 0.1-2 μm fractions. Total contents in the 2-44 μm fractions are presented for iron and manganese, while total contents in bulk samples were obtained for zinc, manganese, copper, and cobalt. A few analyses of iron (as Fe_2O_3) in the >44 μm fractions are reported in Table 12. The average deviation of duplicate trace metal analyses is <3% for total trace metal determinations and -10% for reducible metal analyses. Not presented in a table are the concentrations of oxidizable metals present in the <0.1 μm and 0.1-2 μm fractions, as most analyses gave results below detection limits and some sample contamination was evident in examination of some of the data from the different size fractions as well as the duplicate samples. Oxidizable metal data will be outlined somewhat in the later discussion of trace metal data.

Additional data of interest to this study can be obtained from the well logs. Figure 2 shows the geothermal gradients in the wells from High Island block 110 (from open hole logging data) to be 2.1°C/100 m down to 2800 m and 4.8°C/100 m below that. This is consistent with the range of observed Gulf Coast geothermal gradients (Hower, et al., 1976; Hottman and Johnston, 1965; Weaver and Beck, 1971; Rieke and Chilingarian, 1974). The increased gradient at depth may be

Table 16. Manganese in Solid Samples (110°C Dry).*

Depth	<.1 μm		.1-2 μm		2-44 μm	Bulk
	Total	Reducible	Total	Reducible	Total	Sample
390	725.	329.	540.	205.	250.	286.
538 I	192.	21.	215.	15.	240.	439.
538 II	235.	42.	240.	28.	240.	--
692	412.	143.	405.	142.	960.	540.
844	655.	285.	470.	179.	670.	531.
1000 i	458.	174.	478.	174.	680.	482.
1000 ii	482.	197.	475.	180.	680.	482.
1150 I	292.	89.	305.	99.	770.	--
1150 II	310.	109.	345.	120.	370.	--
1289	338.	79.	322.	62.	520.	331.
2851	192.	45.	170.	37.	230.	116.
2906	160.	47.	162.	37.	330.	197.
2961	225.	80.	230.	77.	490.	--
3007	155.	45.	150.	37.	340.	181.
3038	165.	49.	152.	37.	270.	--
3064	210.	70.	195.	62.	480.	247.
3074	185.	52.	145.	37.	440.	--
3164	190.	55.	158.	46.	570.	282.
3242	208.	65.	235.	82.	1030.	549.

*Data expressed as ppm.

Table 17. Iron and Zinc in Solid Samples (110°C Dry).

Depth	Fe (%)*					Zn (ppm)				Bulk Sample
	<.1 μm		.1-2 μm		2-44 μm	<.1 μm		.1-2 μm		
	Total	Reduce	Total	Reduce	Total	Total	Reduce	Total	Reduce	
390	5.53	.19	4.34	.30	1.96	220.	45.	228.	43.	120.
538I	6.71	.22	4.13	.17	1.33	120.	15.	126.	14.	61.
538II	6.36	.30	4.20	.20	1.26	126.	14.	138.	16.	--
692	4.76	.22	3.78	.47	4.06	140.	24.	132.	20.	130.
844	4.97	.24	3.85	.42	4.76	165.	26.	123.	15.	106.
1000i	5.11	.25	3.92	.30	3.92	132.	23.	130.	20.	108.
1000ii	5.11	.28	3.92	.39	3.99	149.	38.	128.	22.	108.
1150I	5.04	.25	2.94	.26	1.89	119.	17.	146.	16.	--
1150II	4.90	.30	3.71	.40	2.10	123.	22.	110.	23.	--
1289	4.06	.13	3.15	.41	3.36	150.	21.	108.	14.	102.
2851	4.20	.27	4.55	.33	1.89	111.	29.	91.	19.	108.
2906	3.50	.17	3.50	.25	3.22	89.	20.	85.	14.	98.
2961	3.99	.28	3.99	.47	3.29	110.	33.	106.	25.	--
3007	3.92	.22	3.22	.29	3.43	71.	15.	65.	17.	86.
3038	3.64	.19	2.94	.25	3.71	70.	11.	66.	10.	--
3064	3.71	.20	3.22	.22	4.83	80.	17.	75.	11.	86.
3074	3.64	.19	3.29	.17	4.55	68.	12.	65.	12.	--
3164	3.71	.20	3.08	.20	5.11	74.	17.	75.	11.	119.
3242	4.13	.17	3.85	.15	2.94	72.	10.	86.	8.	83.

*See Table 12 for >44 micron Fe data (as Fe₂O₃).

Table 18. Cu, Co, and Cr in Solid Samples (110°C Dry).*

Depth	Copper					Cobalt					Chromium			
	<.1 μm		.1-2 μm		Bulk Sample	<.1 μm		.1-2 μm		Bulk Sample	<.1 μm		.1-2 μm	
Total	Red.	Total	Red.	Total		Red.	Total	Red.	Total		Red.	Total	Red.	Total
390	20.0	1.7	28.0	4.6	16.2	32.0	9.1	30.0	5.8	21.2	130.0	1.0	120.0	2.0
538 I	26.0	4.6	24.0	4.6	12.4	16.0	1.9	22.0	1.0	10.7	112.0	2.0	115.0	1.0
538 II	21.0	3.7	26.0	4.8	—	18.0	1.9	23.0	1.1	—	108.0	2.5	115.0	1.0
692	25.0	4.2	30.0	7.1	24.5	18.0	4.2	18.0	3.3	17.0	118.0	2.0	108.0	1.0
844	22.0	5.0	35.0	8.3	22.9	18.0	4.3	17.0	2.6	18.5	120.0	1.0	115.0	1.0
1000 i	18.0	3.9	22.0	4.8	21.6	16.0	4.2	18.0	3.4	16.8	108.0	1.0	106.0	1.0
1000 ii	18.0	4.3	23.0	6.5	21.6	16.0	4.7	18.0	3.4	16.8	105.0	2.0	112.0	1.0
1150 I	16.0	3.6	22.0	5.4	—	14.0	3.5	12.0	2.5	—	88.0	0.0	85.0	2.0
1150 II	16.0	3.6	20.0	6.5	—	14.0	4.3	16.0	4.1	—	95.0	2.0	100.0	2.0
1289	16.0	2.5	21.0	3.7	16.2	21.0	4.1	15.0	2.5	16.7	105.0	1.0	92.0	2.0
2851	12.0	3.7	12.0	5.2	11.6	14.0	4.5	14.0	3.2	9.1	115.0	2.0	110.0	3.1
2906	7.8	1.9	10.0	3.6	17.7	16.0	6.3	13.0	3.5	14.5	108.0	6.2	108.0	3.7
2061	7.5	1.9	12.0	3.6	—	19.0	9.2	16.0	5.6	—	262.0	78.0	175.0	42.0
3007	7.5	3.2	11.0	3.0	15.2	17.0	6.8	12.0	3.7	11.5	122.0	8.1	115.0	4.4
3038	4.5	.9	7.0	1.8	—	17.0	6.2	11.0	3.2	—	110.0	2.0	118.0	1.0
3064	5.2	1.0	7.0	1.4	14.4	14.0	4.3	11.0	3.1	12.1	120.0	10.5	120.0	7.4
3074	7.5	2.5	9.0	3.0	—	12.0	3.9	11.0	2.6	—	85.0	2.0	98.0	1.0
3164	7.8	2.4	8.8	2.1	20.3	12.0	4.0	10.0	2.7	12.8	95.0	7.4	112.0	4.4
3242	8.5	2.2	8.0	3.0	17.2	8.0	2.5	8.0	1.5	11.5	85.0	1.0	80.0	1.0

*Data expressed as ppm.

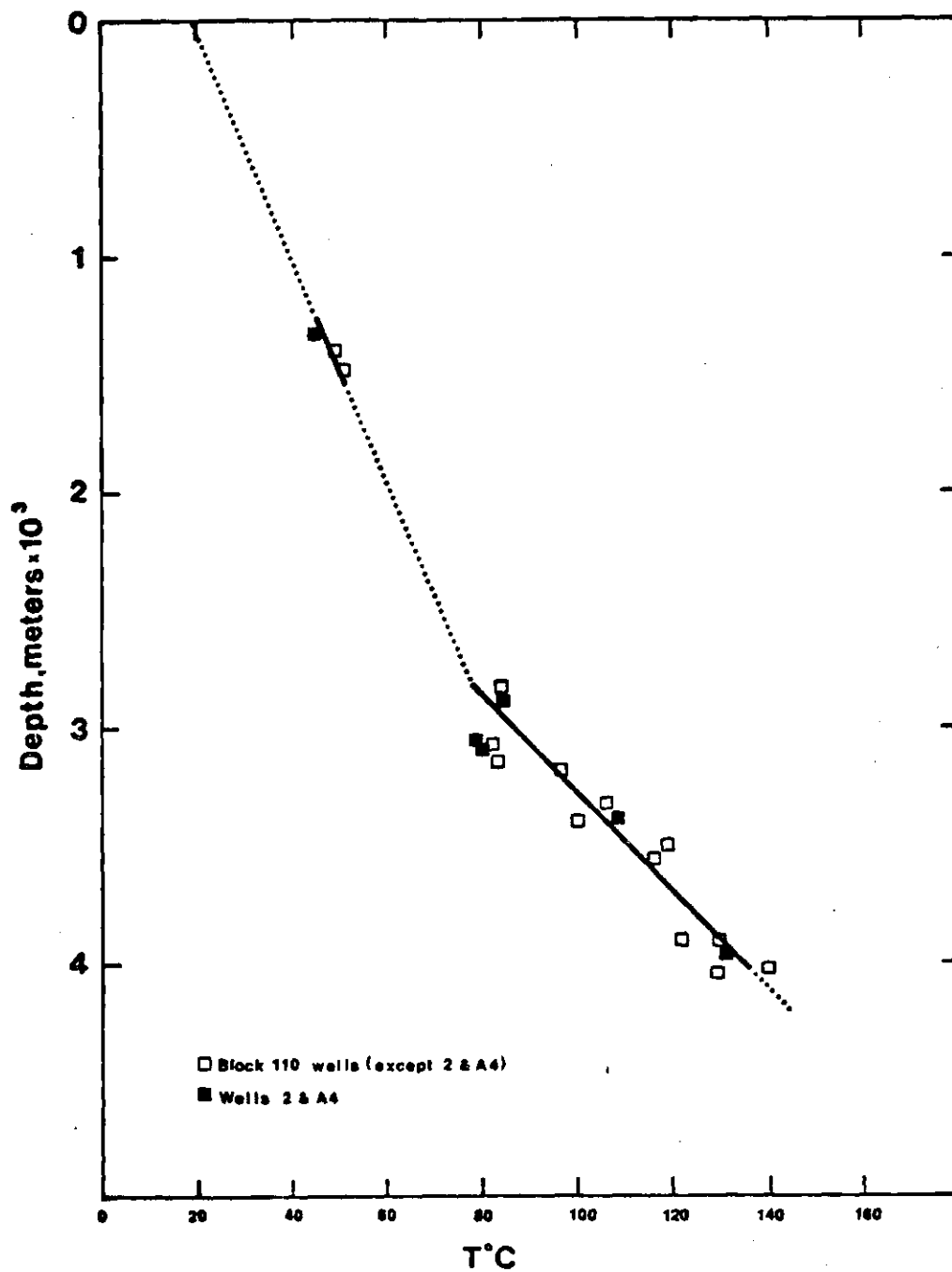


Figure 2. Well Log Temperature Variation with Depth for High Island Block 110 Wells.

due to the insulating capabilities of deeply buried, highly undercompacted sediments (Rieke and Chilingarian, 1974).

Also of interest is the acoustic log which records sonic velocities through the sediments. Using average sonic velocities of the shales (reported as Δt_{sh} in $\mu\text{sec}/\text{ft}$), it is possible to determine formation pressures using the method of Hottman and Johnston (1965). This technique is made possible by the dependence of both the sonic travel time and the fluid pressure on sample porosity. Porosities of the sediments will be estimated later for purposes of correction for evaporation. The formation pressure with depth determined by this method is plotted (over 100' (30.2 m) intervals) in Figure 3 along with the normal hydrostatic and geostatic pressure gradients (Chapman, 1973). Increases in formation pressures above the hydrostatic are termed abnormal pressures and are accompanied by abnormal increases in porosity. The observed zones of abnormal pressures may be caused by: loading of the sediment faster than interstitial water can be expelled (Chapman, 1973); increases in fluid volume due to increasing temperature (Barker, 1972); or the release of mineralogic water (Burst, 1976). The initiation of a very high pressure zone below 2800 m coincides with the increased geothermal gradient of Figure 2.

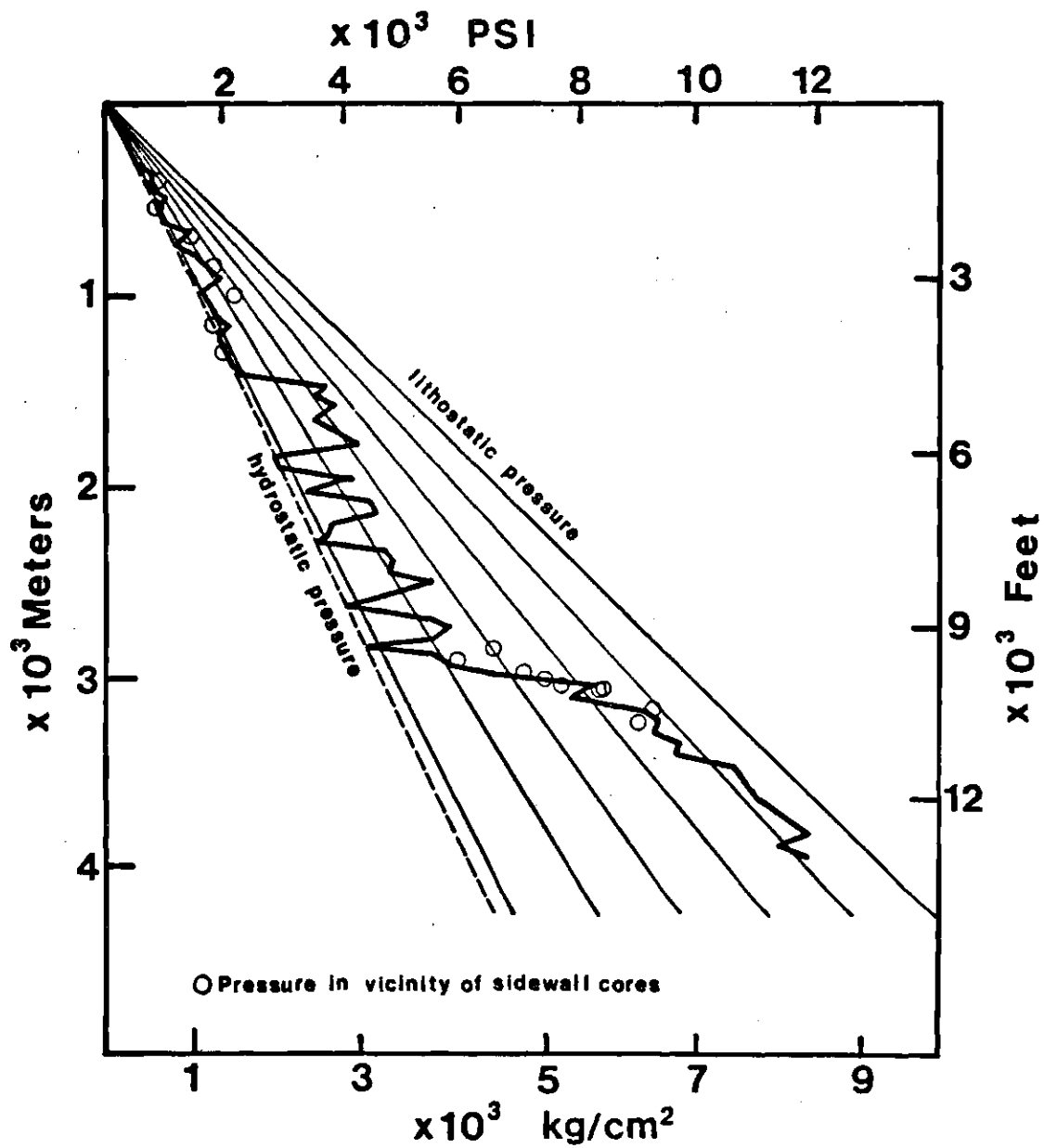


Figure 3. Variation in Fluid Pressure with Depth in Wells 2 and A4 from Acoustic Logs.

CHAPTER IV

DISCUSSION A

The Validity of and Corrections
to Pore Water Analyses

The analysis of interstitial waters of recent sediments for use as indicators of solid chemical reactions has grown in recent years (Manheim and Sayles, 1974; Sayles and Manheim, 1975). The primary technique employed for interstitial water analysis is pressure squeezing (Manheim, 1966; Presley, et al., 1967). Results from this type of analysis are generally concluded to reflect in situ pore water compositions for most ions. However, there are a number of factors which may cause alteration of pore water constituents during recovery and analysis. These major causes of pore water alteration prior to squeeze analysis include: alteration of pore water-solid equilibria due to pressure (Manheim, 1966; Shishkina, 1968) and temperature (Manglesdorf, et al., 1969; Bischoff, et al., 1970; Russell and Fallgatter, 1972; Sayles, et al., 1973a) variations during handling; contamination of pore waters by drill mud; and concentration of ions due to evaporation after recovery of the sediment core.

Additional water analyses have been obtained through use of a leaching method (Weaver and Beck, 1971; Schmidt,

1973). Potential errors inherent in this type of analysis are generally the same as the above with the addition of problems with the desorption and adsorption of ions from the solid caused by dilution of pore waters (Manheim, 1974). Since this study utilizes both squeeze and leach techniques, a detailed examination of potential errors in these analyses is desirable.

1. The Extent of Drill Mud Contamination

In order to prevent fluid in permeable beds from invading the drill hole pressure exerted by the drill mud column is adjusted during operation so that it exceeds that of the highest pressure permeable bed encountered (Martin, 1955). This results in the buildup of a mud cake on the walls of the hole where permeable beds are penetrated and the migration of drill mud fluid into the formation. This zone of invasion is generally greater than 3" deep (Schlumberger, 1958) and thus insures that water recovered from sidewall cores of permeable beds will be contaminated. The situation regarding less permeable beds is not as clearly understood, but it is intuitively obvious that much less invasion would take place and little or no mud cake will build up. An examination for possible drill mud contamination of the cores used in this study was performed using two methods.

The first method involves the determination of pore water constituents from the exterior to the interior of a single core, trimmed sequentially. If the core used (538)

is completely contaminated by drill fluid the pore waters will be similar in ion concentrations to the drill fluid. If contamination is not complete, a gradient will exist such that outermost portions of the core would be nearer to drill mud composition than the central portions of the core. In this case the outermost sample (538 A) consists of the portion of core (top, bottom, and side) which was trimmed from the other samples and disposed of as possibly contaminated. The leach method of analysis was employed as the trimmed samples were too small to allow squeezing. As will be shown later, few of the ion concentrations obtained from leach analysis represent actual pore water chemistries. Ions showing the least signs of leach induced alteration in the 538 m sample are Cl, Br, and Na. These were chosen for the drill mud contamination examination. Figure 4 is a graph of these three ions in the layers of core 538 (Table 6) as well as the Br/Cl and Na/Cl ratios in the layers and drill mud #1 (from Table 4).

It can be seen from this figure that the ratios (Br/Cl and Na/Cl) within the core are relatively constant and do not equal, or approach in the outermost portions, the ion ratios of the drill mud #1 (shallow mud from well 2). This allows the conclusion that drill mud contamination is not a problem for core 538 which, as seen in Table 7, is the sandiest sample squeezed in this work. However, the absolute ion concentrations are seen in Figure 4 to decrease from the outermost layers of the core, inward. This can be taken as

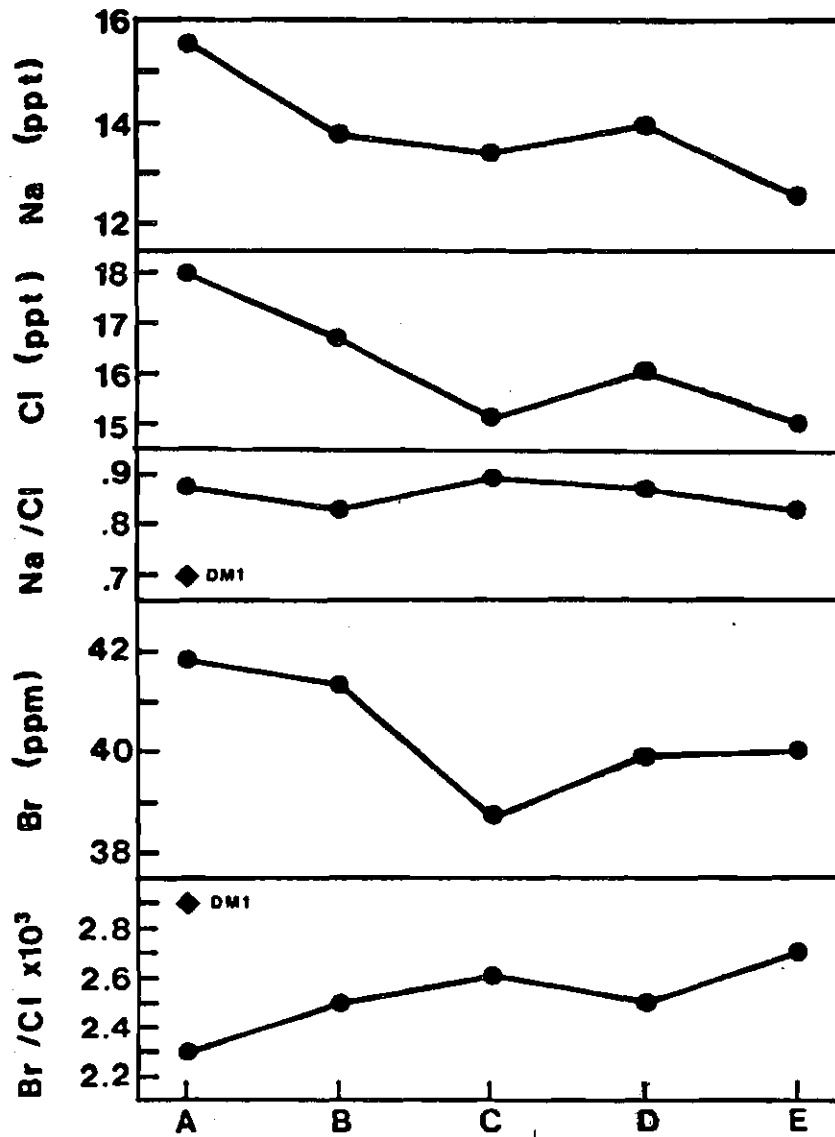


Figure 4. Variations in Na, Cl and Br Determined by Leaching Trimmed Sections of Sample 538. (A = outermost rind, E = central core)

evidence that evaporation has occurred after recovery of the core and prior to analysis.

The second method utilized for the examination of contamination is the analysis of the trace metal chromium, which is frequently added to the drill mud as sodium chromate (Collins, 1975). A value of 13.3 ppm Cr was obtained for drill mud #1 (Table 4) while chromium values from three squeezed samples (Table 3) average 0.3 ppm. This would indicate a <2% contamination of the pore waters by drill mud. However, if the hexavalent chromium from sodium chromate was reduced to trivalent chromium, a decrease in the amount of interstitial chromium would occur due to the high affinity of trivalent chromium for clay exchange positions.

The analyses of total and reducible chromium in the <0.1 μm and 0.1-2 μm fractions of all samples (Table 18) provides evidence for this transfer. All chromium values in both fractions lie in the range 80-130 ppm (total Cr) and 0-10.5 ppm (reducible Cr) except for the sample at 2961 meters which has 261 ppm (<0.1 μm) and 175 ppm (0.1-2 μm) total Cr and 78 ppm (<0.1 μm) and 42 ppm (0.1-2 μm) reducible Cr. From this data it appears that sample 2961 shows the only evidence for contamination by drill fluid. Grain size data (Table 7) provides a possible explanation, as 2961 is the sandiest of the deeper samples.

2. Effects of Squeeze Temperature and Pressure on Pore Water Chemistry

a. Variations in Pressure of Squeezing. The effects of squeeze pressure on pore fluids expelled from clays and shales have been examined by various authors. Chemistry of water expelled during compaction of unconsolidated sediments has been studied by Von Englehardt and Gaida (1963), Hiltabrand, et al., (1973), Chilingarian and Rieke (1973), and Rosenbaum (1976) and will be discussed later. Semi-consolidated sediments have been studied by Manheim (1966), Shiskina (1968), and Russell (1971). These authors agree that squeezing of semi-consolidated sediments ($\phi < 50\%$) up to high pressures has a negligible effect on the resultant chemistry. Shiskina (1968) squeezed a clayey marine sediment up to 3100 Kg/cm^2 ($44,000 \text{ lbs/in}^2$) and a diatomaceous clay up to 1080 Kg/cm^2 ($15,000 \text{ lbs/in}^2$) and found no variations greater than $\pm 0.1\%$ in major ions. In carbonate sediments she found high pressures to promote the dissolution of carbonate. Manheim (1966) examined carbonate rich and clay rich marine sediments at pressures up to 850 Kg/cm^2 ($12,000 \text{ lbs/in}^2$) and found little variation in chloride concentrations ($\pm 0.2\%$). Russell (1971) claims to observe slight freshening of the water expelled from deeply buried Gulf Coast sediments at pressures up to 720 Kg/cm^2 but considers the variations small enough to ignore.

The basis for expecting chemical changes in expelled

water of semi-consolidated sediments is the chemical fractionation which is seen to take place (McKelvey and Milne, 1962; Milne, et al., 1964) when solutions are passed through clay membranes of low porosity. It can be said that non-charged species (H_2S , HCO_3 , H_2O) will migrate more readily through clay membranes while anions are generally retarded (White, 1975). The retardation of anions also promotes retardation of cations as charge balance must be maintained. In general, the larger and/or more positively charged the cation, the greater its retardation should be (White, 1965).

All samples in this study were squeezed at pressures less than 320 Kg/cm^2 (4500 lb/in^2). Two of the samples (390 and 1150II) have enough fluid on squeezing to allow collection of samples representing different squeeze pressures and the investigation of squeeze pressure as a variable (Table 2). All of the ions analyzed have ranges less than $\pm 10\%$ with Na, Ca, Cl and total dissolved species varying less than 5%. Some systematic variations as a result of squeeze pressure are readily apparent. Figure 5 shows the variations among Ca/Na, Mg/Na and K/Na ratios with increasing pressure. Assuming that the initial water squeezed is approximately equal to the pore water composition, an increasing ratio in Figure 5 would imply a greater mobility for the species in the numerator in the ratio. From this figure it can be seen that the mobility (U_x^+) sequence for the major cations is $U_{Mg}^{2+} > U_{Ca}^{2+} > U_{Na}^+ > U_K^+$. This sequence agrees with that

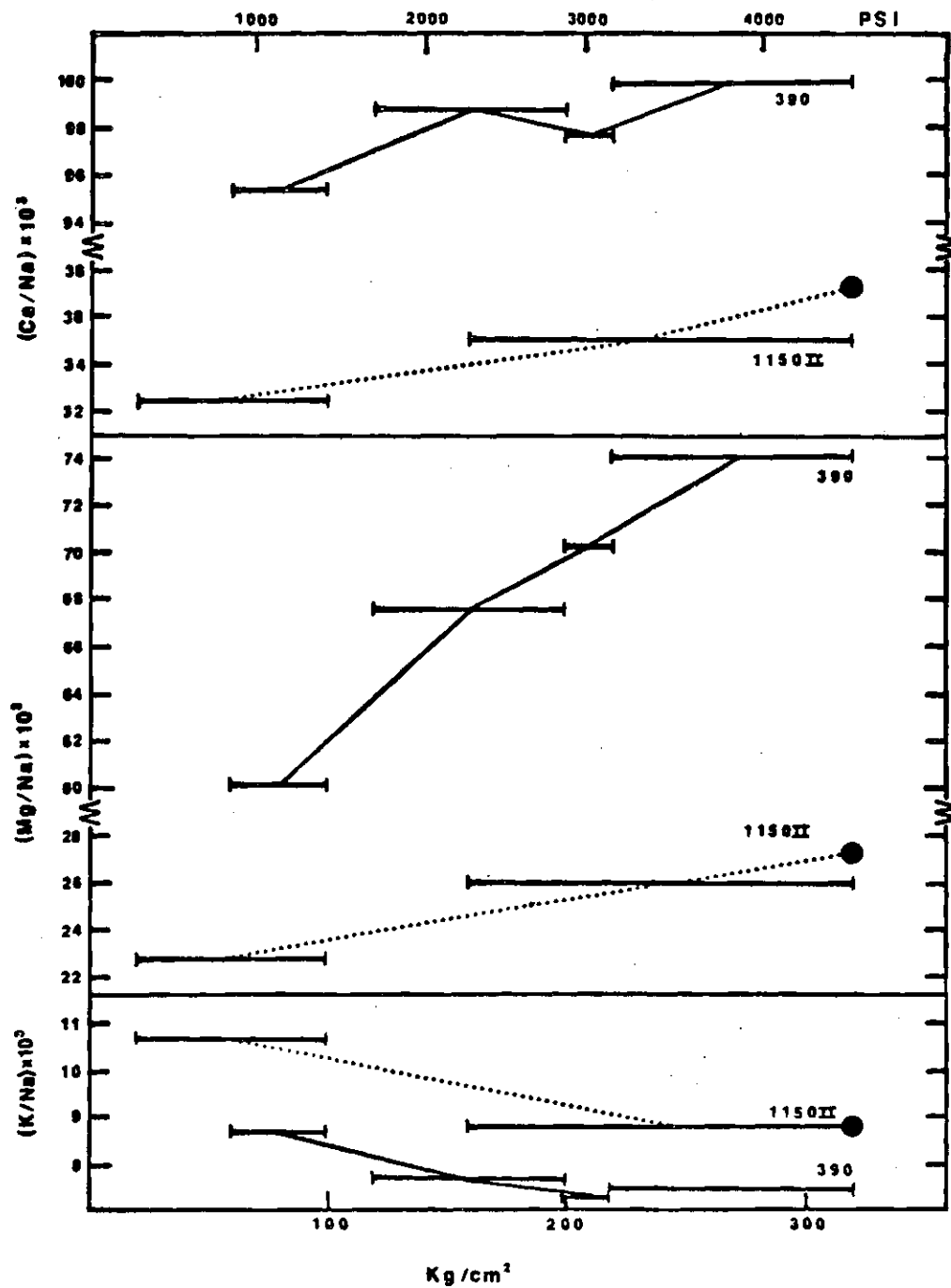


Figure 5. Ratio of Ca, Mg and K to Na for Interstitial Waters Extracted at Different Pressures.

found experimentally (Kharaka and Berry, 1973) for bentonite, illite and shale compacted membranes with sea water flowing through the pores. This greater mobility of divalent cations (the reverse of the expected trend) is attributed by Kharaka and Berry (1973) to the high hydraulic flow of compaction experiments.

The pore water analyses of this study represent the cumulative collection of liquids up to the maximum pressures employed and therefore there may be slight systematic errors between higher porosity (shallow) samples and deeper, less porous samples. Figure 6 is a plot of the cumulative composition of solution expelled with increasing pressure for 390 and 1150II. If one assumes the actual pore water chemistry is that of the initial fluid expelled, then the maximum deviations of ions in the total liquid expelled from the true pore water composition are seen to be relatively small (Figure 6). For most ions the deviation is <5% in either the positive or negative direction with potassium being more severely depleted (10-12%) and magnesium strongly enriched (4.4-7%) in the final liquid. It might be possible to apply corrections to arrive at an approximate original pore water composition; however, it is not important to the developments of this thesis since all samples (being squeezed to approximately the same maximum pressure) should deviate equally from true values thus making pressure induced deviations between samples negligible.

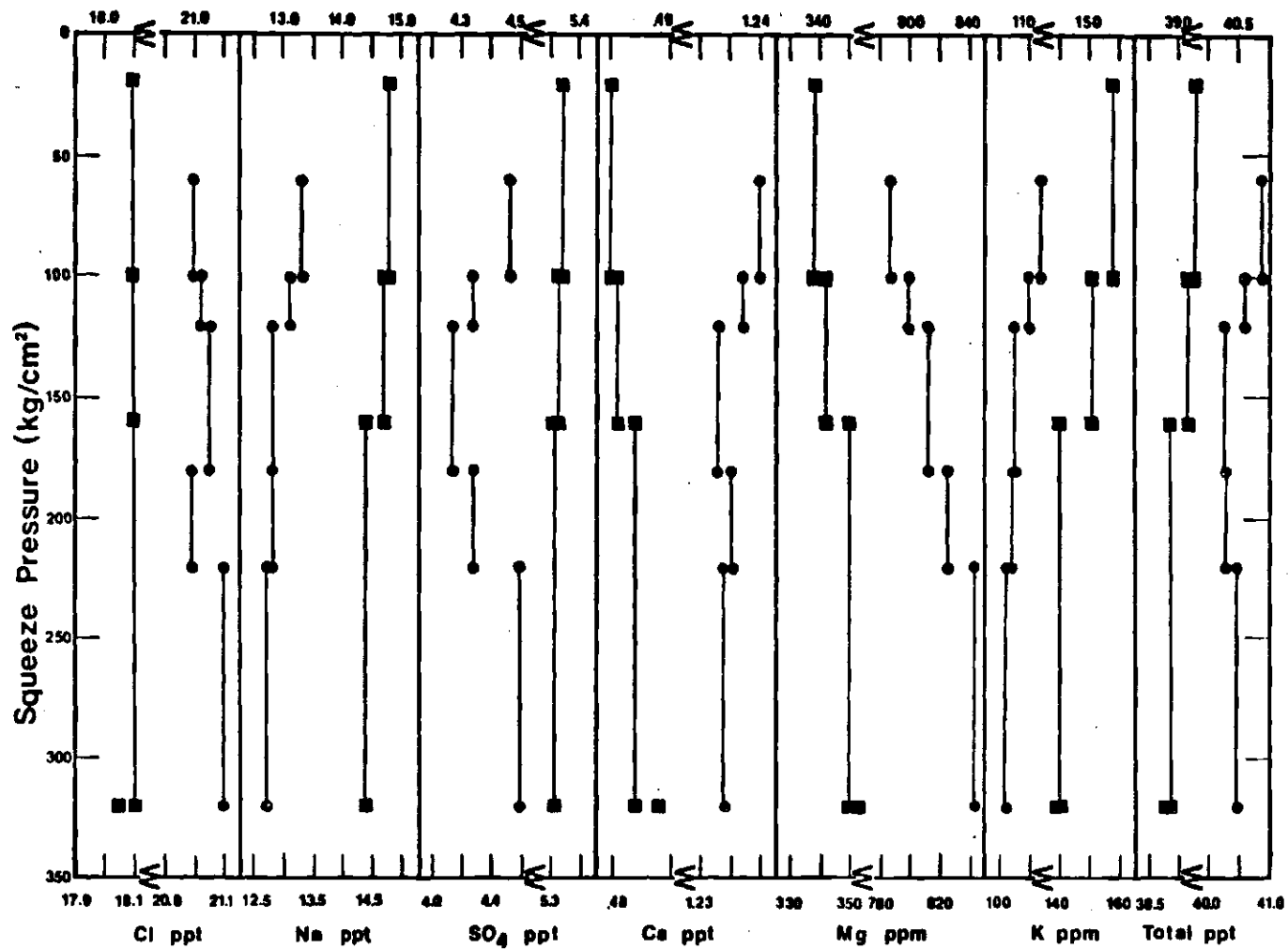


Figure 6. Cumulative Composition of Interstitial Waters Expelled with Increasing Pressure. (■ = 1150 II, ● = 390)

Also of interest in Figure 6 is the cumulative plot of total dissolved solids, which indicates that the final waters squeezed from the samples are slightly fresher than the initial liquid. This observation (also noted by Russell, 1971) will be discussed later, along with the significance of ion mobilities, when the effects of compaction and dewatering of sediments on their pore water compositions are examined.

b. Effects of Temperature of Squeezing. In the process of sidewall recovery, the temperature is altered from that of the in situ sample. Extractions of the samples of this study were performed at ambient laboratory temperatures (25-27°C). From Figure 2 it can be seen that the shallow samples (390-1289) cover an in situ temperature range of 27-47°C while the deep samples (2851-3241) range from 80-100°C. Thus drops in temperature of up to 75°C were experienced prior to squeezing. As the solubilities of most compounds are temperature dependent, this temperature change prior to analysis can be expected to have altered the pore water chemistry. The decreased solubility of many minerals upon lowering of temperature may have resulted in the precipitation of solids during recovery and storage.

Manglesdorf, et al., (1969) demonstrated that an increase in temperature from sea floor (0-5°C) to laboratory (20-25°C) produced an appreciable increase in the potassium concentration (~0.67%/°C) accompanied by a smaller increase

in sodium and a decrease in magnesium in a sample composed of 50% montmorillonite and 50% sea water. They attribute this change to the alteration of clay exchange equilibria with changing temperature such that increases in temperature promote release of K^+ and Na^+ in exchange positions and the absorption of Mg^{2+} . Bischoff, et al., (1970) confirm these observations using a reducing, green, clayey sediment from the Sao Pedro basin. They fail to observe an enrichment on warming for sodium, perhaps due to the swamping effect of the high sodium content of the interstitial water. However, in addition to the decrease in interstitial Mg and increase in K, they report an enrichment upon warming for Cl which they attributed to anion exchange reactions and a depletion in Ca which is consistent with migration of divalent ions to exchange positions on warming. Sayles, et al., (1973a) examined the effects of warming on major and minor elements of the interstitial waters of a number of oceanic sediments. They found general enrichments in interstitial K and Na and depletions in Ca, Mg and Sr which they also attribute to an increased affinity for divalent ions in exchange positions at higher temperatures. The percentage change in the interstitial water content for K was the largest of those observed at $-1\%/^{\circ}C$ for clays and marls. No apparent changes were observed for Li, Cl and SO_4 in their analyses, while large enrichments of interstitial B and SiO_2 were observed in most samples. The increase in interstitial silica on warming has also been observed by Fanning and Pilson (1971) in water

obtained by squeezing a foraminiferal lutite with 30-40% CaCO_3 . They attribute this increase on heating to increased solubility of silica compounds. Fanning and Pilson observed no changes in interstitial salinity, alkalinity or phosphate content, while warming produced a slight pH increase in their experiment.

For analysis of near surface ocean sediments an in situ water extraction mechanism has been developed (Sayles, et al., 1973b), but this device is not suited to the extraction of waters from deeply buried sediments. Instead of in situ extraction, most authors recommend re-equilibration and squeezing at in situ temperatures (Sayles, et al., 1973a; Horowitz, et al., 1973; Geiskies, 1974), although the reversibility of temperature induced trends has not been established (Bischoff, et al., 1970). In fact, experiments performed by Hulbert and Brindle (1975) indicate that the temperature effects and effects of storage and handling exhibit a more complex behavior. As in the above mentioned studies, they found that, upon warming, their Gulf of Mexico abyssal sediments (5-8°C in situ) to 20-22°C, enrichments of interstitial K and perhaps Na and depletions of Ca and Mg occurred. However, storage and squeezing at 5°C did not eliminate these effects. Surprisingly, storage at 22°C and re-equilibration to 5°C prior to squeezing resulted in a closer approximation of the original composition (determined by squeezing at in situ temperature at site). Hulbert and Brindle recommend standardization of storage procedures

as a method of detecting relative differences in ion concentrations between samples when in situ extraction is not possible.

Thus far the discussion has concerned temperature effects resulting from increases in sample temperature from sea floor (0-5°C) to laboratory (20-25°C). The samples of this study, however, were subject to temperature drops of up to 75°C. The continuation of observed trends to higher temperatures must be established in order to fully interpret the effect of temperature changes on interstitial water contents of the samples studied here. Russell and Fallgatter (1972) equilibrated a Gulf Coast mud with an artificial brine and squeezed it ($P_{\max} = 720 \text{ Kg/in}^2$) at various temperatures (up to 91.3°C) (Figure 7). They note that, with increasing temperature, K and HCO_3 increase markedly, while pH, Mg and Cl decrease. Ca and SO_4 show a marked depletion at 51°C and then increase again. The complex behavior of these two species during pressure variations (Figure 6) as well as temperature variations cannot be adequately explained at this time. The magnitude of enrichment for potassium ($\sim 0.7\%/^\circ\text{C}$) is consistent with that observed in ocean bottom sediments, however the K increase is not linear. At low temperatures, Figure 7 shows a rate of K increase of $0.24\%/^\circ\text{C}$ and at higher temperatures it reaches $1.2\%/^\circ\text{C}$. The direction of trends shown by Russell and Fallgatter (1972) are also consistent with deep sea samples for Ca, Mg, and Na.

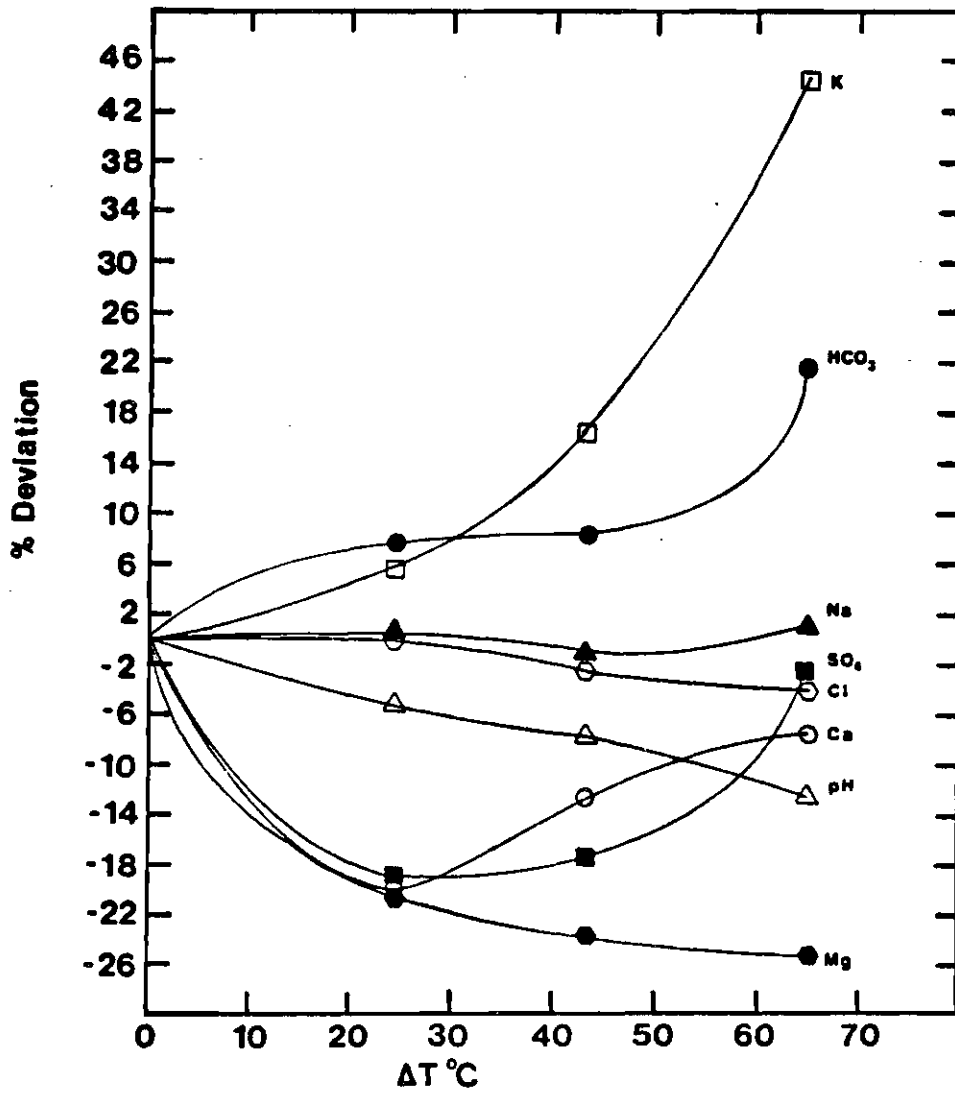


Figure 7. Deviation of Squeezed Pore Water Chemistry with Changes in Extraction Temperature. (from the data of Russell and Fallgatter (1972))

Combining the results of investigations of temperature of squeezing, it is possible to conclude that for pelitic sediments in the range of 0-100°C:

1. The effects of temperature of squeezing on the interstitial abundances of Na, Cl, Li and total ions are small enough (<5%/100°C) to be ignored.
2. Temperature effects for SO_4 , Ca, HCO_3 and pH are larger but are poorly defined. Corrections for these errors will not be attempted. The relative temperature induced errors should be <10% within the shallow sample group or the deep sample group, and the absolute error should be similarly small for the shallow samples. Absolute errors for the deep samples, especially for HCO_3 determinations, may be somewhat higher.
3. Temperature effects for K and Mg are large and systematic (Figure 7). Relative errors within the two sample groups could be as large as 30% for K and 15% for Mg, while absolute errors may reach 60% for K and 26% for Mg (Russell and Fallgatter, 1972). Assuming reversibility of the temperature induced K and Mg changes it is possible to correct the laboratory determined concentrations of this study to original in situ K and Mg contents. The in situ temperature of each sample can be determined from Figure 2 and subtracting the laboratory temperature

(-26°C) to give the change in temperature. Figure 7 can then be used to determine the correction necessary to convert determined values (Table 1) to in situ concentration. Using the laboratory determined interstitial water K and Mg concentrations for each sample the corrected K and Mg concentrations can be calculated (Table 19).

4. Temperature effects for SiO₂ and B are quite large with warming providing ~2.5%/°C enrichments of the interstitial solutions. However, this data is derived only from lower temperature studies. In this study a different temperature range is involved, so precise interpretation and correction for the temperature effect is impossible. Maximum increases should be less than 200%.

3. Effects of and Correction for Evaporation Prior to Squeezing

The sequential leach of sample 538 suggests that evaporation in the outermost layers of the cores, during storage, may have occurred. The samples from well 2 were all wrapped in plastic film and aluminum foil while those from well A4 were not wrapped prior to storage in jars. This would promote greater evaporation in the A4 samples. In addition to this, the length of storage time prior to squeezing varied from 3 to 64 days and could also be expected to control the degree of evaporation prior to squeezing. Figure 8 is a plot of the chloride content of the squeezed pore waters (from Table 1)

Table 19. Temperature Corrections for K and Mg in Squeeze Pore Waters

Depth (meters)	T°C in situ	ppm K Squeezed	K Correction %*	ppm K Corrected	ppm Mg Squeezed	Mg Correction %*	ppm Mg Corrected
390	27	102	+0.1	102	840	-3.8	810
538 I	30	130	+0.3	130	415	-9.1	380
538 II	30	110	+0.3	110	397	-9.1	360
692	34	198	+1.1	200	1625	-13.1	1410
844	37	180	+1.5	183	1490	-15.1	1270
1000	40	128	+2.3	131	662	-16.8	550
1150 I	43	110	+3.2	114	275	-18.2	240
1150 II	43	139	+3.2	143	353	-18.2	290
1289	46	135	+4.1	141	594	-19.3	480
2851	79	183	+27.	232	--		--
2906	82	87	+31.	114	37.6	-25.1	28.2
2961	85	102	+35.	140	45.0	-25.3	33.6
3007	87	98	+38.	135	30.0	-25.4	22.4
3038	88	125	+40.	175	68.8	-25.4	51.4
3064	90	119	+43.	170	33.8	-25.5	25.2
3074	90	78	+43.	112	52.0	-25.5	38.7
3164	94	65	+51.	98	32.0	-25.6	23.8
3242	98	295	+59.	470	59.0	-25.6	43.9

*From Figure 7 (squeeze T \cong 26°C).

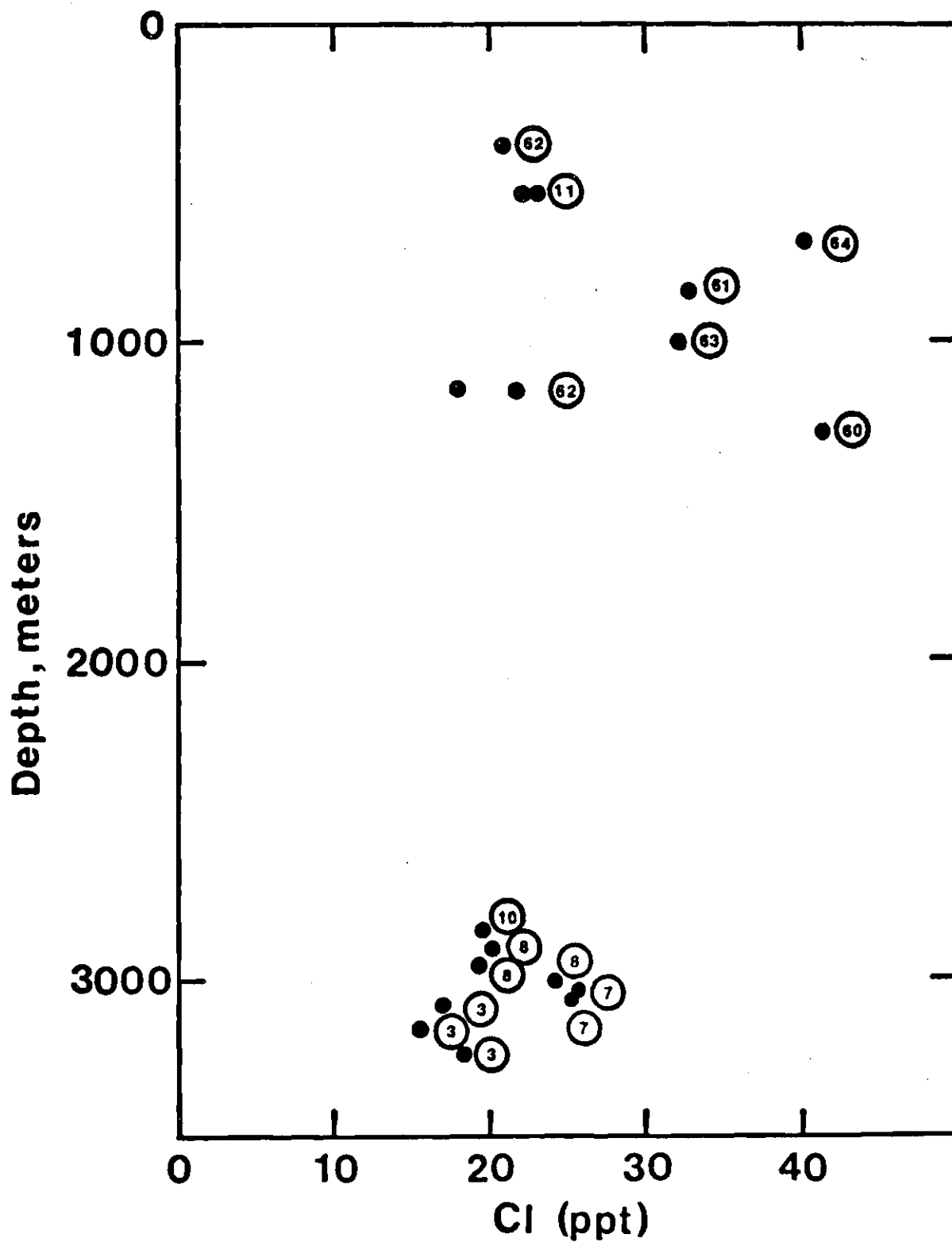


Figure 8. Uncorrected Chloride Content of Squeezed Pore Waters. (Circled numbers represent time in days from core recovery to squeezing.)

against depth with the circled number after each point representing the lag time in days. As would be expected, if some of the samples were not completely sealed during storage, all of the samples with Cl >30 ppt have lag times ≥ 60 days. The two samples, 844 and 1289, which show evidence of gypsum precipitation in the outermost layers (which were trimmed prior to squeezing) both had lag times ≥ 60 days and Cl contents >30 ppt. The presence of gypsum in the outermost portions of samples which appear, on the basis of lag times and chloride contents, to be highly evaporated; indicates that gypsum precipitation was caused by evaporation in these two samples. It is also possible that decreased gypsum solubility, due to the temperature drop experienced by the cores, is a factor as well.

Thus the evaporation of pore waters during storage can result not only in the straightforward concentration of ions in solution which would leave the ion ratios constant, but also in the alteration of solid:aqueous equilibria and the transfer of ions between solid and liquid phases. This aqueous:solid transfer can be due either to precipitation of a mineral which has become supersaturated during evaporation (i. e., gypsum, CaCO_3 , SiO_2) or to the alteration of equilibria controlling exchange ion populations, and will result in changes in ion ratios during evaporation. The fact that gypsum precipitation has occurred in the outermost portions of some cores, does not necessarily mean that this precipitation

has affected the inner portions (those squeezed), however the possibility of gypsum precipitation during evaporation or cooling warrants further investigation.

Assuming sea water activity coefficients and degrees of complexation (Berner, 1971) it is possible to calculate ion activity products $(Ca^{2+}) \cdot (SO_4^{2-})$ using the data from Table 1. Five of the samples (390, 692, 844, 1289 and 2851) have ion activity products between $10^{-4.5}$ - $10^{-5.0}$ (solubility product for gypsum is $10^{-4.6}$). Two of these samples (844 and 1289) are the samples which showed gypsum precipitation in the outermost layers and four of the five have lag times of ≥ 60 days. All samples other than these five can thus be considered free from gypsum precipitation in the squeezed sample while the case for the above five is less clear.

The extent of alteration of those samples suspected of gypsum precipitation can be examined by plotting the Ca/Cl ratio vs. depth (Figure 9) using the data from Table 1. The separate, straight line relationships apparent for the shallow and the deep samples probably represent depth related trends. The largest deviation from these trends is shown by sample 538 which, as is seen in Table 7, is by far the most sandy sample of this study. As post recovery evaporation is not depth dependent one would expect to see deviations from the depth related trends if evaporation has caused significant precipitation of gypsum (or calcite). Of all the samples likely to be affected by evaporative precipitation only one of these

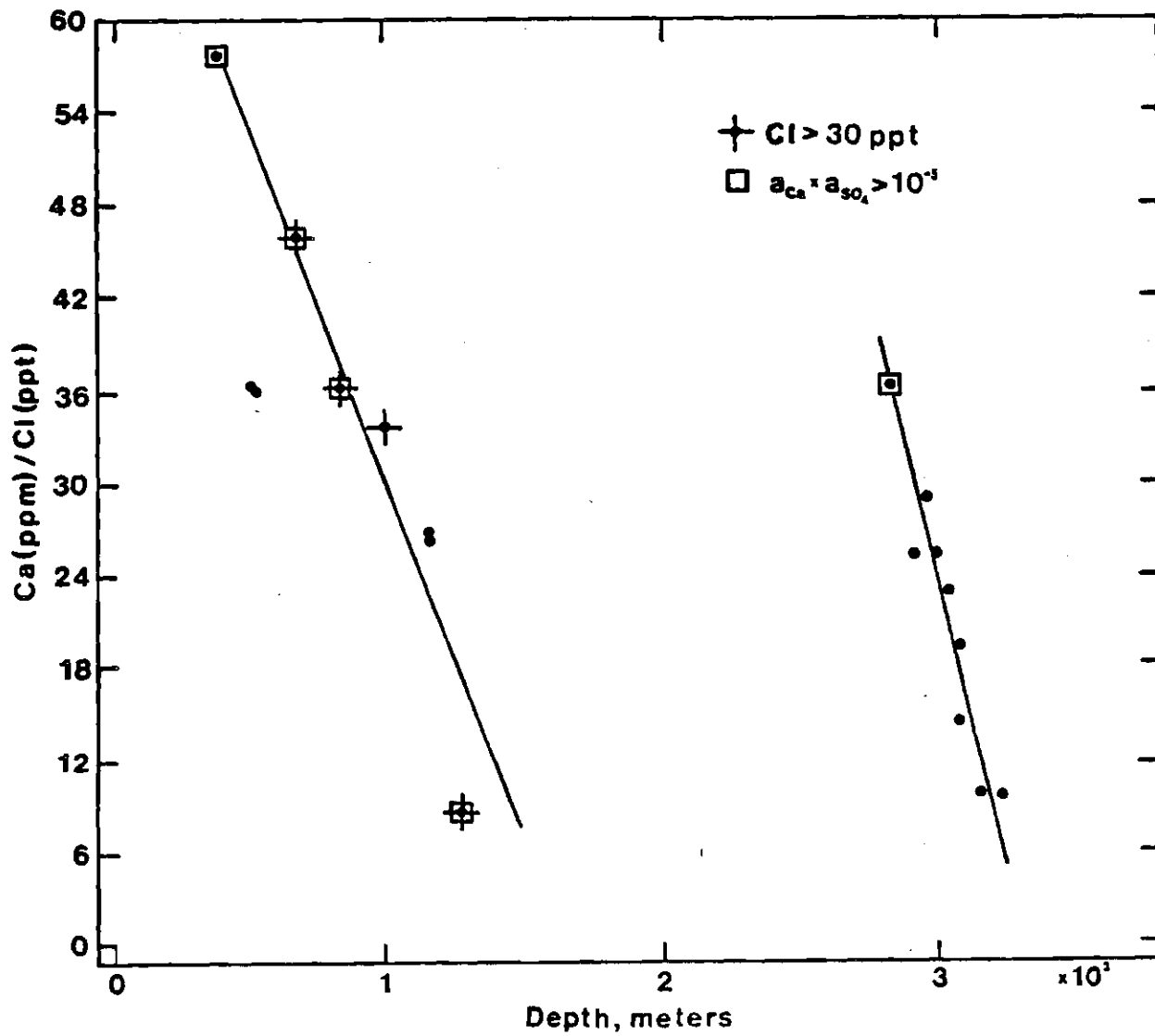


Figure 9. Variation of the Ca to Cl Ratio with Depth for Squeezed Samples.

(1289) has a Ca/Cl ratio that is appreciably lower than that which might be expected if the Ca/Cl ratio were truly depth dependent. Therefore, sample 1289 can be considered the only sample that is likely to be altered appreciably by evaporative precipitation.

Evaporation will also possibly cause alteration of equilibria between the pore waters and silicate minerals. The effect of evaporation on silica (and boron) contents is not clear, although in general increased evaporation should promote silica precipitation. The effect of evaporation on exchange ion populations should be relatively small as evaporation increases salinity, activities and complexation while exchange ion populations depend primarily on ion activity ratios which should remain fairly constant. Increased pore water salinity will tend to decrease the selectivity of exchange positions for divalent cations (Stumm and Morgan, 1970), however this effect will only be significant if the original pore water concentrations are considerably less than those of sea water.

The amount of evaporative loss during core storage can be estimated by comparing pore water content of the core determined prior to squeezing, with in situ porosities determined from acoustic well logs. Sonic travel times (Δt in μ sec/ft) from the acoustic log can be related to the formation porosity by the equation:

$$\phi = \frac{\Delta t_{\log} - \Delta t_{\text{matrix}}}{\Delta t_{\text{fluid}} - \Delta t_{\text{matrix}}} \cdot C_p \quad \text{Eq. 1} \quad (\text{Schlumberger, 1958, 1972})$$

where ϕ = porosity

Δt_{\log} = formation travel time

Δt_{matrix} = solid material travel time

Δt_{fluid} = pore fluid travel time

C_p = correction factor for shale content

This equation can be applied to the determination of the porosity of reservoir rocks that are of uniform porosity and free from shale where $C_p = 1$. Magara (1968) found a linear relationship between porosity and Δt_{\log} for mudstones from the Negato Plain, Miocene of Japan. This line can be described by Eq. 1 (using values of $\Delta t_{\text{matrix}} = 60 \mu\text{sec/foot}$, $\Delta t_{\text{liquid}} = 180 \mu \text{ sec/foot}$ and $C_p = 1.6$) and will be used here (Figure 10) as an estimate of the in situ porosity, Δt relationship.

Weight loss on air drying of a sub-sample taken prior to squeezing of the main sample (% P. W.) is used here as a measure of the percent by weight pore water. It is likely that a few percent pore water remains behind on room temperature drying, however at higher temperatures structural water loss may occur. Percent P. W. is converted to porosity using:

$$\phi = P_g / [P_f \left(\frac{1}{0.01 \cdot (\% \text{ P. W.})} - 1 \right) + P_g] \quad \text{Eq. 2}$$

where p_g = grain density = 2.65 g/cc

p_f = fluid density = 1.02 g/cc

ϕ = fractional porosity.

This porosity, determined for each sample (except for 1150 II and 2851 for which no % P. W. value was obtained) is plotted on Figure 10 against the Δt_{10g} using the average Δt for a five foot interval bracketing the sample depth.

As would be expected, it can be seen from Figure 10 that most of the samples are lower in porosity than the value expected from the empirical in situ data. In fact, the only sample which plots appreciably higher is 2961, which, as was shown earlier, is contaminated with drill mud and therefore can be ignored. If it is assumed that all samples which plot below the line do so because of evaporation, then it is possible to obtain the in situ porosities of the samples by using Magara's relationship and the acoustic log values of Δt .

Table 20 gives the laboratory determined fraction pore water by weight, porosities, the Δt_{10g} values and the in situ porosities and fractions of pore H_2O determined from Figure 10 as well as the evaporation correction factor (F_{H_2O} lab/ F_{H_2O} in situ). This correction factor, when multiplied by the pore water chemistry data of Table 1 (Table 19 for K and Mg after temperature correction) gives the pore water concentrations of the original unevaporated sample (Table 21) assuming no evaporative precipitation has occurred. Samples 1150 II, 2851 and 2961 are excluded from Table 21 for reasons stated

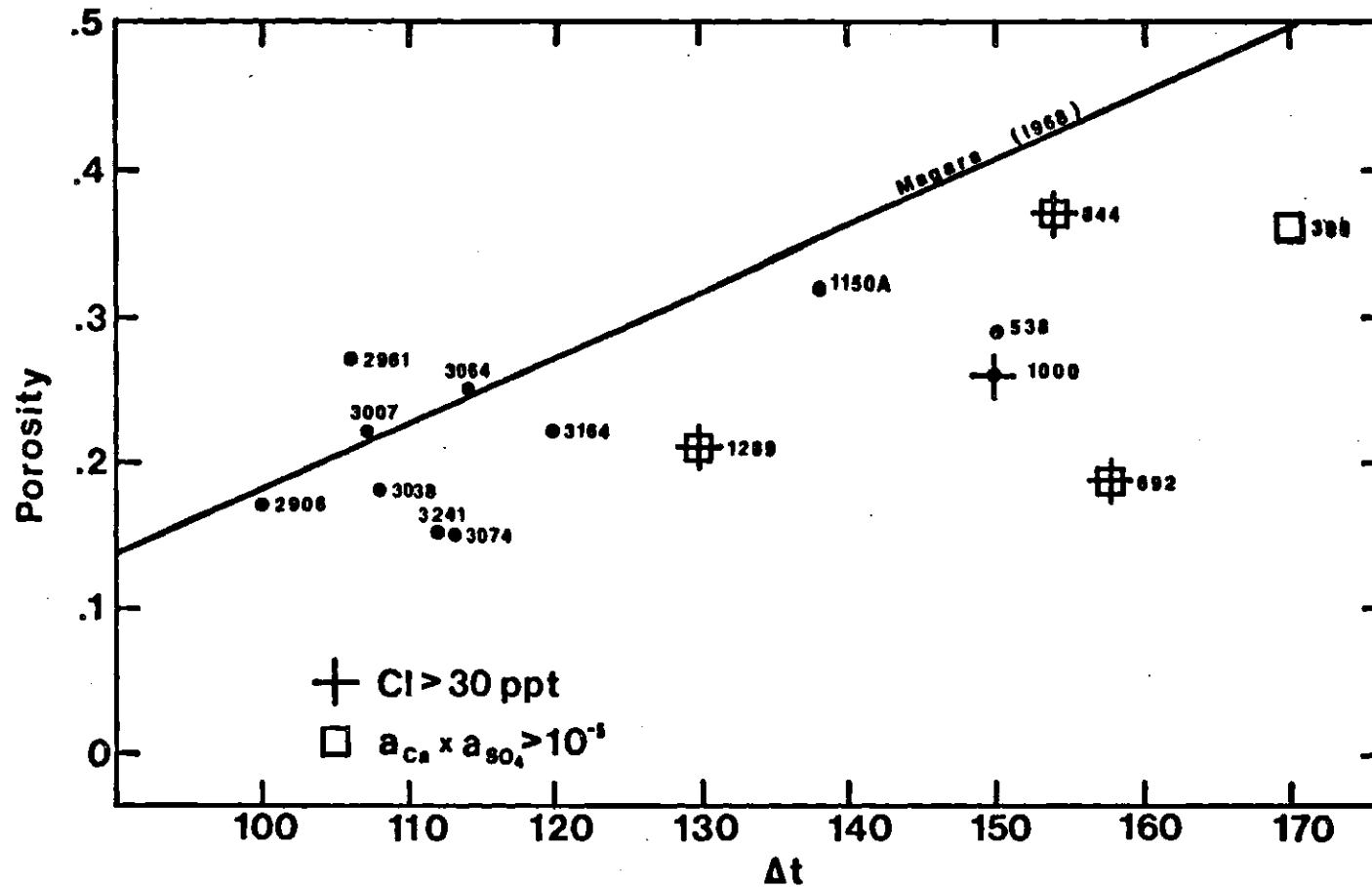


Figure 10. Porosity vs. Acoustic Travel Time for Cores Studied, Relative to In Situ Relationship of Magara (1968).

Table 20. Extent of Evaporation During Transportation and Storage.

Depth (meters)	F Pore H ₂ O (laboratory) (1)	φ (porosity) (laboratory)	Interval Transit Time μsec/ft (2)	In Situ φ (porosity) (3)	In Situ F Pore H ₂ O	Evaporation Factor (4)
390	.177	.36	170	.50	.274	.65
538	.133	.29	150	.40	.201	.65
692	.080	.19	158	.44	.230	.35
844	.179	.37	154	.43	.220	.80
1000	.115	.26	150	.40	.200	.60
1150 I	.148	.32	138	.35	.170	.90
1289	.091	.21	130	.32	.150	.60
2851	--	--	107	.22	.095	--
2906	.072	.17	100	.18	.076	.95
2961	.122	.27	106	--	--	--
3007	.095	.22	107	.22	.095	1.00
3038	.077	.18	108	.22	.095	.80
3064	.110	.25	114	.25	.110	1.00
3074	.063	.15	113	.24	.106	.60
3164	.098	.22	120	.27	.122	.80
3242	.064	.15	112	.24	.106	.60

(1) Table 1

(2) From well logs (5' interval around sidewall core)

(3) Estimated from Figure 10

(4) Evaporation factor = F pore H₂O (lab)/F pore H₂O (in situ)

Table 21. Pore Water Chemistry of Squeezed Cores, Corrected for Evaporation.

Depth (meters)	In Situ % Pore Water	Cl ppt	SO ₄ ppm	HCO ₃ ppm	Organic Carbon ppm	Na ppt	K ppm*	Mg ppm*	Ca ppm	Br ppm	F ppm	B ppm	SiO ₂ ppm
390	27	14.0	2900	130	20	8.3	66	530	800	7.	0.2	0.2	4.7
538 (avg)	20	15.0	1400	--	--	9.0	78	240	530	37.	0.6	0.3	1.6
692	23	14.0	1400	--	--	7.9	70	490	660	4.	--	0.3	1.2
844	22	26.0	5200	--	--	16.0	150	1000	950	7.	--	1.7	--
1000	20	19.0	700	70	30	12.0	79	330	660	22.	0.5	0.6	1.3
1150 I	17	19.0	3500	100	50	14.0	103	220	530	16.	0.8	0.9	2.4
1289	15	25.0	4400	--	--	23.0	85	290	230	--	--	--	--
2906	7.6	19.0	5200	660	700	15.0	108	27	500	13.	--	0.9	2.4
3007	9.5	24.0	4900	--	--	18.0	135	22	620	8.	--	1.1	2.7
3038	9.5	20.0	4600	40	270	15.0	140	41	480	--	--	--	--
3064	11.0	25.0	5300	--	--	19.0	170	25	510	6.	--	--	--
3074	10.6	10.0	4400	--	--	7.4	67	23	160	--	--	--	1.7
3164	12.2	12.0	7800	--	--	11.0	78	19	130	--	--	--	--
3242	10.6	11.0	--	--	--	9.0	280	26	110	--	--	--	--

*Corrected for temperature.

above.

The errors involved in this calculation are difficult to assess quantitatively. Based on duplicate measurements of weight loss on drying, the laboratory water values are reproducible to within $\pm 5\%$. Travel times determined from 5' sections bracketing the cored depth represent the average travel time for that section to within $\pm 2 \mu\text{sec}/\text{ft}$ although the interval cored may not represent the average material of that section. Using the shale travel times from the acoustic logs and Magara's ϕ vs. travel time relationship it is possible to determine porosity vs. depth and bulk density vs. depth profiles that are consistent with other data from the Gulf Coast (Dickenson, 1953; Kerr and Barrington, 1961; Eaton, 1969; Schmidt, 1973). Assuming a similar error range for the in situ line as was estimated for the laboratory determined porosities and Δt_{log} values of the samples of this study, results in an error range for the evaporation correction factor of about $\pm 10\%$. However, the possibility of errors not included in this estimate is relatively high, therefore these corrected data will only be employed when ion ratios are insufficient.

4. Comparison of Squeezing and Leaching Methods of Pore Water Recovery

An alternative method employed for pore water analysis (Schmidt, 1971; Weaver and Beck, 1971) involves leaching a sample containing a determined mass of pore water, with a known amount of distilled water or other solution. The original

pore water chemistry is determined by analysis of the leach solution and correction for dilution assuming little or no interaction with air or solid during leaching. Murthy and Farrell (1972) state that a series of leaches, of different leach liquid:pore water ratios, performed on the sample allows extrapolation to a non-leached, original pore water chemistry that is more precise than that determined by squeezing. However, the problems they attribute to the squeezing technique are either of little importance (i. e., pressure of squeeze variations) or will be present in both squeeze and leach procedures (i. e., temperature variations, evaporation); and the accuracy of the extrapolation they perform depends on the linearity of solid-aqueous interrelations during leaching. In fact, this work provides a framework for the discussion and correction of errors encountered during squeeze analysis while the dissolution of solids and the alteration of exchange equilibria during leaching are much more difficult to quantify. As the work of Weaver and Beck (1971) and Schmidt (1973) represent most of the pore water data from deeply buried pelitic sediments, and their data were obtained with constant dilution factor leaching techniques, an examination of some of the samples of this study by leaching was performed.

Five cores (Table 5) were leached using approximately a 1:25 (pore water:leach water) dilution. Four of these samples (538, 2906, 3007 and 3064) were semi-homogenized

splits of samples that were also squeezed, while the fifth (2961b) was a separate core, taken adjacent to the core squeezed (2961, Table 1). Table 22 shows the squeeze/leach concentration ratios for the four duplicate samples (from Tables 1 and 5) along with the squeeze/leach ratios determined by Murthy and Farrell (1972) for shallow Gulf Coast muds using a 1:10 (pore water:leach water) dilution. A squeeze/leach ratio of less than one, as shown by HCO_3 , B, SiO_2 , organic carbon, K and Br is indicative of elements being released to the liquid from solid phases (or from the atmosphere in the case of HCO_3) upon leaching. Ca and Mg show squeeze/leach ratios significantly greater than one, while variations for SO_4 , Na and Cl average to within 20% of unity. As discussed earlier, large errors are possible in equating weight loss on room temperature drying with percent pore water. This may account for some of the deviation in the SO_4 , Na and Cl values. However, the systematic nature of the slight SO_4 and Na enrichments and Cl depletions in the leach determinations indicate that inaccurate pore water determinations are not the only factor contributing to these squeeze/leach differences.

The variation in the major cations (Ca and Mg loss and Na and K gain in the leach determinations) are consistent with an increase in selectivity of the clay exchange sites for divalent cations due to the reduction in interstitial salinity upon leaching. This is predicted by the double layer theory of ion exchange in clays (Stumm and Morgan, 1970).

Table 22. Ratio of Squeeze/Leach Determined Pore Water Chemistries.

Sample	Cl	SO ₄	HCO ₃	OC*	Na	K	Mg	Ca	Br	F	B	SiO ₂
538	0.96	0.79	--	--	0.83	0.60	13.8	12.6	0.90	0.06	0.03	0.02
2906	1.00	0.57	.02	.38	0.59	0.32	0.7	5.9	0.10	--	0.02	0.02
3007	1.35	1.13	--	--	0.81	0.54	0.8	7.9	0.13	--	0.02	0.02
3064	1.49	0.76	--	--	0.87	0.66	1.0	7.7	0.31	--	--	--
Average	1.20	0.81	.02	.38	0.78	0.52	4.1	8.5	0.36	0.06	0.02	0.02
Murthey And Farrell (1972)	--	--	--	--	0.89	0.45	1.7	1.5	--	--	--	--

*OC = Organic Carbon.

Boron, silica and organic carbon increases during leaching are caused by dissolution of solid (or suspension of colloidal) material. HCO_3 increases in leach determinations may be due in part to CaCO_3 dissolution but organic decomposition or atmospheric CO_2 absorption are probably more important. The causes of Cl, SO_4 and Br variations are not clear. Alteration of anion exchange equilibria may be important.

Due to the complexity of the reactions involved, it is necessary for leaching techniques to be rigidly standardized with regard to dilution factors and duration of leaching, in order to obtain consistent results. Even then, these analyses will not only represent interstitial water content but will also reflect aqueous:solid interactions initiated by the leaching process.

CHAPTER V

DISCUSSION B

Mineralogic and Chemical Variations
During Gulf Coast Burial Diagenesis1. The Occurrence and Recognition of Non-Diagenetic, Mineralogic Variations

The mineral suite that is observed in a sediment sequence is the result of a long history of processes involving weathering, transportation, deposition, and burial. Chemical and mineralogic transformations and segregations may occur during all of these stages. The recognition of changes, in vertical sediment sequences, which are non-diagenetic in nature is an important step toward describing diagenetic variations. In particular, the Gulf Coast consists of many sedimentary provinces containing various amounts of the common sedimentary minerals. A large vertical sequence of sediments will consist of sediments from a number of different sources deposited in a variety of environments.

A pertinent example of the large degree of variation possible with varying sedimentary province is the areal distribution of the illite/smectite ratio in $<2 \mu\text{m}$ clays from surface sediments in the Gulf of Mexico (Figure 11). This figure is compiled from the data of Pinsak and Murray (1960) (75 samples) and Devine, et al., (1973) (48 samples) using

their 17 A and 10 A peak heights and dividing the 17 A peak height by 3 to equate peak intensity with clay content. This experimentally determined correction factor was used by Pinsak and Murray (1960) in calculating clay contents, while Devine, et al., (1972) used a theoretically determined correction factor of 8, necessitating correction of their clay analyses to allow comparison of the two sets of data. The data of these two studies, upon correction, are found to agree favorably, both in comparison of nearby samples and in the average Gulf Coast illite/smectite ratio (0.75; Pinsak and Murray (1960) and 0.67; Devine, et al., (1973)).

Figure 11 shows a number of interesting features. The most noticeable include:

1. Large scale variations in the ratio for the entire Gulf (<0.5 - >2.0) as well as the northwestern Gulf (<0.5-1.5),
2. Major illite concentrations on the Yucatan and Florida carbonate platforms,
3. Major smectite sources in the Mississippi and northwest Gulf rivers,
4. A general increase in smectite in the deep Gulf, and
5. Several narrow, illite rich, zones in close proximity to the Mississippi delta.

From the above example, it is obvious that even the most pertinent diagenetic indicator, the illite/smectite ratio, may show large variations in vertical sequences that could be

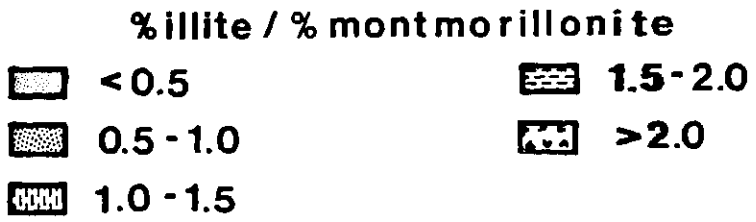
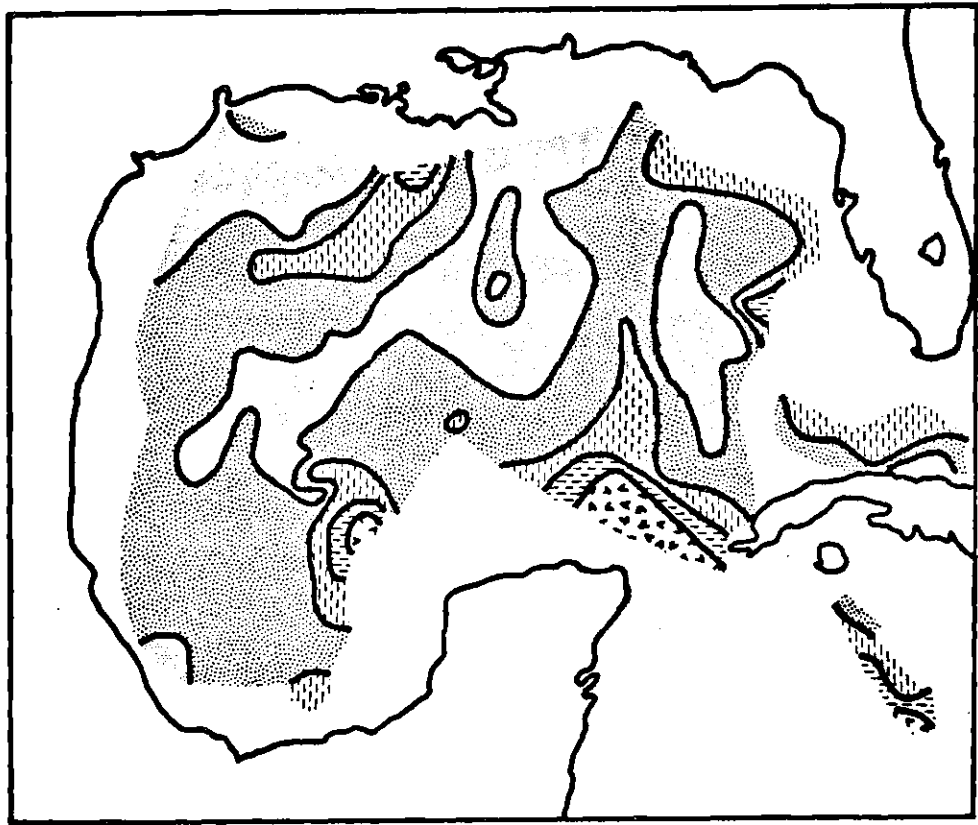


Figure 11. Illite/Montmorillonite Ratio in Gulf of Mexico <2 μm Surface Sediments. (from the data of Pinsak and Murray (1960) and Devine, et al., (1973))

entirely due to changes in the material deposited rather than diagenesis. Thus, care must be exercised when examining sedimentary sequences, so that non-diagenetic variations are not interpreted as diagenetic. One criterion helpful in recognizing non-diagenetic transformations will be the presence of abrupt chemical or mineralogic changes, occurring over a short interval and/or coinciding with unit or facies boundaries. Much of the scatter in various component vs. depth trends can probably be attributed to small scale variations in source material or environment of deposition. On the other hand, smooth transformations, occurring over an extended vertical range, regardless of facies and unit boundaries, would suggest diagenesis. The recognition of similar transformations occurring in different regions at similar temperatures and pressures would also be indicative of diagenesis.

2. Mineralogy of the Sidewall Cores and Relation to Burial Diagenesis

Phyllosilicates are present in all of the size fractions studied. The coarse (2-44 μm and $>44 \mu\text{m}$) fractions, consisting primarily of quartz, were examined by microscope ($>44 \mu\text{m}$ only) and X-ray diffraction (2-44 μm and $>44 \mu\text{m}$). Most coarse fractions contain small amounts of detrital mica. Chlorite and glauconite were observed in grain mounts of some samples. Many of the samples contain clay clasts. These clasts, which resisted disaggregation by sonification, increase in frequency in the deeper samples. The $>44 \mu\text{m}$ fraction of samples 2961

and 3007 have abundant clasts, up to 1 cm in length, which are cemented by silica. Calcium carbonate is present in most 2-44 μm and $>44 \mu\text{m}$ samples, increases with depth, and is particularly abundant in the deepest sample (3242). In most samples, shell fragments (especially 1150) and foraminifera (especially 3074 and 3164) make up much of the CaCO_3 while in sample 3242, the abundant carbonate is mainly in the form of grains and cement with few foraminifera. Dolomite is present in minor amounts in the shallow sample coarse fractions but is undetected in the deeper samples with the exception of 3242 where it is less abundant than calcite. Pyrite, present in most coarse fractions, increases with depth. In the $>44 \mu\text{m}$ fraction pyrite is present as small ($<0.2 \text{ mm}$) nodules and fillings in foraminifera. Samples 3074 and 3164 contain abundant pyrite in these forms. Several feldspars were identified in the coarse fractions of all samples, however no depth related trends are observed. Siderite was tentatively identified on the basis of the peak at 2.79 A ($\text{CuK}\alpha$), however secondary peaks are either masked or too small to use to substantiate the identification. If present, siderite increases in the deepest samples. Barite is present in the coarse fractions of a few of the deepest samples (3007 and 3164). This cannot be due to contamination as barite was not used in the drill mud. A series of broad reflections occur from coarse fraction powder packs between 12° and $18^\circ 2\theta$ ($7.4\text{-}4.9\text{A CuK}\alpha$). These are believed to be indicative of intermediate stages in silica

diagenesis (Mizutani, 1970) and will be discussed later.

Clay minerals of the 2-44 μm fraction, which comprise <25% of these fractions, were estimated from X-ray patterns. The small 001 clay reflections obtained from oriented slides and the presence of halloysite? and expanded chlorite in some of the samples make accurate determination of clay percentages (particularly relative proportions of 17 A and 10 A layers in the mixed layer clay) difficult. Illite in the 2-44 μm fraction can be seen to decrease (from ~62 to 41% of total clay in 2-44 μm) while mixed layer illite/smectite (18% shallow, 28% deep), kaolinite (12% shallow, 19% deep) and chlorite (7% shallow, 10% deep) increase.

The 0.1-2 μm fraction is almost entirely clay minerals although sample 3242 contains some CaCO_3 and all 0.1-2 μm samples contain <10% quartz. Clay distribution in the 0.1-2 μm fractions is shown in Figure 12. There is no systematic variation in the chlorite content (5% average) of the 0.1-2 μm clay. Kaolinite shows a systematic increase with depth in the shallow samples (from 13-23%) and a decrease in the deep samples (from 18-12%). The 2:1 clays of this fraction are shown in X-ray patterns to consist of discrete illite (10 A 001) and a mixed layer illite/smectite (17 A 001, <5.67 A 003). Normalizing the 0.1-2 μm clay mineralogy to 100% 2:1 clays allows the calculation of average 2:1 clay distributions of: Shallow (390-1289 m); illite = 45%; illite/smectite: 7% (10 A), 48% (17 A)

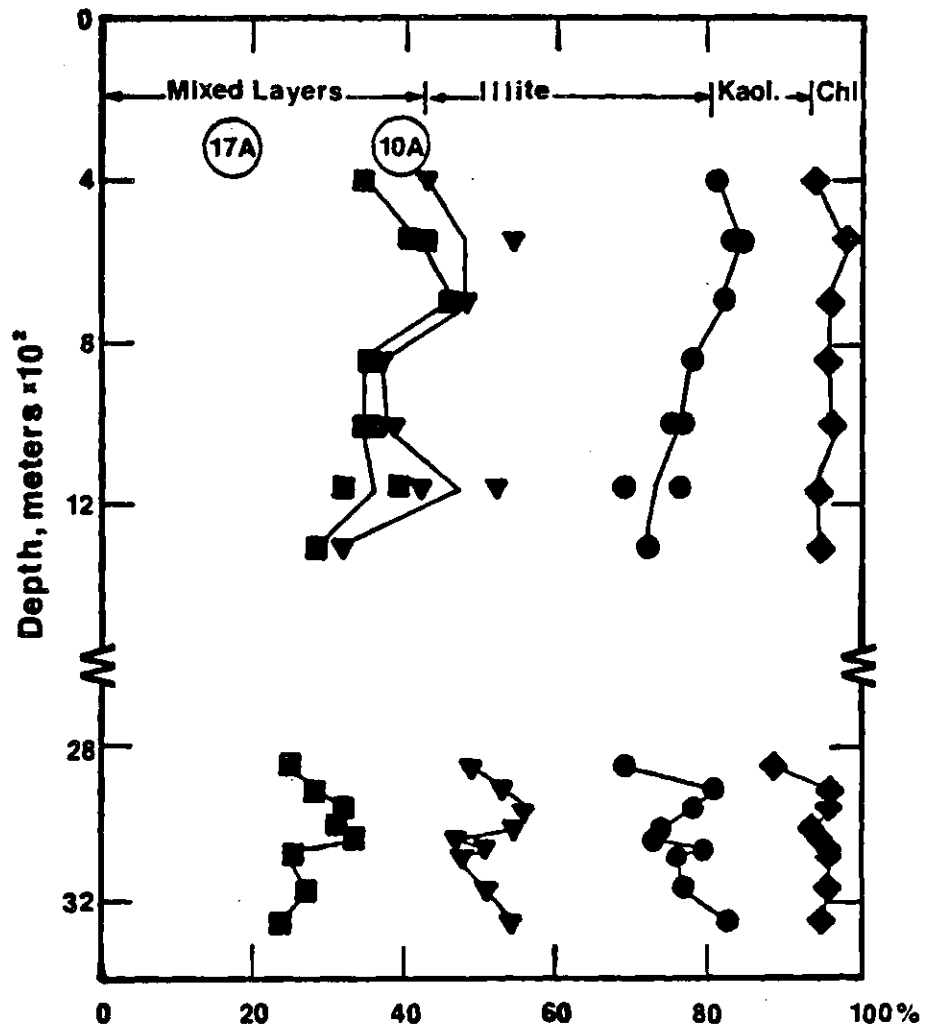


Figure 12. Variation of the 0.1-2 μm Clay Minerals with Depth.

Deep (2851-3242 m); illite = 33%; illite/smectite - 30% (10 A), 37% (17 A).

As with the 2-44 μm clay minerals, discrete illite decreases and illite/smectite increases with depth. In fact, in the 0.1-2 μm 2:1 clays near equal decreases from shallow to deep samples of 12% discrete illite and 11% smectite in the illite/smectite phase are balanced by a 23% increase in 10 A layers in the illite/smectite phase.

The <0.1 μm fractions consist entirely of clay minerals. The broad X-ray diffraction peaks do not permit delineation of kaolinite and chlorite. The sum of these two clays is plotted along with the <0.1 μm 2:1 clays in Figure 13. The 2:1 clays comprise >90% of the <0.1 μm material and there is no apparent depth related change in the kaolinite + chlorite content. However, as in the 0.1-2 μm clays a decrease with depth of discrete illite layers and 17 A layers in the illite/smectite is balanced by increases in 10 A layers in the illite/smectite. Normalized to 100% 2:1 clays, the <0.1 μm average percentages are:

Shallow (390-1289 m); illite 27%; illite/smectite 30% (10 A), 43% (17 A)

Deep (2851-3242 m); illite 20%; illite/smectite 43% (10 A), 37% (17 A).

The most commonly recognized diagenetic reaction is the transformation of smectite to illite, which has been observed in the thick shale sequences of the Gulf Coast

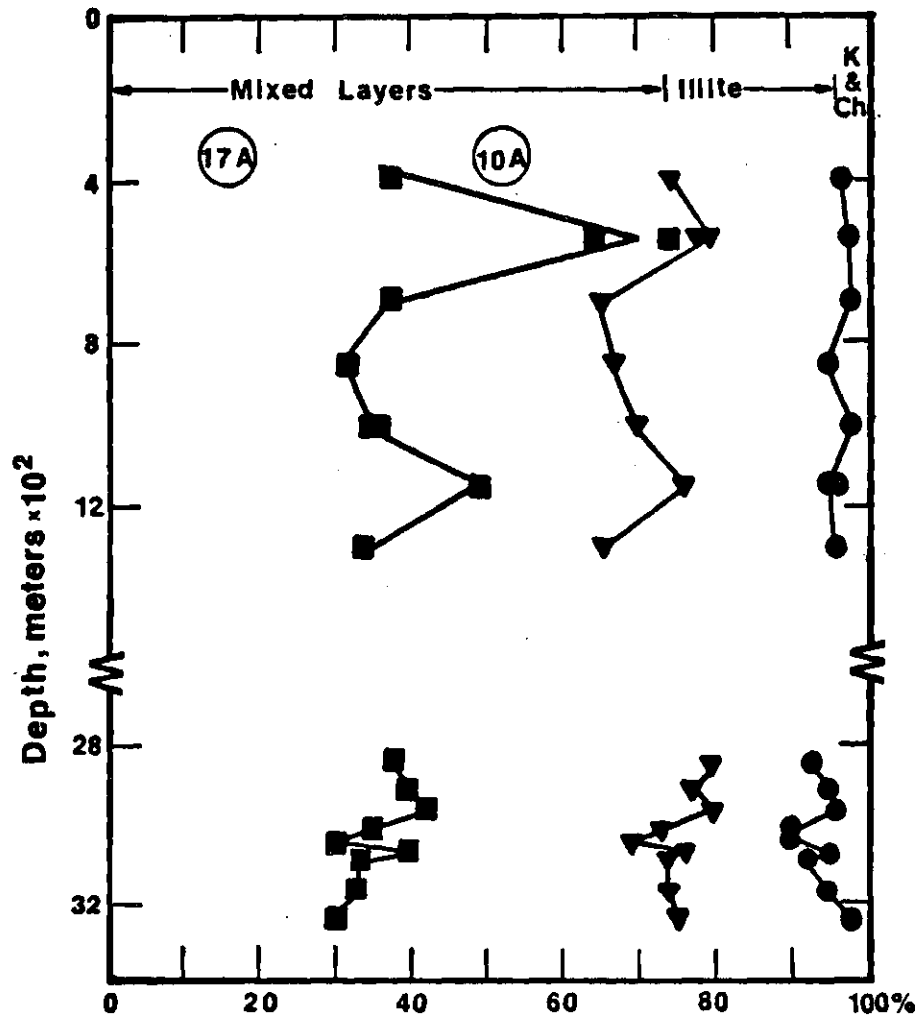


Figure 13. Variation of the <0.1 μm Clay Minerals with Depth.

(Powers, 1967; Burst, 1969; Perry and Hower, 1970; Weaver and Beck, 1971; Van Moort, 1971; Schmidt, 1973) and in other areas (Dunoyer de Segonzac, 1969; Weaver and Beck, 1971; Van Moort, 1971; Foscales and Kodama, 1974; Helig, 1974). Dunoyer de Segonzac (1970) is a summary of diagenetic clay alterations during deep burial. The most sensitive indicator of this diagenetic reaction is the increase in 10A layers in the mixed layer illite/smectite. Data on the illite/smectite mixed layer clay obtained by Hower, et al., (1976) and in this study are plotted in Figure 14. Data obtained by Hower, et al., (1976) consists of X-ray patterns of the size fractions of cuttings from a Gulf Coast Oligocene well with a geothermal gradient similar to the wells of this study. They observe a systematic increase in 10 A layers in the illite/smectite with depth with a major increase from 2860-3400 m. The data from this study (Table 8 and Figure 14) show a much greater variation over small distances. This is possibly due to the difference in sampling techniques as cuttings would tend to smooth out short term variations while sidewall cores would not. Nonetheless the 10 A layers in the illite/smectites of $<0.1 \mu\text{m}$ and $0.1-2 \mu\text{m}$ fractions can be seen to increase with depth. The data of both studies show an increased degree of expandibility in the coarser clay fractions of each sample. This may be the result of the accumulation of degraded $>2 \mu\text{m}$ material in the $<0.1 \mu\text{m}$ fraction due to sonification, or a faster 17 A \Rightarrow 10 A transformation in the smaller grain sizes. The nature of the sampling technique may

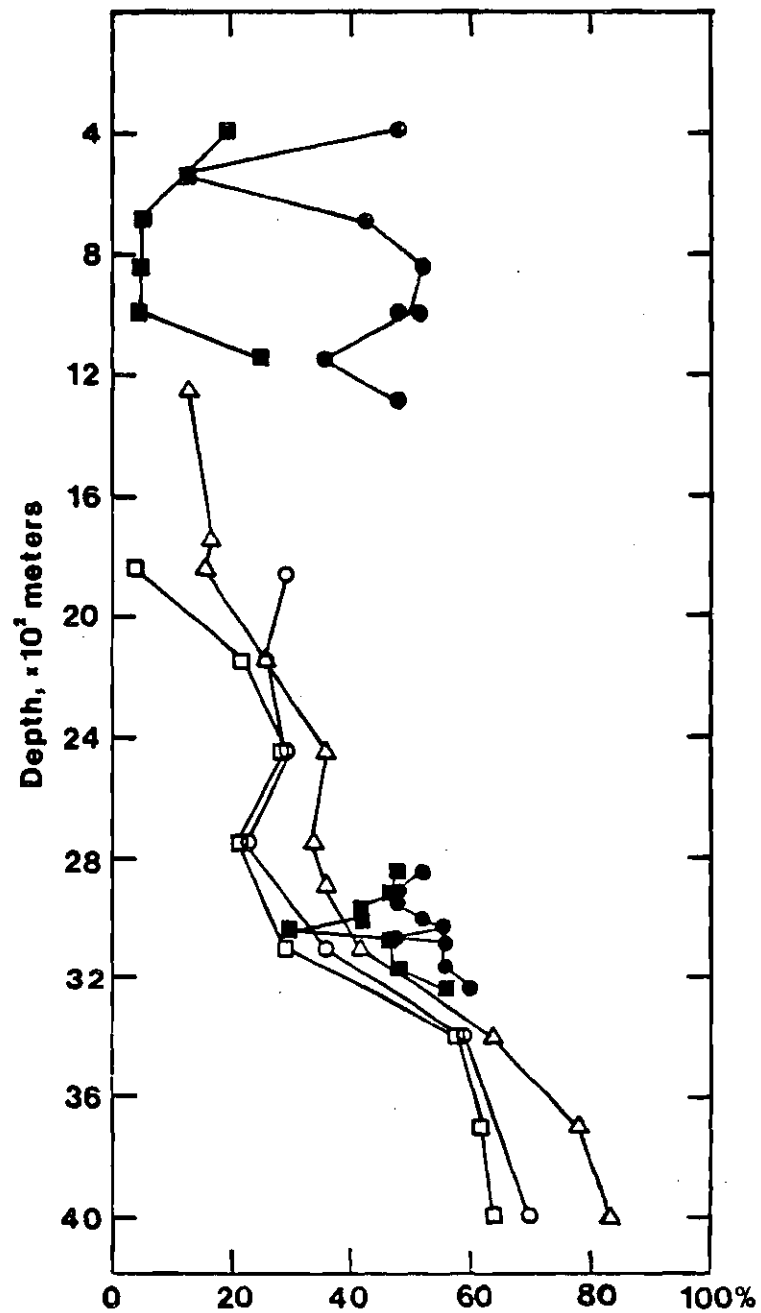


Figure 14. Variation of the Percent 10A Layers in the Illite/Smectite Mixed Layer Clay with Depth. (● = $<0.1 \mu\text{m}$, ■ = $0.1-2 \mu\text{m}$; This Study. Δ = $<0.1 \mu\text{m}$, ○ = $0.1-0.5 \mu\text{m}$, □ = $0.5-2 \mu\text{m}$; Hower, et al., (1976))

be of further importance in explaining the high 10 A content of the shallow <0.1 μm samples of this study. The very sandy sample, 538, contains a large percentage of 17 A material which is more consistent with an extension of the trend shown by the samples of Hower, et al., (1976) than the other, less sandy, samples. This presence of greater 17 A layers in sandier shallow samples may result in sidewall cuttings being generally more 17 A rich than the sidewall cores of this study which were placed in shale layers only. As the sand layers in a vertical Gulf Coast sediment sequence diminish with depth this effect would also decrease.

Despite this ambiguity, the data of this study agree favorably with those of Hower, et al., (1976). The deep samples are in close agreement with their data and appear to cover the initiation of the major 17 A \Rightarrow 10 A transformation. The acceleration of the major transformation at \sim 2800 m, in the wells studied, coincides with the change in the slope of the geothermal gradient (Figure 2) and the top of the main high pressure zone (Figure 3).

In addition to the increase in 10 A illite/smectite layers in the clays, Hower, et al., (1976) observe decreases with depth in discrete illite. This decrease with depth is also observed in this study. Hower, et al., (1976) observe discrete illite only in their coarser fractions, while the samples of this study contain discrete illite in all fractions.

Hower, et al., (1976) postulate a basic diagenetic

reaction, confirmed by this study, whereby 17 A layers are converted to 10 A layers by the addition of potassium derived from the decomposition of detrital K bearing minerals. In the samples of this study, the increase in mixed layer 10 A component of the $<2 \mu\text{m}$ clays, with depth, (Figure 12 and 13) result in part from the discrete illite of the same fraction while the slight increases in total $<1 \mu\text{m}$ and $1-2 \mu\text{m}$ 10 A layers (discrete and mixed layer) must be due to K loss from coarser fractions or pore water. Additional diagenetic reactions which have been proposed include:

1. Loss of kaolinite with depth (Dunoyer de Segonzac, 1964; Weaver and Beck, 1971; Hower, et al., 1976),
2. Formation of authigenic chlorite below $\sim 3200 \text{ m}$ (Dunoyer de Segonzac, 1964; Weaver and Beck, 1971; Van Moort, 1971),
3. Loss of K-feldspar below $\sim 3000 \text{ m}$ (Weaver and Beck, 1971; Hower, et al., 1976),
4. Precipitation of silica with depth (Mizutani, 1970, Hower, et al., 1976, and this study),
5. Precipitation of reduced iron compounds (siderite and pyrite) (Weaver and Beck, 1971 and this study),
6. Precipitation of a carbonate caprock above the high pressure zone (Weaver and Beck, 1971; and this study).

3. Solid Chemical Changes in Gulf Coast Sediments with Depth

Accompanying the mineralogic changes during burial diagenesis are changes in the solid sample chemistry. Weaver

and Beck (1971) in a Mississippi delta Plio-miocene well, Hower, et al., (1971) in the Mio-oligocene near Galveston and Van Moort (1971) in the western Louisiana Eocene Wilcox formation report analyses of major elements in the bulk samples as a function of depth of burial. Average chemical compositions of depth related groups of their samples are compiled in Table 23a. To compare these data with the results of this study it is necessary to calculate a bulk composition from the compositions of the individual size fractions (Tables 9-12). However, as only six $>44 \mu\text{m}$ fractions were analyzed and this fraction was generally a minor part of the bulk (except 538), the $<44 \mu\text{m}$ can be considered representative of the bulk sample. Calculating the $<44 \mu\text{m}$ chemistry from the data in Tables 7 (recalculating size fraction percentages to 100% .03-44 μm), 9, 10, and 11 and averaging the shallow (390-1289) and deep (2851-3241) samples results in the data from this study in Table 23a. Using the difference between the sum of the oxides and 100% as a measure of loss on ignition, these values can be converted to an ignited basis for comparison with Van Moort (1971) and Hower, et al., (1976) or left as is for comparison with Weaver and Beck (1971). The need for this correction can be eliminated and all data examined together by comparing the oxide/ Al_2O_3 ratios from the wells (Table 23b and Figure 15a-g). Any change or difference in these data will be due to either differences in source and depositional environment or a diagenetic event that removes or adds material.

Table 23a. Bulk Chemistry of Gulf Coast Pelitic Sediments (Avg. of Sample Sets)*

Sample Sets	SiO ₂ %	Al ₂ O ₃ %	Total Fe		MgO %	CaO %	K ₂ O %	Na ₂ O %	TiO ₂ (%)	# of Samples in Set
			as Fe ₂ O ₃ %	FeO						
(1)										
1850-2750 m	63.4	12.3	5.43		2.59	9.95	2.56	1.61	0.76	4
3100-4000 m	68.4	12.8	5.57		2.06	4.53	2.75	1.28	0.83	4
4300-5500 m	70.9	13.7	5.27		2.20	1.81	3.43	0.91	0.89	5
(2)										
			Fe ₂ O ₃	FeO						
1530-1630 m	70.6	19.1	2.55	2.00	1.55	0.25	2.41	1.52	1.03	2
3060-3200 m	64.3	22.0	1.86	3.76	2.16	0.94	3.04	1.58	0.95	7
3690-4230 m	66.5	21.1	1.58	3.01	2.10	0.71	2.43	1.47	0.94	8
4740-4840 m	68.0	16.5	0.81	5.33	2.45	1.29	2.23	2.01	0.82	2
(3)										
390-1289 m	67.9	17.8	5.85		2.15	1.07	3.29	0.88	0.98	7
2850-3242 m	67.5	18.5	5.66		1.80	2.45	2.60	0.59	0.91	9
(4)										
<3000 m	--	13.2	3.30		1.65	1.13	2.49	0.78	--	8
3000-4000 m	--	16.1	3.82		1.67	0.33	2.67	0.53	--	7
4000-5000 m	--	13.4	4.56		1.64	0.93	2.36	0.39	--	5

*Data expressed as weight percent.

(1) Hower, et al., (1976) Ignited.

(2) Van Moort (1971) Ignited.

(3) This study <44 μ Ignited (assuming all unanalysed components are ignitable).

(4) Weaver and Beck (1971) 110°C Dry.

Table 23b. Bulk Oxide/ Al_2O_3 Ratios of Gulf Coast Pelitic Sediments.

	$\text{SiO}_2/\text{Al}_2\text{O}_3$	$\text{Fe}_2\text{O}_3/\text{Al}_2\text{O}_3$	$\text{MgO}/\text{Al}_2\text{O}_3$	$\text{CaO}/\text{Al}_2\text{O}_3$	$\text{K}_2\text{O}/\text{Al}_2\text{O}_3$	$\text{Na}_2\text{O}/\text{Al}_2\text{O}_3$	$\text{TiO}_2/\text{Al}_2\text{O}_3$
(1)							
1850-2750 m	5.15	0.44	.210	.810	0.20	0.130	0.062
3100-4000 m	5.34	0.44	.160	.350	0.21	0.100	0.065
4300-5500 m	5.18	0.38	.160	.130	0.25	0.070	0.065
(2)							
1530-1630 m	3.70	0.25	.081	.013	0.13	0.080	0.054
3060-3200 m	2.92	0.27	.098	.043	0.14	0.072	0.043
3690-4230 m	3.14	0.23	.099	.033	0.11	0.069	0.044
4740-4840 m	4.12	0.40	.148	.078	0.14	0.122	0.050
(3)							
390-1289 m	3.81	0.33	.121	.060	0.18	0.049	0.055
2850-3242 m	3.65	0.31	.097	.130	0.14	0.032	0.049
(4)							
<3000 m	--	0.25	.125	.086	0.19	0.059	--
3000-4000 m	--	0.24	.104	.020	0.17	0.033	--
4000-5000 m	--	0.34	.122	.069	0.18	0.029	--

(1) Hower, et al., (1976) Ignited.

(2) Van Moort (1971) Ignited.

(3) This study <44 μ Ignited (assuming all unanalysed components are ignitable).

(4) Weaver and Beck (1971) 110°C Dry.

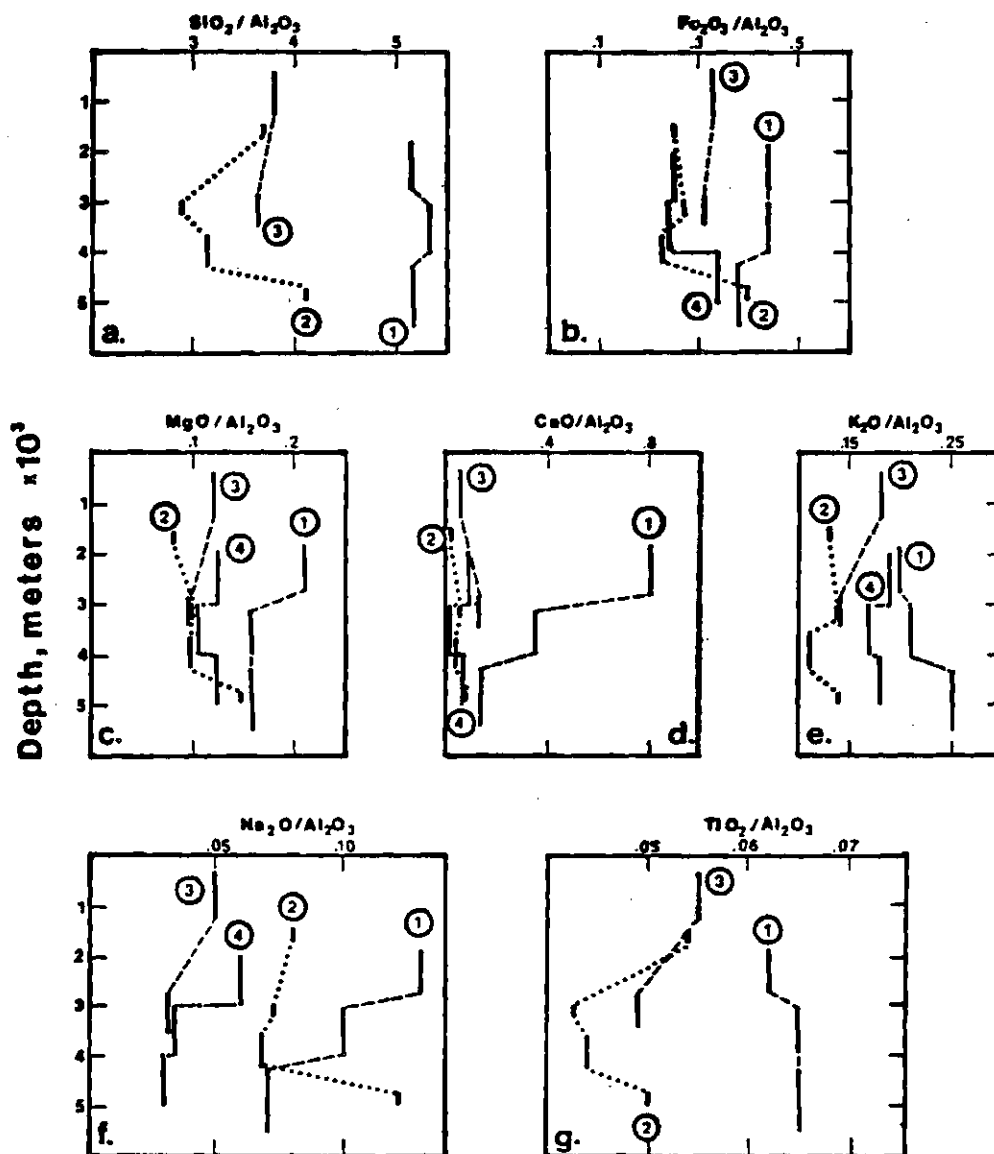


Figure 15. Bulk Sample Oxide/ Al_2O_3 Ratio Variations with Depth for Gulf Coast Pelitic Sediments. (1. Hower, et al., (1976), 2. Van Moort (1971), 3. This Study, 4. Weaver and Beck (1971)).

The large variations in both wt% oxides and the oxide/ Al_2O_3 ratios is indicative of the importance of variations in facies, depositional environments and possibly sampling techniques in determining bulk chemistries. In this respect, it can be noted that the bulk sample data of Hower, et al., (1976) consistently plots Al_2O_3 poor relative to the other wells indicating, perhaps, slightly greater sand contents. The only ratio which shows signs of a systematic depth related trend in all four studies, thus suggesting a diagenetic effect, is the $\text{Na}_2\text{O}/\text{Al}_2\text{O}_3$ decrease with depth observed in all samples except the deepest of Van Moort. This drop in solid Na could be the result of Na-feldspar decomposition or the loss of Na from exchange sites with increasing depth of burial.

In order to recognize facies or source variations and better assess the nature of chemical diagenesis it is necessary to examine alterations which occur within the closed system represented by the solid sample. In order to do this, some method of sample segregation must be employed. The easiest and least damaging to the sample is size fractionation which, by the data of Hower, et al., (1976) and this study, allows the segregation of pure clay suite in the $<0.1 \mu\text{m}$ fraction, a clay, quartz and calcite suite in the $0.1-2 \mu\text{m}$ fraction and a complex multi-component system containing clay, quartz, feldspars, carbonates, pyrite, barite and perhaps other common minerals in the $>2 \mu\text{m}$ material. In a system that is closed with respect to the bulk solid sample, elements involved in

diagenetic reactions will move from one mineral to another (Weaver and Wampler, 1970) and may thus move from one size fraction to another. Figures 16-24 are plots of depth vs. wt. % oxide (or element) (110°C dry basis) in the various size fractions of the samples of this study.

The 2-44 μm chemistry, with its large scale chemical variations, generally reflects detrital influence. This is particularly true in the shallow samples where apparently samples 692, 844, and 1000 are quite distinct from the other shallow samples in terms of a lower SiO_2 content and higher Fe_2O_3 , MgO and K_2O . This is probably the result of the higher sand contents of the samples 390, 538, 1150 I and II and 1289. In the deep 2-44 μm sample chemistries there is evidence of silica loss and Al_2O_3 , Fe_2O_3 , MgO and CaO gain with depth. This may be the result of increased distance from the lower most massive sand unit (~2800 m) with depth or the initiation of diagenetic reactions upon entering the high pressure zone and is probably associated with the increase in clay clasts in these samples. The high CaO and low Sr contents of the deepest sample indicates precipitation of some sort of caprock over the high pressure zone (Weaver and Beck, 1971). Increases in Fe_2O_3 in the coarse fraction of the deep samples, are a result of pyrite and/or siderite precipitation.

The composition of the finer size fractions can reflect variations in the 2-44 μm fraction related to facies or source, however a dampening of such differences with finer grain sizes

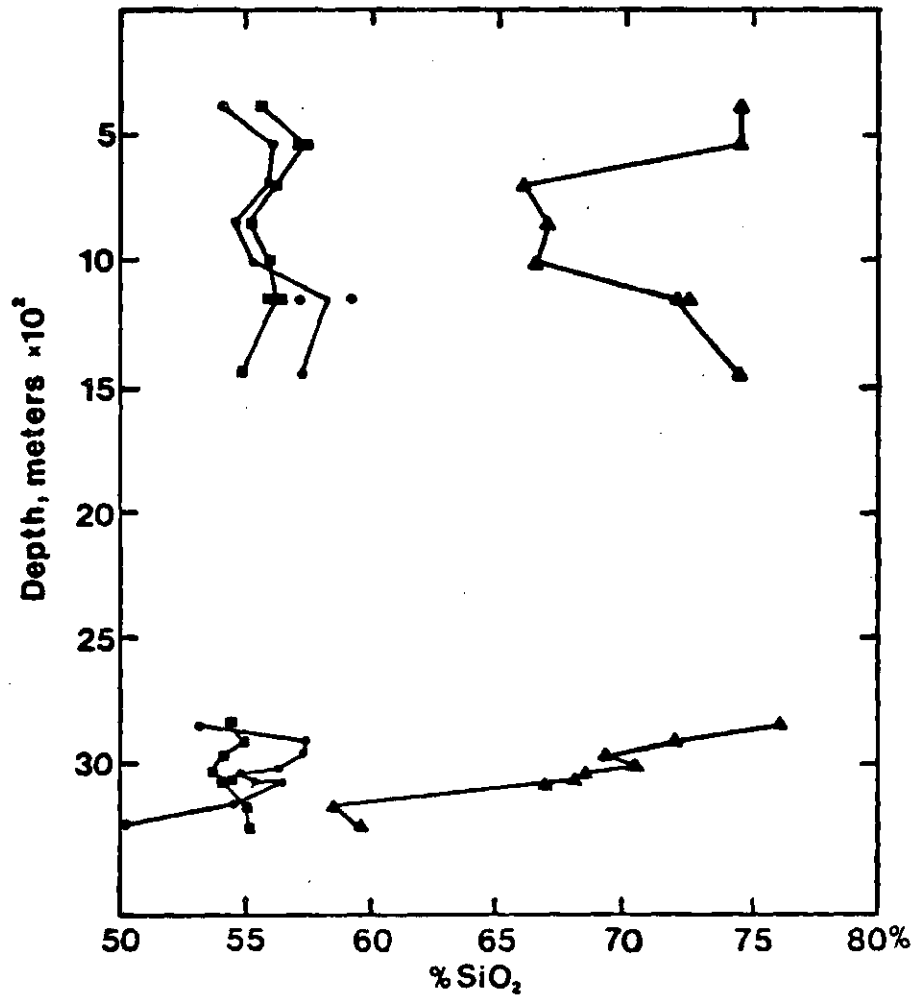


Figure 16. SiO₂ Variation in <44 μm Size Fractions (110°C Dry) with Depth. (■ = <0.1 μm, ● = 0.1-2 μm, ▲ = 2-44 μm)

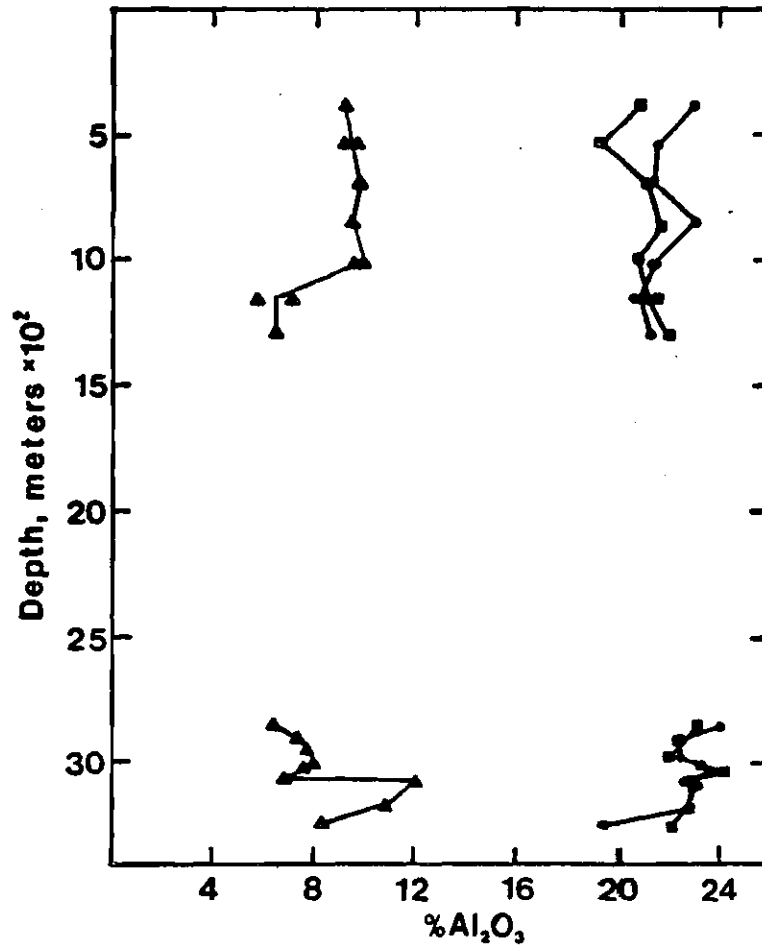


Figure 17. Al_2O_3 Variation in $<44 \mu\text{m}$ Size Fractions (110°C Dry) with Depth. (\blacksquare = $<0.1 \mu\text{m}$, \bullet = $0.1-2 \mu\text{m}$, \blacktriangle = $2-44 \mu\text{m}$)

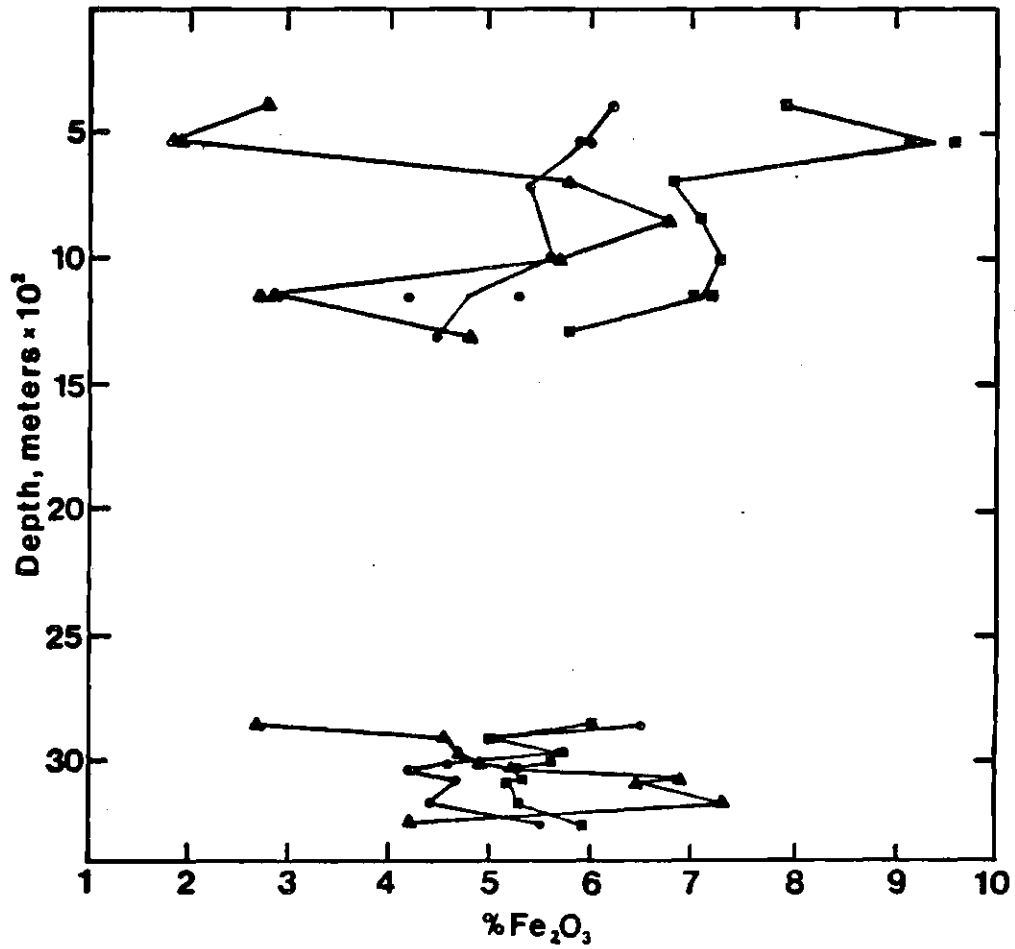


Figure 18. Fe (as Fe₂O₃) Variation in <44 μm Size Fraction (110°C Dry) with Depth. (■ = <0.1 μm, ● = 0.1-2 μm, ▲ = 2-44 μm)

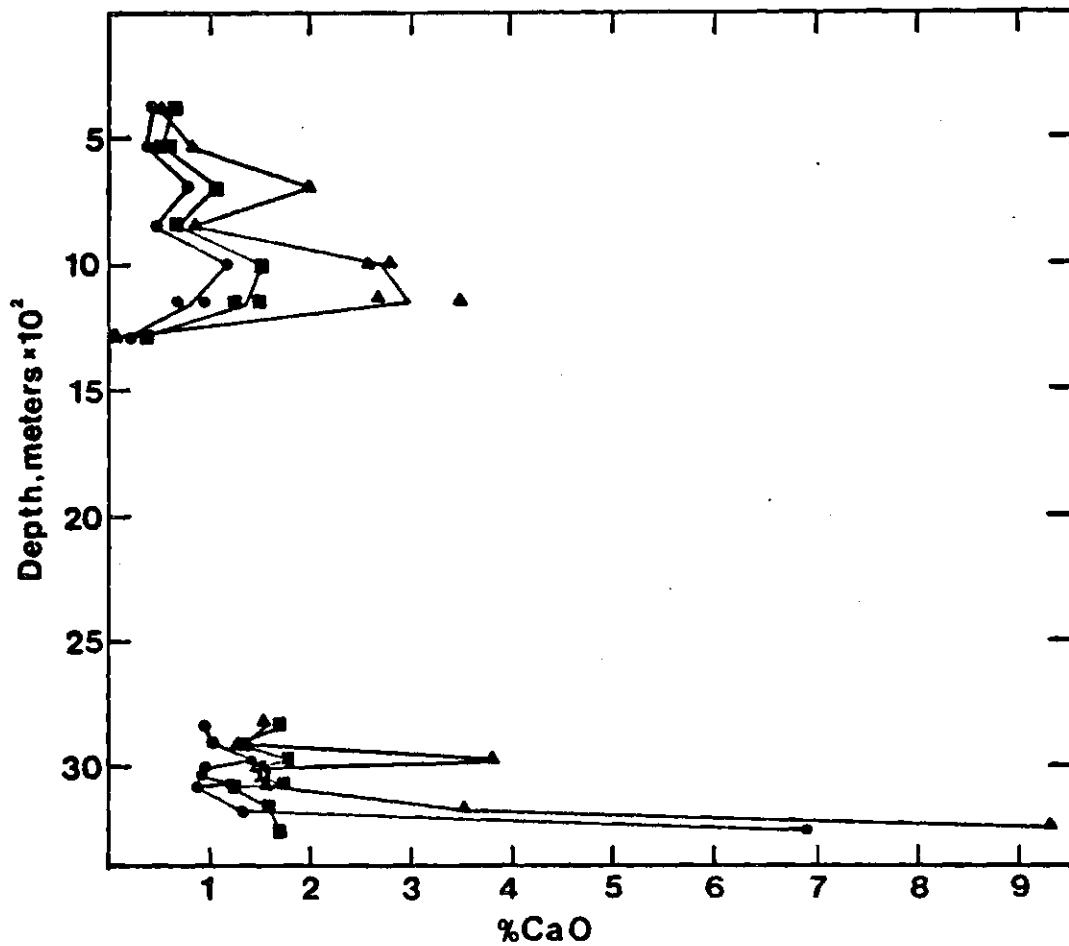


Figure 19. CaO Variation in <44 μm Size Fraction (110°C Dry) with Depth. (\blacksquare = <0.1 μm , \bullet = 0.1-2 μm , \blacktriangle = 2-44 μm)

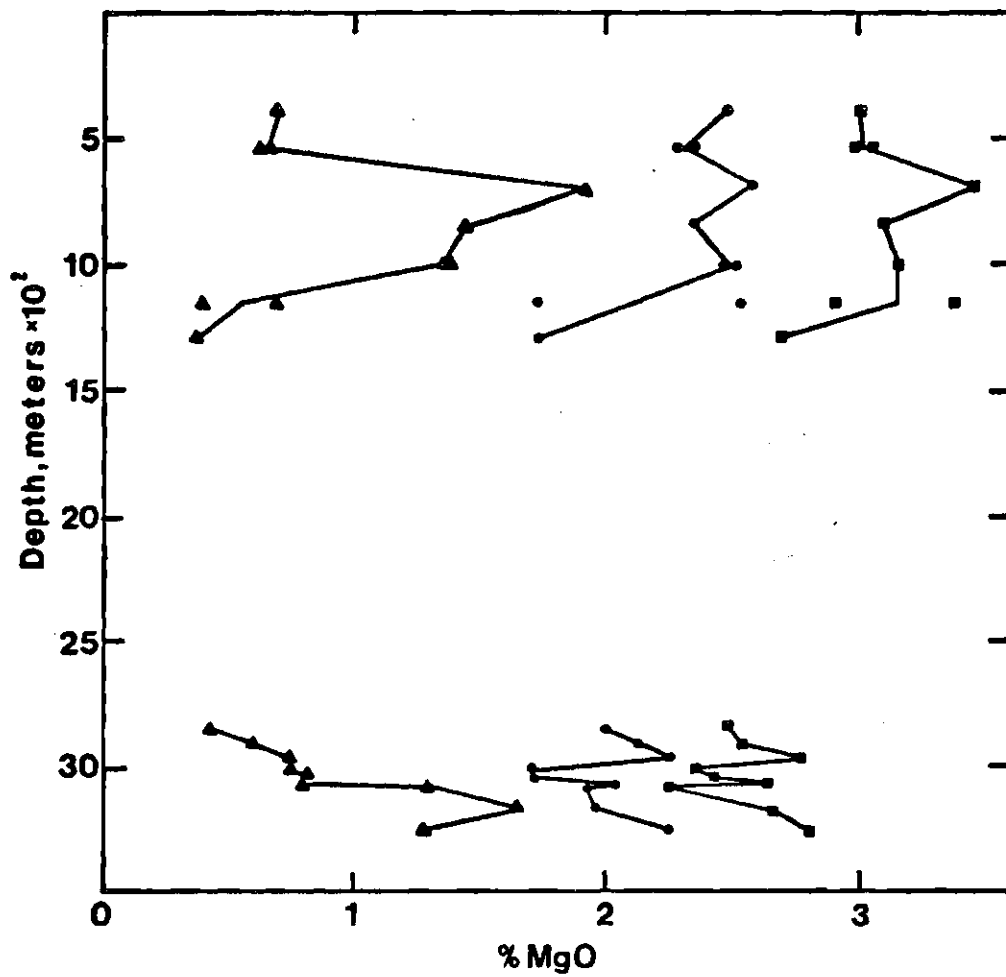


Figure 20. MgO Variation in <44 μm Size Fractions (110°C Dry) with Depth. (\blacksquare = <0.1 μm , \bullet = 0.1-2 μm , \blacktriangle = 2-44 μm)

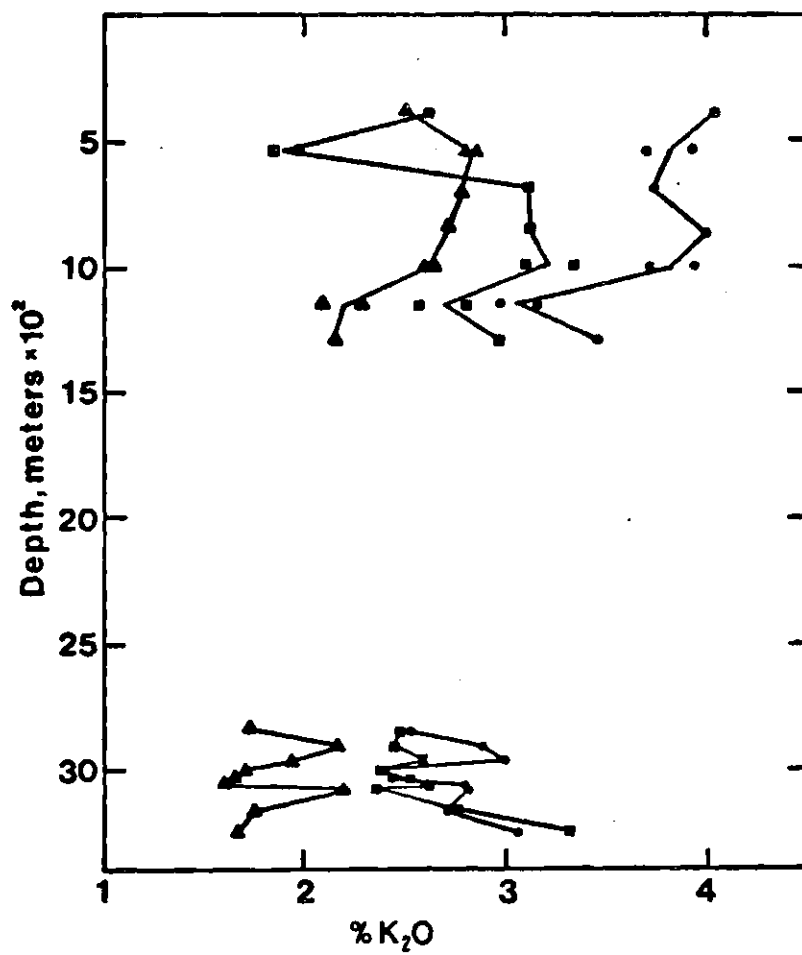


Figure 21. K₂O Variation in <44 μm Size Fractions (110°C Dry) with Depth. (■ = <0.1 μm, ● = 0.1-2 μm, ▲ = 2-44 μm)

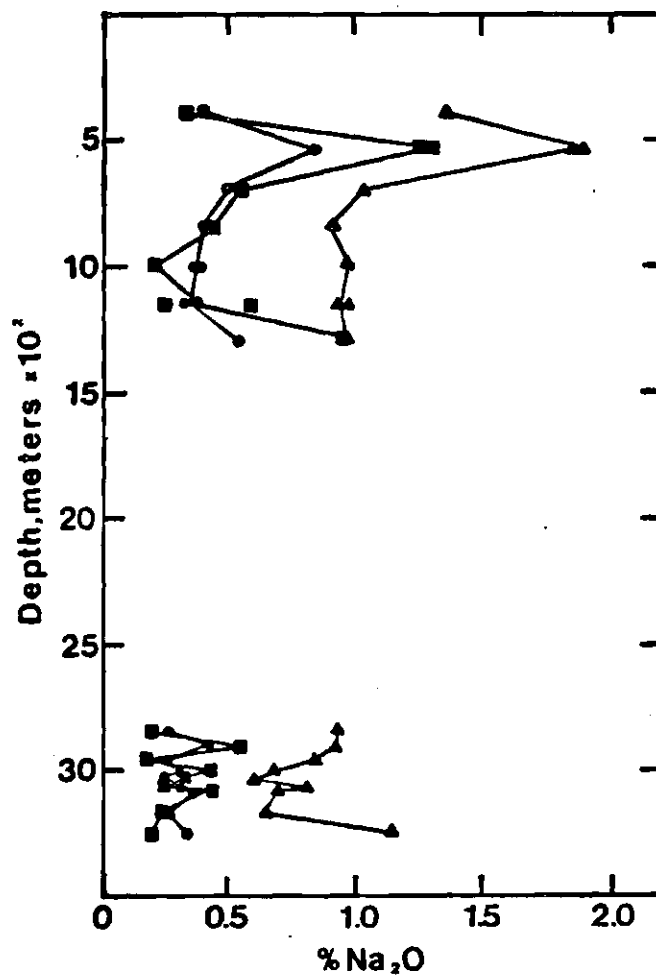


Figure 22. Na₂O Variation in <44 μm Size Fractions (110°C . Dry) with Depth. (\blacksquare = <math><0.1 \mu\text{m}</math>, \bullet = $0.1-2 \mu\text{m}$, \blacktriangle = $2-44 \mu\text{m}$)

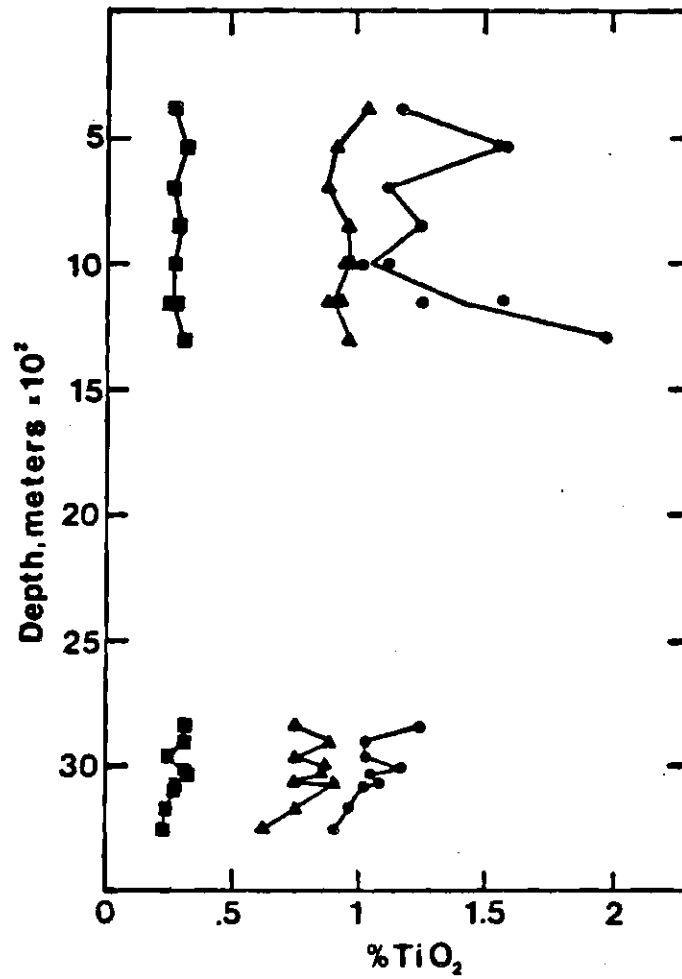


Figure 23. TiO₂ Variation in <44 μm Size Fractions (110°C Dry) with Depth. (■ = <0.1 μm, ● = 0.1-2 μm, ▲ = 2-44 μm)

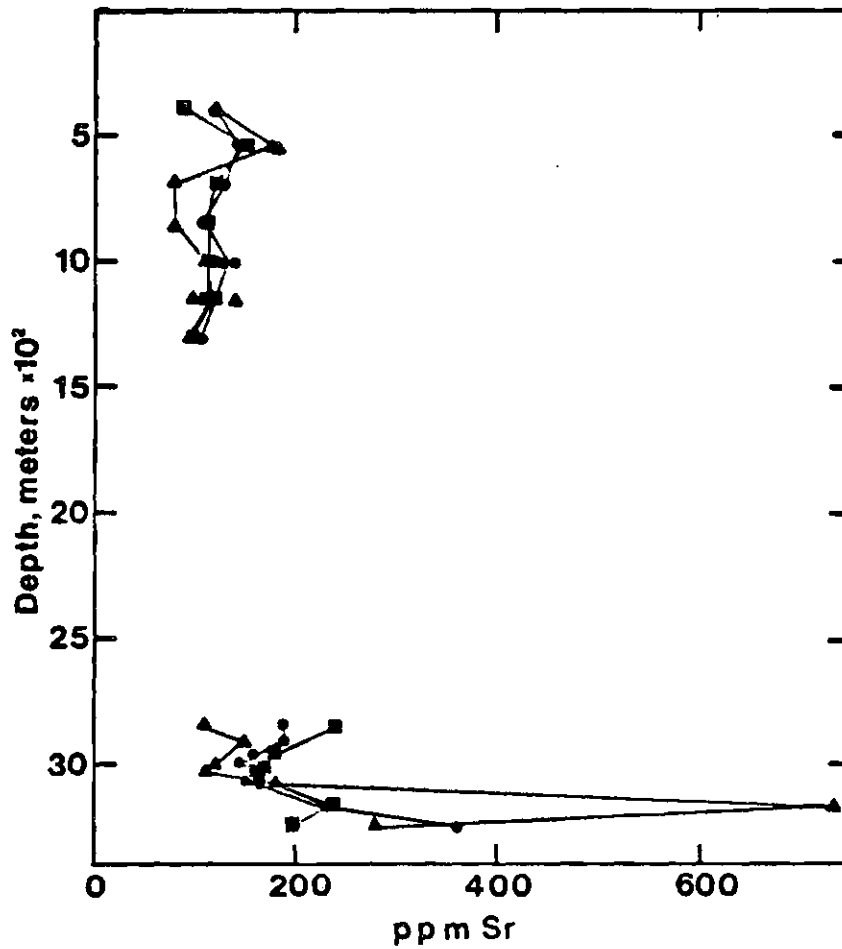


Figure 24. Sr Variation in <44 μm Size Fractions (110°C Dry) with Depth. (\blacksquare = <0.1 μm , \bullet = 0.1-2 μm , \blacktriangle = 2-44 μm)

is observed. Hopefully diagenetic additions and subtractions from the finest size fraction will be visible without too much facies and source interference. The $<0.1 \mu\text{m}$ fraction chemistry of Gulf Coast samples has been analyzed by Hower, et al., (1976) and in this study. Hower, et al., (1976) describes the $<0.1 \mu\text{m}$ chemistry of well cuttings covering evenly the depth range 1850-5500 m. Their data record the chemical transition in this fraction during the diagenetic conversion from 80% to 20% expanded layers in the illite/smectite. They observe an increase in K_2O , an increase in Al_2O_3 and decreases in MgO , SiO_2 and Fe_2O_3 with depth. All of these oxide percentages are seen to change primarily in the 3000-4000 m range. Also Na_2O and CaO are seen to decrease abruptly between 3100 and 3400 meter samples. The samples in the present study must be converted to an ignited basis in order to allow comparison. The basis for this conversion, the normalization of 110°C chemistries to 100%, is sound as the components not measured include mostly H_2O , CO_2 , sulfur compounds and other ignitable elements. The compositions of the $<0.1 \mu\text{m}$ fractions of the samples of this study on an ignited basis are reported in Table 24 and compared with the data of Hower, et al., (1967) in Figure 25a & b. Closer agreement than would be expected on the basis of the bulk chemistries or the $<0.1 \mu\text{m}$ mineralogy can be seen, for K_2O , Fe_2O_3 , and Al_2O_3 where the two studies overlap. SiO_2 values from this study average about 0.5 wt % higher and MgO values are lower by about 0.5 wt. % than the corresponding data of

Table 24. Major Element Chemistry of the <.1 μm Fraction (Ignited).

Depth	SiO ₂ %	Al ₂ O ₃ %	Fe ₂ O ₃ %	MgO %	CaO %	K ₂ O %	Na ₂ O %	TiO ₂ %
390	61.0	22.8	8.7	3.27	.71	2.84	.37	.30
538 I	61.3	20.7	10.3	3.27	.63	2.10	1.40	.34
538 II	61.9	20.7	9.9	3.23	.52	2.02	1.36	.35
692	60.7	22.8	7.4	3.73	1.15	3.35	.58	.29
844	60.3	23.6	7.8	3.38	.75	3.40	.48	.33
1000 i	60.5	22.6	7.9	3.42	1.71	3.37	.22	.29
1000 ii	60.4	22.5	7.9	3.41	1.65	3.60	.23	.29
1150 I	60.8	23.0	7.8	3.12	1.36	2.98	.62	.30
1150 II	61.0	22.7	7.6	3.69	1.63	2.79	.26	.27
1289	61.0	24.5	6.5	2.99	.38	3.29	1.09	.33
2851	59.9	25.6	6.6	2.75	1.84	2.75	.22	.33
2906	61.3	25.2	5.6	2.85	1.41	2.73	.60	.33
2961	60.5	24.7	6.4	3.11	2.01	2.91	.18	.28
3007	60.1	26.0	6.3	2.62	1.62	2.65	.47	.33
3038	59.9	26.3	5.8	2.72	1.66	2.81	.35	.36
3064	60.7	25.0	5.9	2.96	1.86	2.94	.29	.31
3074	61.0	25.8	5.9	2.51	1.34	2.65	.48	.32
3164	60.7	25.2	5.9	2.93	1.77	3.03	.27	.25
3242	60.3	24.2	6.5	3.07	1.83	3.64	.22	.24

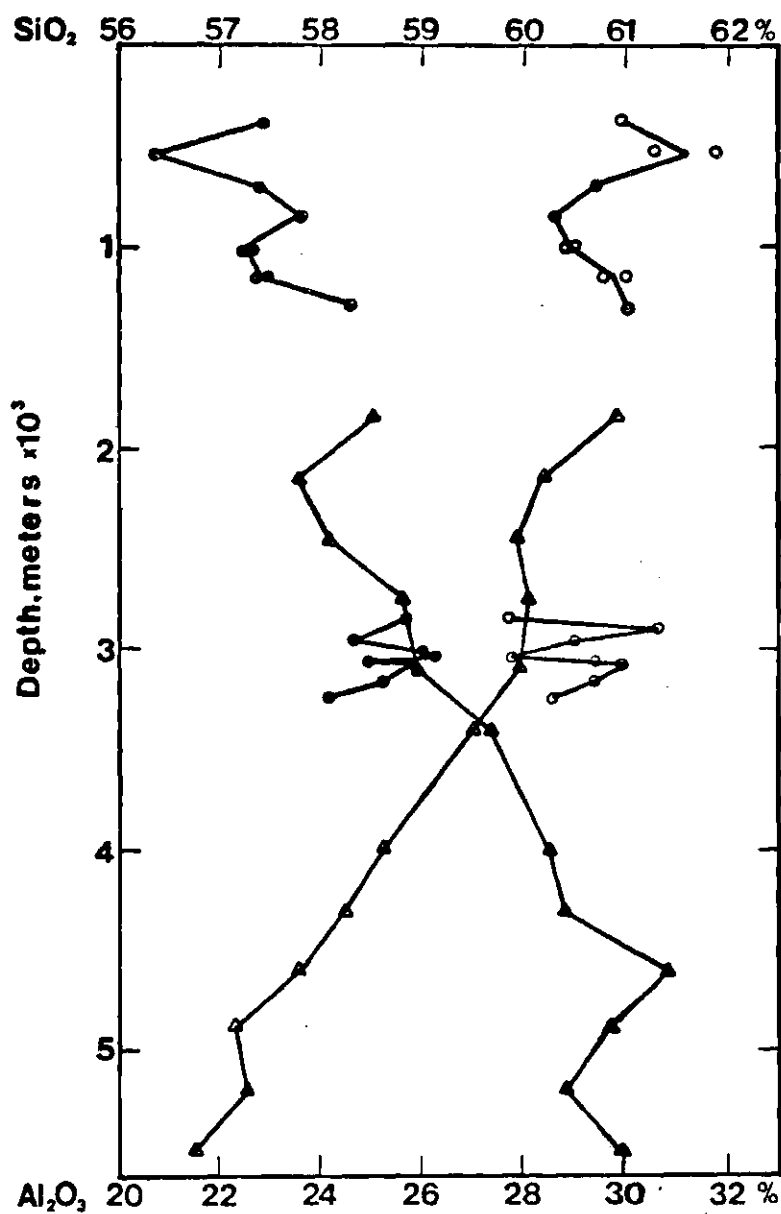


Figure 25a. SiO₂ and Al₂O₃ Variation in <0.1 μm Gulf Coast Samples (Ignited Basis) with Depth. (O = SiO₂, ● = Al₂O₃; This Study. Δ = SiO₂, ▲ = Al₂O₃; Hower, et al., (1976)).

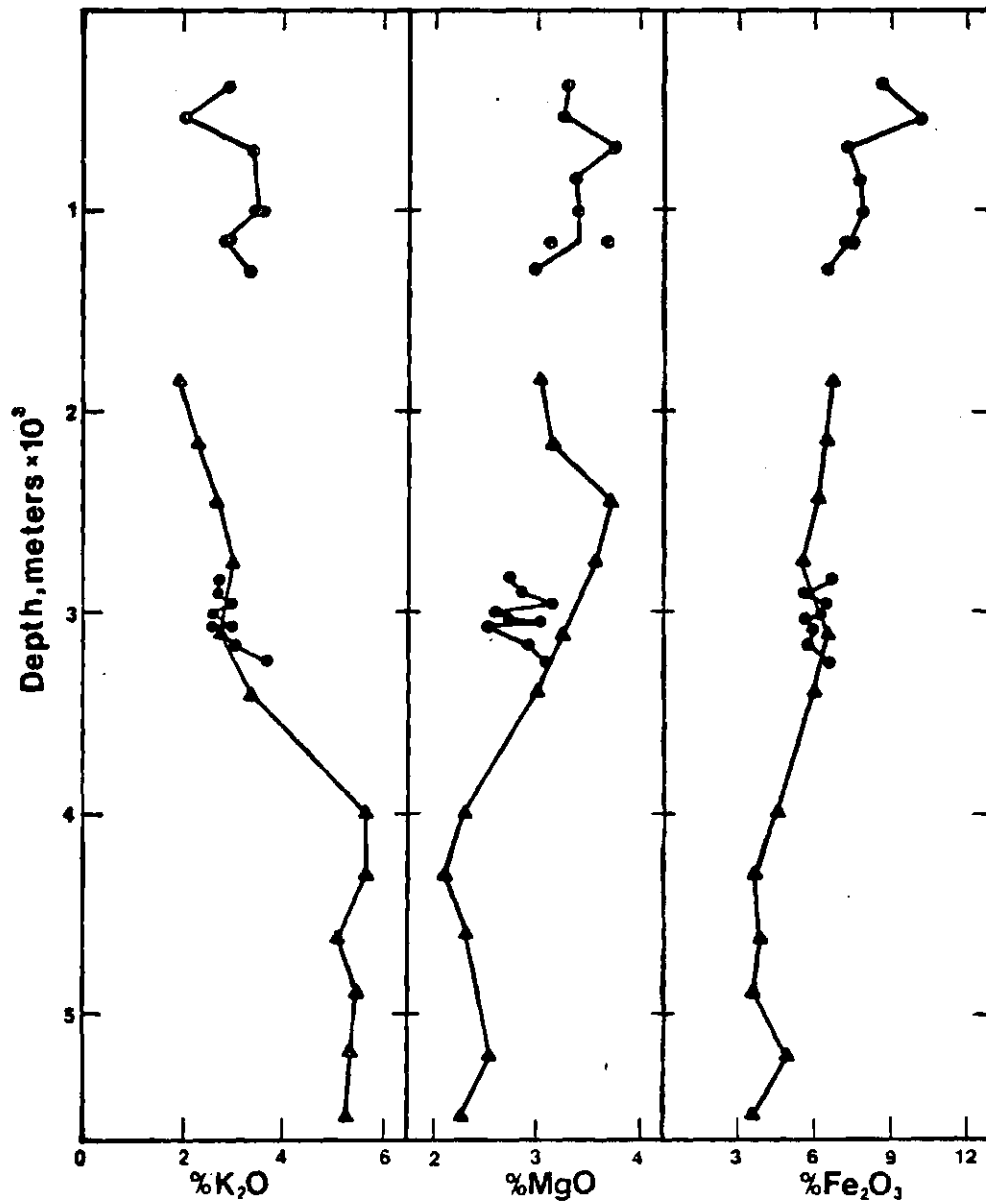
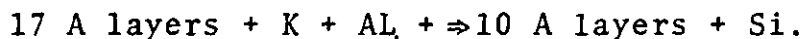


Figure 25b. K₂O, MgO and Fe₂O₃ Variation in <0.1 μ m Gulf Coast Samples (Ignited Basis) with Depth. (● = This Study, ▲ = Hower, et al., (1976))

Hower, et al., (1976). The increased scatter in the samples of this study probably represents the true variations in the small samples recovered from the single layers that the side-walls represent.

Including the shallow samples of this study in the picture generally confirms and extends the chemical trends indicated by Hower, et al., (1976) with the exception of potassium, which appears systematically high in the samples from 690 to 1290 m. The cause of this discrepancy can be seen in the mineralogy of this fraction (Figure 14) where the % 10 A layers in the mixed layer clay averages 40-50% instead of the $\leq 20\%$ of Hower, et al., (1976). The samples of this study also contain appreciable discrete illite in this fraction. Some discrete illite may be present in some of the $<0.1 \mu\text{m}$ samples of Hower, et al., (1976) (see their Figure 1) but not as much as is apparent in the present samples. The increased illite content in the shallow $<0.1 \mu\text{m}$ material may be the result of differing facies or may be caused by the diagenetic loss of discrete 10 A material with depth.

In any event, the chemistry of the $<0.1 \mu\text{m}$ material from this study is consistent with the diagenetic reaction proposed by Hower, et al., (1976);



In addition to the above reaction, the confirmation of observed decreases in Fe_2O_3 and MgO indicate that diagenetic Mg and Fe

loss (Hower, et al., (1976) also occurs and the reaction can be written;



The sources of potassium and aluminum for this reaction are primarily the decomposition of detrital mica and K-feldspar (Weaver and Beck, 1971; Hower, et al., 1976) although input of K from elsewhere becomes necessary at the high pressure zone. Fe lost from the fine fraction results in the precipitation of reduced iron compounds (FeS and FeCO₃). A shift from trivalent to divalent iron species with depth, described by Weaver and Beck (1971) and Van Moort (1971), apparently results from this reaction. Fe loss from clays and precipitation of pyrite is a depth dependent reaction proposed by Drever (1971b). Silica loss from fine fractions may result in the precipitation of silica as grain coatings and cement (Hower, et al., 1976 and this study).

The cause of variations in the CaO and Na₂O contents of the <0.1 μm fractions of High Island samples can be explained through an examination of the exchange ion chemistry of these fractions (Table 15). Figure 26 shows the individual exchange ions and total exchange ions in meq/100 g vs. depth for the <0.1 μm fraction. From this graph it can be seen that Ca²⁺ increases with depth while K⁺, Mg²⁺, and Na⁺ decrease. As the majority of the Ca²⁺ and Na⁺ ions in the <0.1 μm fractions are in exchange positions, these

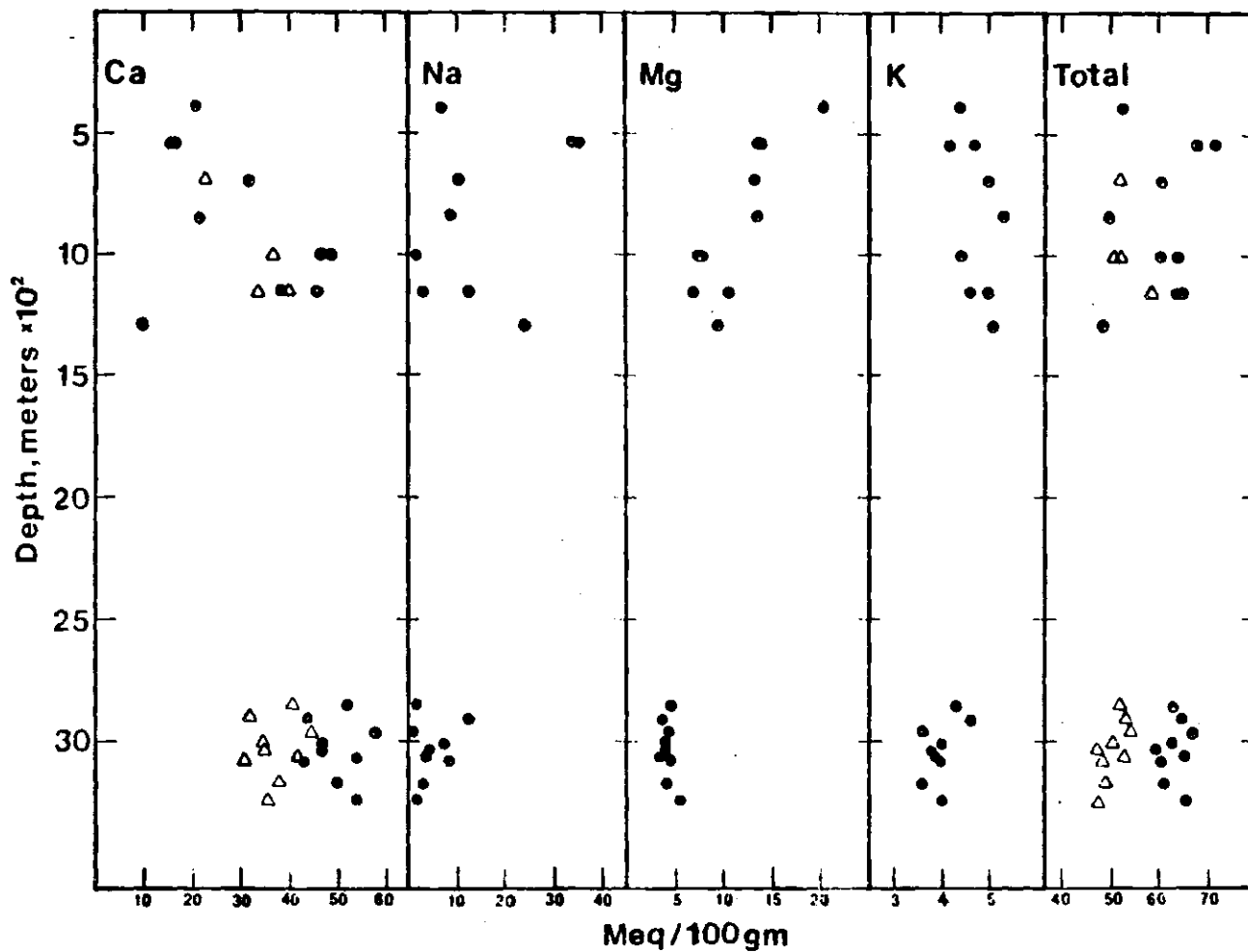


Figure 26. Variation in the Exchange Ion Chemistry of the $<0.1 \mu\text{m}$ Fraction with Depth. (● = Uncorrected, Δ = Corrected for CaCO_3 Dissolution During Ba^{II} Replacement)

trends will regulate the Na and Ca trends in the $<0.1 \mu\text{m}$ fraction. The increase in Ca^{2+} at the expense of other exchange ions was also noted by Weaver and Beck (1971) in their bulk sample exchange ions. Interpretation of these trends is not straightforward as the methods used in washing and fractionation can readily alter the exchange ion population. As discussed earlier in examining the H_2O leach chemistrys, the dilution of the interstitial solution increases the exchange site selectivity of the exchange medium for divalent ions thus tending to replace K^+ and Na^+ with Mg^{2+} and Ca^{2+} . The amount of replacement would depend on ion concentrations in the solution in contact with the clay as well as treatment methods employed. The dissolution of solids during washing and fractionation can provide additional ions to participate in ion exchange (particularly Ca^{2+} from CaCO_3). If CaCO_3 still remains in the sample when it is treated with BaCl_2 , then additional Ca^{2+} will be present in the liquid analyzed and the sum of the exchange ions that are measured will be greater than the actual total exchange capacity by the amount of Ca^{2+} added. The extent of this effect in the $<0.1 \mu\text{m}$ fractions can be estimated by plotting the $<0.1 \mu\text{m}$ percent 17 A layers (from Table 8) vs. total exchange capacity (Table 15) in Figure 27. This figure shows that most of the points plot above a line which runs from 20 meq/100 g at 0% 17 A to 90 meq/100 g at 100% 17 A. The four samples lowest in exchangeable or total Ca which are

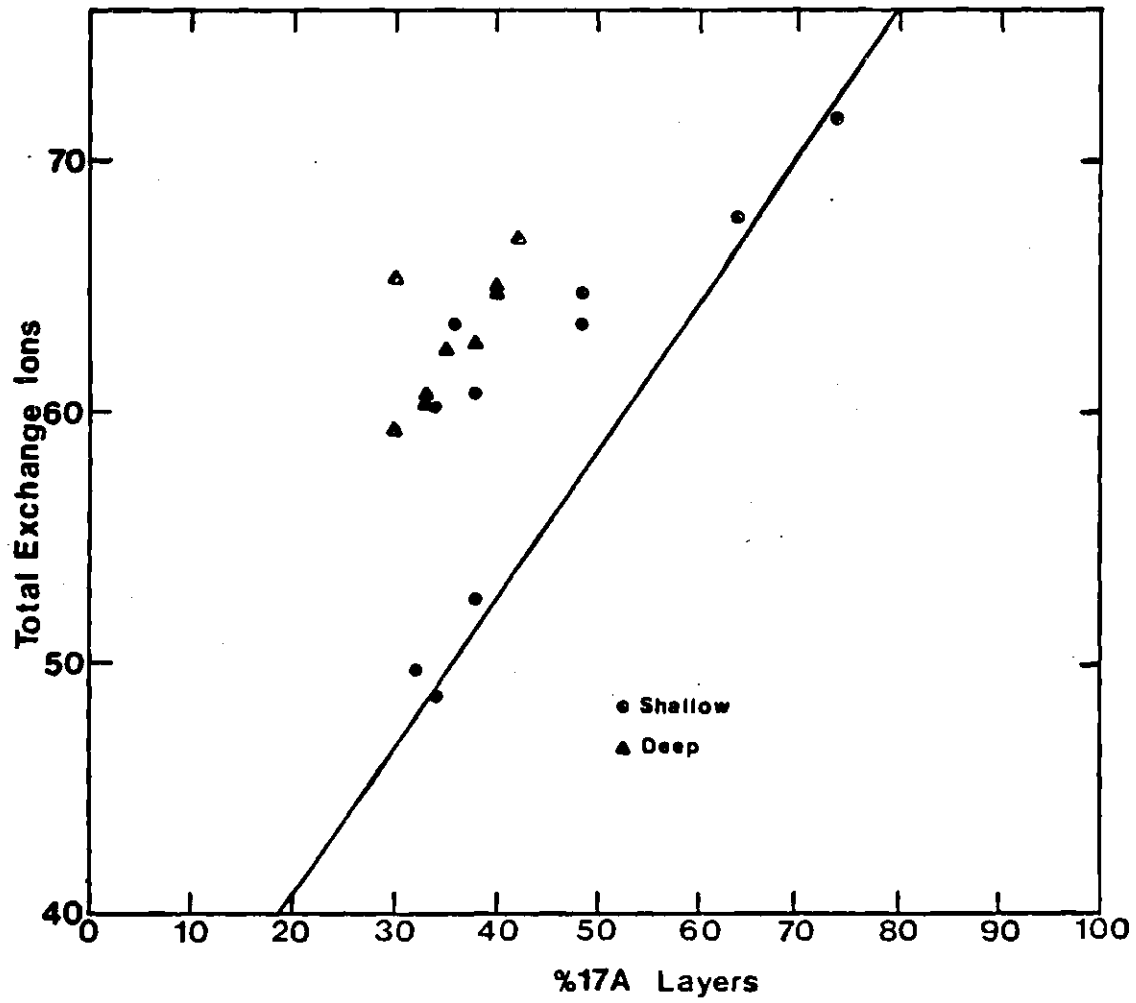


Figure 27. Total Exchange Ions (as Meq/100 gm) vs. % 17A Layers in <math><0.1 \mu\text{m}</math> Fraction.

also low in coarse fraction calcite plot along this line. If it is assumed that all of the excess apparent exchange capacity is due to dissolution of non-exchange calcium (from CaCO_3) during BaCl_2 treatment, then the apparent total exchange and apparent calcium in exchange values are all to high by about 10 meq/100 g except 390, 538 I and II, 844 and 1289. This corresponds to ~0.02 weight percent calcium coming from a source other than exchange ions. It is likely that these samples, which all contain CaCO_3 in the coarse fraction, have had their exchange ion populations altered by the dissolution of CaCO_3 during washing and fractionation and the subsequent migration of Ca^{2+} to exchange positions. While exchange values (Ca and Total) in the $<0.1 \mu\text{m}$ fraction can be corrected for dissolution of CaCO_3 during BaCl_2 leaching (crosses in Table 26) it is still uncertain what the extent of population alteration is. In the corrected $<0.1 \mu\text{m}$ exchange ions Ca^{2+} still increases and other ions decrease with depth. However, the corrected total exchange capacity now shows signs of a depth related decrease. Except for this decrease, which is probably the result of diagenetic loss of exchange capacity, the corrected exchange ion values will not necessarily represent in situ exchange populations. The presence of a depth related exchange ion Ca increase in Gulf Coast bulk samples similar to the increase seen in the $<0.1 \mu\text{m}$ fraction of this study (Weaver and Beck, 1971) where sample treatment, and thus sample alteration, should be less

severe, suggests that exchange of divalent ions for monovalent ions in exchange positions with depth may be diagenetic.

4. Variation of Interstitial Waters During Pelitic Sediment Burial

The interstitial waters of terrigenous sediments undergoing marine deposition can be chemically altered by a number of processes. Proposed processes resulting in interstitial solutions differing from sea water composition include:

1. Osmotic flow of water across semi-permeable membranes from a dilute solution to a more concentrated solution (Hanshaw and Zen, 1965; White, 1965).
2. Migration of ions across semi-permeable membranes in response to a pressure gradient exceeding osmotic pressures (reverse osmosis) (DeSitter, 1947; Marshall, 1948; McKelvey and Milne, 1962; Beck and Berner, 1965; White, 1965; Berry, 1969; Hanshaw and Coplan, 1973; Kharaka and Berry, 1973).
3. Formation of chemical inhomogeneities in the pore solutions due to the presence of exchange media, and subsequent expulsion of the more mobile, chemically distinct, waters furthest from the clay surfaces, during early compaction (Von Englehart and Gaida, 1963; Chilingarian, et al., 1973; Rosenbaum, 1976).
4. Gravity settling of ions in solution and migration of ions due to thermal gradients (Soret effect,

Thermal pumping) (Manglesdorf, et al., 1970).

5. Migration of ions due to electric potentials in sediments (Adamson, et al., 1966; Reike, et al., 1966).
6. Removal or addition of ions or water through diagenetic interaction with the solid sample (DeSitter, 1947; Manheim and Sayles, 1974; Beck and Berner, 1965; Powers, 1967; Burst, 1969; Sayles and Manheim, 1975).
7. Variations in the chemistry of water trapped in the sediments during deposition (DeSitter, 1947; Broecker, 1974).
8. Mixing of subsurface waters of varying compositions (Rittenhouse, 1967; Billings, et al., 1969; Manheim and Sayles, 1974; Sayles and Manheim, 1975).

Once the above processes have acted to create chemical gradients the process of diffusion can act to smooth the original gradients (Anikouchine, 1967; Manheim, 1970; Berner, 1971; Gieskies, 1975). The magnitude and effects of these processes in situ are at present poorly understood, particularly with regard to the role of variable sediment composition, permeability and porosity, pressure and temperature with depth and the effects of the various processes on individual ions.

In general the effects of gravity settling and thermal pumping (Manglesdorf, et al., 1970) will be to increase concentrations with depth. However, these effects should only

be recognizable in thick, permeable units since thermal, physical, and electrical discontinuities at unit boundaries will alter sediment conditions.

Semi-permeable membranes can also provide for changes in interstitial salinity with burial as reservoir solutions are concentrated relative to effluent solutions due to membrane filtration (McKelvey and Milne, 1962). This phenomena can be attributed to the exclusion of anions from the negatively charged pores of clays rich in exchange sites (White, 1965; Hanshaw and Coplan, 1973; Kharaka and Berry, 1973). When two solutions of differing salinity are separated by a clay membrane, osmotic water flow will take place from the low salinity side to the high salinity side (Van Everdingen, 1968) creating increased pressures on the high salinity side (Hanshaw and Zen, 1965). If pressures in excess of the osmotic pressure are applied to the high salinity side, reverse osmosis (membrane filtration) will occur. In laboratory experiments, Lutz and Kemper (1959) determined that large, non-polar organic molecules pass through clay membranes 10^5 - 10^6 times faster than the polar water molecule and Mokady and Low (1968) observed a flux for H_2O approximately 500 times greater than $NaCl$. Since deeper sediments have generally lost more of their original pore fluid than shallow sediments and had more fluid pass through their pores, the probability of encountering more saline, residual solutions at depth is enhanced. The formation and location of

membrane concentrated solutions is complicated by the alternating nature of large and small sand and shale units in a depth sequence.

Van Everdingen (1968) states that Na is more mobile than Ca during membrane filtration. Berry (1969) concludes that monovalent ions are more mobile than divalent. Kharaka and Berry (1973) observed cation mobility sequences of Li (most mobile) > Na > K > Rb > Cs for monovalent ions and Mg (most mobile) > Ca > Sr > Ba for divalent ions. The greater retardation of divalents relative to monovalents was not observed by Kharaka and Berry (1973). They attribute the lack of this effect to the high hydraulic flow, relative to natural systems, used in their experiments.

During the early stages of compaction, where sediment porosities are high, membrane filtration does not appear to take place (McKelvey and Milne, 1962; Bischoff and Ku, 1970). However, in sediments with appreciable exchange capacities, undergoing early compactive dewatering, changes in the composition of the water expelled may occur. During low pressure compaction experiments with montmorillonite, Von Engelhardt and Gaida (1963) observed a higher salinity solution being expelled than the original pore water salinity and calculate a decrease in the residual pore water salinity with increasing pressure resulting from this. Chilingarian, et al., (1973) conclude that the expulsion of a solution more concentrated than the initial pore water is responsible for decreasing the

concentration of the remaining solution during early compaction. Rosenbaum (1976) observed decreases in the salinity of the solution expelled with increasing compaction which is consistent with a lowering of pore water salinity if the initial solution expelled were more saline than the original pore water. Failure to observe this effect in kaolinitic clays (Von Engelhardt and Gaida, 1963) indicates that an inhomogeneous pore water chemistry, resulting from the presence of an exchange medium, is responsible for early compactive chemical fractionation and that the furthest solution from clay, being more mobile, is expelled first and must thus be more saline (Rieke and Chilingarian, 1974).

Wyllie (1949, 1951) demonstrated that the self-potential measured in electric well logging may result from the electric potential of semi-permeable membranes. These natural electric currents can result in the migration of anions and cations to the cathode and the anode respectively, and may promote the formation of segregated environments and the precipitation of various minerals (Rieke, et al., 1966; Serruya, et al., 1967). The operation of this process should be confined to single units as electrical discontinuities typify sediment boundaries.

Variations in the chemistry of the bottom waters included with deposition can result from changes in the proximity of the sedimentation site to nearshore sources of low salinity water or to changes in the composition of sea

water with time (Broecker, 1974).

The mixing of subsurface waters of different compositions will occur primarily in permeable sand units as a result of the influx of waters from distant or near by sources. The invading waters can include fresh waters from recharge zones in subareally exposed extensions of the permeable unit (Rittenhouse, 1967; Billings, et al., 1969; Manheim and Sayles, 1974), waters high in dissolved NaCl as a result of contact with buried salt deposits (Manheim and Bischoff, 1969; Manheim, 1970) or waters expelled from shales during compaction (Chapman, 1973; Magara, 1974).

The lack of equilibrium between the solid and aqueous phases during burial can result in mineral instabilities and in the formation of new assemblages. This may or may not result in large changes in the water chemistry depending on the nature of the reaction involved. If changes occur in the aqueous chemistry due to diagenetic events, they may potentially be significant in magnitude as the loss of a small percentage of an element from the solid (comprising ~90% of the bulk sample weight) to the liquid (10%) will result in a prominent increase in the interstitial content.

After one or more of the above mentioned processes have provided variations in composition of interstitial waters over vertical sections, the process of diffusion can act to modify the existing chemistry. In sediments of low porosities and high porosities (Gieskies, 1974; Berner, 1975)

diffusion is seen to be a prominent mechanism for chemical alteration. Diffusion phenomena can be observed in operation near the sediment-water interface (Anikouchine, 1967; Geiskies, 1975) and near zones of NaCl emplacement (Manheim, 1970). Diffusion may be important in producing nodules and concretions and authigenic layer-type sediments. These would result from migration and precipitation of ions at environmentally maintained chemical boundaries (Berner, 1969, 1971). This process may be the cause of appreciable siderite, pyrite, and calcite nodules in deeper sediments (Weaver and Beck, 1971; Sayles, et al., 1972 and this study). In general, in shallow clay sediments, anions should show high diffusion rates followed by monovalent cations and then divalents cations (Berner, 1971). With increasing depth, the anion exclusive properties of compacted clays with negatively charged surfaces, should act to inhibit diffusion.

Data on the interstitial water chemistry of Tertiary pelitic sediments is available from the following sources:

1. Waters flowing from reservoir rocks, penetrated during exploration for oil,
2. Leaching analysis of deep Gulf Coast shales,
3. Squeezing analyses of shallow marine pelitic sediments, and
4. Squeezing analyses of deep pelitic shales.

Sandstone water analyses are presented by a number of authors. Of particular interest to this study are the

sandstone water analyses from Gulf Coast Tertiary formations (Dickey, et al., 1972; Schmidt, 1973; Collins, 1975). These data have been plotted in Figure 28a-f as Gulf Coast Tertiary sandstone analyses.

Leaching techniques, discussed earlier, were used by Weaver and Beck (1971) and Schmidt (1973) to analyze deep shale samples from the Gulf Coast Tertiary. Murthy and Farrell (1972) provide leach analyses for three shallow Gulf Coast pelitic sediments (no Cl values). These data are not presented in Figure 28a-f as absolute values and ratios are suspect in leaching methods. Depth related trends revealed by leaching may have some significance and will be described where warranted.

The bulk of the available data on interstitial waters of pelitic sediments is concentrated in the area of shallowly buried, slowly accumulating, terrigenous sediments mixed with varying amounts of marine pelagic sediments. The Deep Sea Drilling Project (DSDP) (Manheim, et al., 1968; Chan and Manheim, 1970; Sayles, et al., 1970; Manheim, et al., 1970; Manheim, et al., 1973; Sayles, et al., 1972; Waterman, et al., 1973; Manheim, et al., 1974; Gieskies, 1974; White, 1975) provides major element chemical analyses of interstitial waters, obtained by squeezing, from ~40 holes which penetrate predominantly Tertiary terrigenous sediments with sedimentation rates ranging from 1 to 100 cm/10³ years (the samples of this study have much higher sedimentation rates). None

of the wells except one (site 241 TD = 1200 m) have pore water analyses below 800 m and on only ~35 of these wells have reasonably complete interstitial water compositions been determined. Additional squeeze data is available from some near shore Gulf of Mexico cores studied by Manheim and Bischoff (1969). The DSDP data on Manheim and Bischoff (1969) data are plotted in Figure 28a-f as shallow pelitic sediments.

The only squeeze analyses of deep Tertiary pelitic sediments available for comparison with the data from this study are the data of Russell (1971). This consists of two deep (3200 m and 3962 m) Gulf Coast sediment squeeze analyses.

Examination of Cl content with depth for the Gulf Coast Tertiary sandstones, pelitic sediments (shallow), Russell's two deep samples and the data of this study (corrected for evaporation), allows the recognition of several systematic variations in Cl content (Figure 28a). The interstitial Cl in shallow pelitic sediments shows no major systematic deviations from sea water. Above 800 m, the shallow pelitic sediment Cl values range from 17 to 23 ppt except for samples associated with salt intrusions which may have considerably higher Cl contents. The DSDP well with the deepest pelitic pore water analyses (site 241 TD = 1200 m) shows a constant decrease in salinity to ~15 ppt. This may be due to the early compactive removal of more saline waters (Von Englehardt and Gaida, 1963; Rosenbaum,

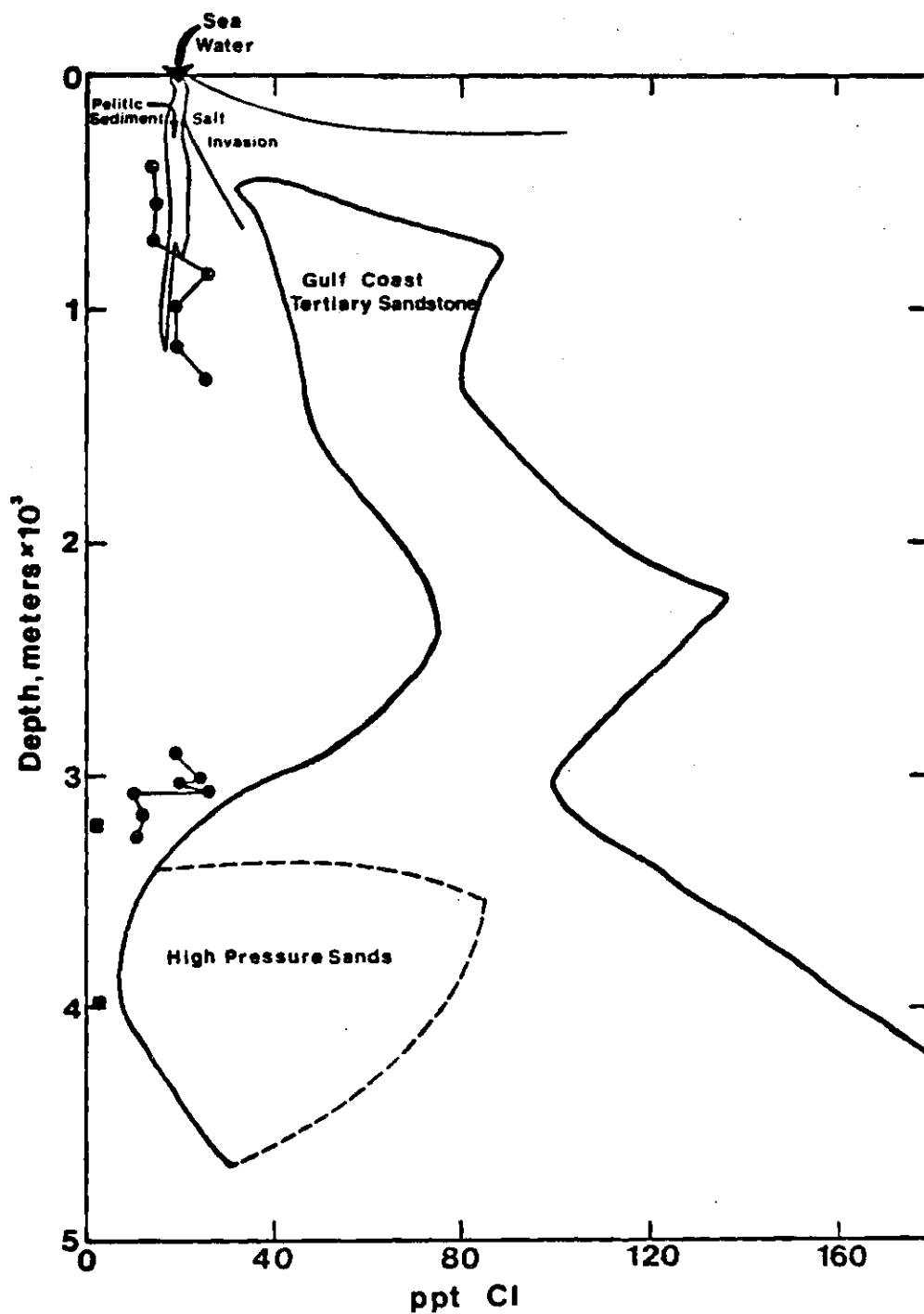


Figure 28a. Interstitial Chloride Variations with Depth in Pelitic Sediments and Gulf Coast Tertiary Sands. (Pelitic sediment data from Deep Sea Drilling Project Reports and Manheim and Bischoff (1968); sandstone data from Schmidt (1971), Dickey, et al., (1972), and Collins (1975); ■ = Deep Gulf Coast shale waters, Russell (1971); ● = This Study, corrected for evaporation.)

1976; and others) or meteoric exchange (Manheim and Sayles, 1974; Gieskies, 1974). The shallow samples of this study show no definite trend in view of the $\pm 20\%$ error associated with the evaporation correction, however the lower than sea water values obtained for the shallowest three samples (390, 538 and 692) would tend to confirm the operation of a shallow mechanism in pelitic sediments that results in lower Cl contents in the interstitial water of the shale. Invasion of meteoric waters into fine grained sediments of less than 700 m depth in the Gulf Coast does not seem likely as a source for the observed Cl reduction nor does changes in the salinity on deposition as the wells studied were offshore in water depths of ~25 meters. If the evaporation correction is accurate, salinity of the shale waters exceeds average sea water below 800 m. This may be the result of the initiation of reverse osmosis below 800 m, where the porosity is reduced sufficiently. Better evidence for reverse osmosis is present in the sandstone water Cl analyses (Figure 28a) where a general trend toward increasing salinity with depth is consistent with membrane filtration of water passing out of sandstones if, in general, greater depth of burial implies filtration of greater amounts of solution. As thick shale units will block water flow from sands (Champman, 1973; Magara, 1974a) the filtration of reservoir sand waters must result from passage of water along faults and fractures, through thin shale units and laterally. Some of the initial

sandstone Cl increase may result from the loss of more saline water from the shallow shales to the sands. This Cl increase in the sands with depth, which is visible throughout the entire range of normally pressurized sandstones, is not evident in the sands associated with the main high pressure zone. This reduction in sandstone Cl is apparently associated with the presence of over-pressurized shales (Schmidt, 1973). The deep shale samples from this study have essentially the same range (19-26 ppt) as the shales from 800-1300 m indicating that if membrane filtration is occurring in the thick shales, it is moderated by some other process. The deepest three samples of this study (all from well A4), which are apparently within the high pressure zone (Figure 3), show no depth related trend, however they do show considerably lower Cl contents (10-12 ppt) than the shallower samples. The squeeze data of Russell (1971), which are apparently also within the high pressure zone, show further reduction in chloride. The leach data of Weaver and Beck (1971) (~1:20d) confirm the presence of a reduction in Cl into the high pressure zone although their Cl values are all apparently too low. The leach data of this study (Table 6), corrected for evaporation using the correction factor of Table 20, indicates ~19 ppt for samples 538 and 2906 and a decrease below this (17.9 ppt at 3007 m and 16.8 ppt at 3064 m). The shale data (leach) of Schmidt (1973) (ethanol-H₂O leach) show generally lower Cl values than those of this study, which rise

to a maximum of around 10 ppt at about 600 meters above the high pressure zone and then decrease again with depth. These decreases in Cl concentration associated with the high pressure zone could be evidence that the release of structural water (Burst, 1976) low in Cl to the pores is responsible for the lower interstitial water Cl contents of the shales and the sands as well as the higher fluid pressures below ~3000 m.

The use of ion/Cl ratios in examination of variations of ions other than Cl will eliminate the uncertainty in the evaporation correction. However, the problem of temperature correction still remains. Cl and Na require little if any correction. Corrections for K and Mg have been estimated. Ca and SO₄ showed no single systematic temperature change in the data of Russell and Fallgatter (1972) used to analyze temperature variations. The maximum Ca and SO₄ loss from interstitial waters upon heating is ~20% at temperatures of about 70°C (Figure 7).

The Na/Cl ratio (Figure 28b) for shallow pelitic sediments shows no systematic variation from average sea water (average = .55 Na/Cl) although some of the salt invaded samples have Na/Cl ratios considerably below other samples of similar depth. The reason these low Na/Cl ratios in salt invaded samples is not clear, as mixing with water containing dissolved NaCl (Na/Cl = ~.65) should result in higher Na/Cl ratios. The shallower samples of this study show a constant

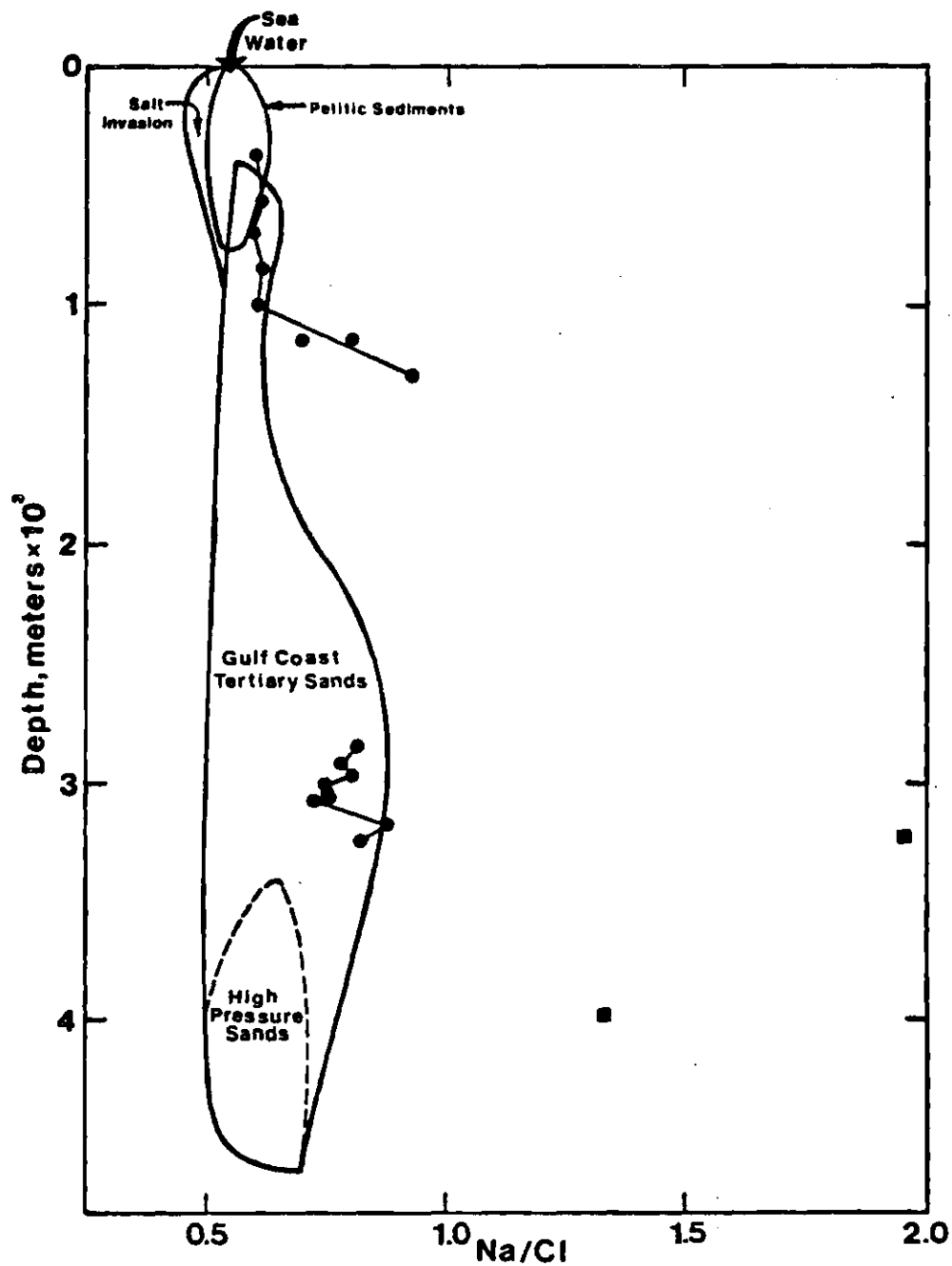


Figure 28b. Interstitial Na/Cl Variations with Depth in Pelitic Sediments and Gulf Coast Tertiary Sands. (Pelitic sediments data from Deep Sea Drilling Project Reports and Manheim and Bischoff (1968); sandstone data from Schmidt (1971), Dickey, et al., (1972), and Collins (1975); ■ = Deep Gulf Coast shale waters, Russell (1971); ● = This Study.)

Na/Cl ratio of $.60 \pm .02$ down to 1000 m. Below this depth the Na/Cl ratio increases, remaining above .70 for the remaining shallow samples as well as the deep samples. A similar increase in the Na/Cl ratio of some Gulf Coast Tertiary sands occurs below 1800 m. The loss of Na from exchange positions (discussed earlier) to the interstitial waters may be responsible for the increase in interstitial Na. Na-feldspar decomposition may also contribute. No clear effect on the Na/Cl ratio can be seen entering the high pressure zone in either sands or shales, although the data of Russell (1971) suggests that the Na/Cl ratio is extremely high below 3000 m. As can be seen in Figure 28c-f, the other ion/Cl ratios of Russell (1971) consistently plot higher than would be expected from pore water data of other sources. This may be the result of faulty Cl data for these analyses. If the Cl values are actually 2-4 times the recorded value (particularly the shallower sample) this would reduce most of Russell's ion/Cl ratios to values more consistent with the other analyses while still retaining Cl values below the lowest encountered in this study. The leach data of Weaver and Beck (1971) and Schmidt (1973) provide Na/Cl ratios all in excess of 1.0. The Na/Cl ratios for the leach samples of this study (from Table 5) are also high. This is due to the systematic error induced by the leaching technique (Na leached from the solid). Despite the inaccuracy of the absolute Na/Cl leach data, Weaver and Beck (1971) and Schmidt (1973)

observe a general Na/Cl increase with depth.

K/Cl ratios, presented in Figure 28c will be affected by the temperature of squeezing. As discussed earlier, raising the temperature above in situ temperatures will result in increases in the interstitial K content. Corrections have been applied to correct the K data of this study to the concentrations at in situ temperatures (Table 19). Evidence of this temperature induced deviation can be seen in the shallow pelitic sediment data (Figure 28c) where the K/Cl ratios of the shallowest samples range from .020 to .028 (sea water = .020). Despite the temperature ambiguity a noticeable K decrease occurs in the shallow pelitic sediments. A similar marked K depletion is already apparent in the shallowest samples of this study. Shallow sands are also depleted in K relative to Cl. This loss of interstitial K during early burial must be the result of uptake of K into the solid. As there is apparently not enough exchange K to account for interstitial K loss the bulk of this potassium probably enters non-exchange clay sites. The loss of 300 ppm K from the interstitial water of a sample containing 20% by weight pore water, would result in the addition of .01% K to the solid. Thus the shallow diagenetic uptake of K into the solid can best be observed by examining interstitial water chemistry. K/Cl ratios remain fairly constant after the initial drop off until the high pressure zone is encountered. At this depth there is evidence for increases

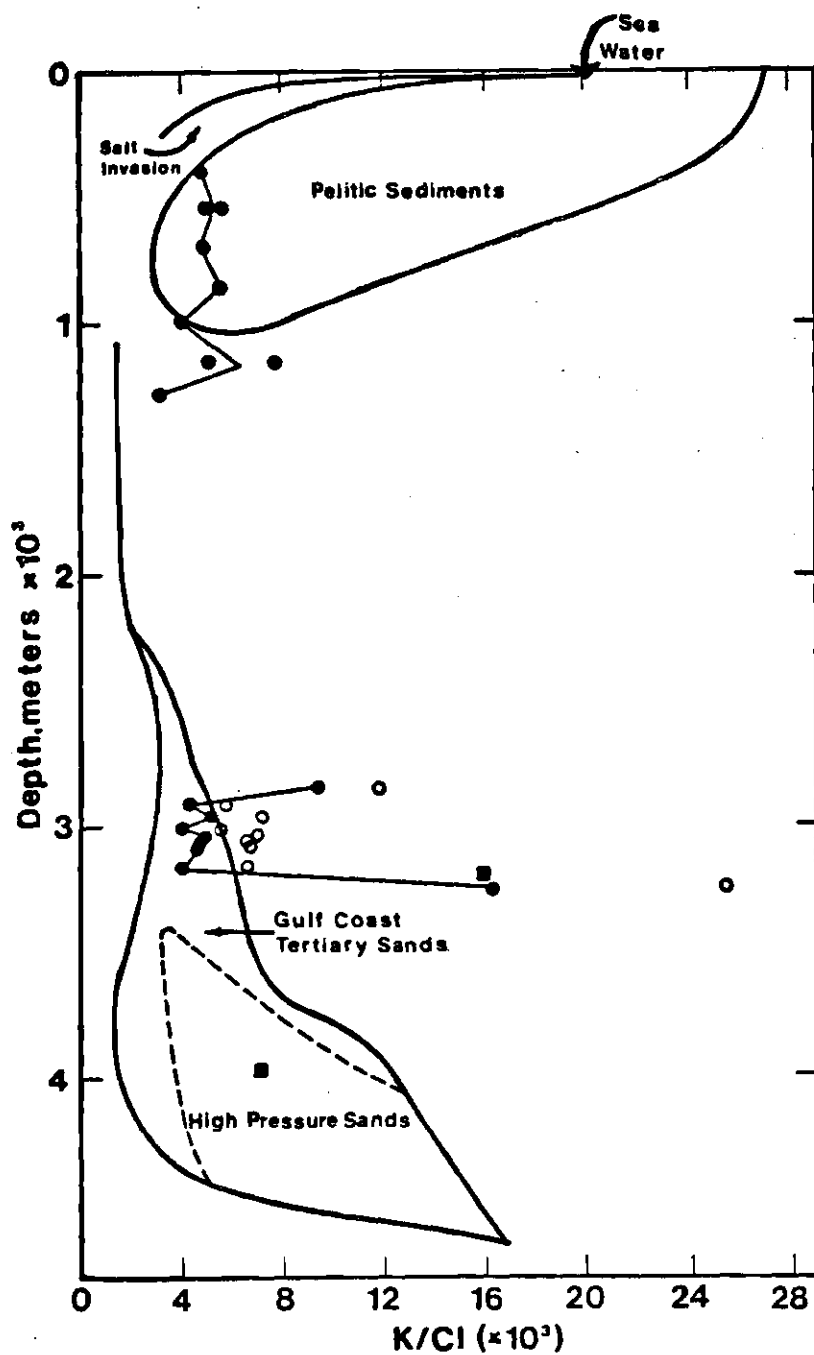


Figure 28c. Interstitial K/Cl Variations with Depth in Pelitic Sediments and Gulf Coast Tertiary Sands. (Pelitic sediment data from Deep Sea Drilling Project Reports and Manheim and Bischoff (1968); sandstone data from Schmidt (1971), Dickey, et al., (1972), and Collins (1975); ■ = Deep Gulf Coast shale waters, Russell (1971); ● = This Study; ○ = This Study (temperature corrected).)

in interstitial K in the sample at 3241 m of this study as well as the high pressure sand waters and possibly the data of Russell (1971). Weaver and Beck (1971) and Schmidt (1973) also show an increase in their leach K/Cl ratios at the high pressure zone, although again their ratios are abnormally high. This increase in interstitial K at depth could be the result of release of K from clays during dewatering or the decomposition of K-feldspars (Hower, et al., 1976). High K/Cl ratios in sandstones below 3000 m, in the high pressure zone, would result from invasion of high K/Cl waters from the shales during dewatering of the over-pressurized zone.

Interstitial Mg/Cl ratios (Figure 28d) show effects similar to K/Cl during early burial. Since the magnesium content of waters is depleted in cores warmed from sea bottom to laboratory temperatures the range of shallowest pelitic sediment Mg/Cl ratios is expanded in the low Mg direction from average sea water. Rapid loss of interstitial Mg with depth occurs in both the shallow pelitic sediments and the shallow samples of this study. Shallow Gulf Coast tertiary sandstone waters are also depleted in Mg. As was the case with K, the interstitial Mg loss can probably be attributed to absorption by the solid. However, the Mg decrease in exchange positions with depth observed in this study (if real) rules out migration of Mg into exchange sites. The most likely sites for migration of Mg into the solid include interlayer ($Mg(OH)_2$) or octahedral clay positions or

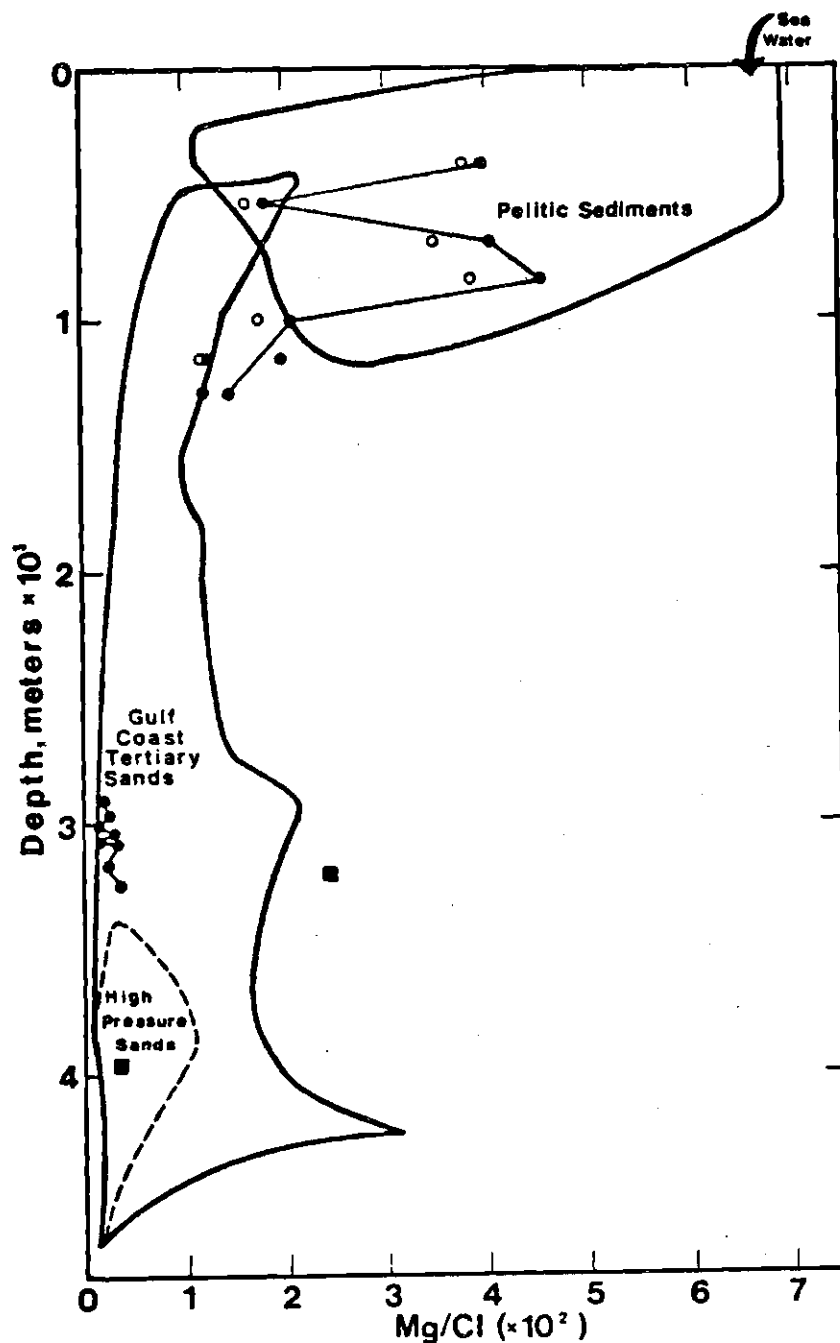


Figure 28d. Interstitial Mg/Cl Variations with Depth in Pelitic Sediments and Gulf Coast Tertiary Sands. (Pelitic sediment data from Deep Sea Drilling Project Reports and Manheim and Bischoff (1968); sandstone data from Schmidt (1971), Dickey, et al., (1972), and Collins (1975); ■ = Deep Gulf Coast shale waters, Russell (1971); ● = This Study; O = This Study (temperature corrected).)

carbonate minerals. The absence of dolomite peaks on X-ray patterns of most of the deep samples of this study and the decrease in $<0.1 \mu$ MgO with depth would indicate the minor effect on the solid content of this absorption. Another possible Mg sink would be the formation of Mg rich calcite, however this is seen to be diagenetically improbable (Berner, 1971). The precipitation of Mg rich compounds in the sands accompanied by diffusion may result in loss of Mg from the shale waters. It is also possible for facies changes with depth to mask the addition to the solid of Mg provided by the pore water. The role of Mg in release of iron from clays (Drever, 1971b) is apparently filled, in these samples by aluminum. The Mg/Cl ratio continues to decrease from shallow to deep samples of this study, while there may be some evidence for Mg release to the water in the suspect data of Russell (1971). Although Mg migrates to the solid during leaching thus causing errors in leach determined Mg/Cl ratios, both Weaver and Beck (1971) and Schmidt (1973) report Mg/Cl shale water increases with depth into the high pressure zone. However this increase is not seen in the high pressure sands and any increase in the deep samples of this study is probably below detection limits.

The Ca/Cl ratio (Figure 28e) in shallow pelitic sediments shows both increases and decreases relative to average sea water. This is probably caused by varying degrees of CaCO_3 saturation in the initially deposited sediments. In

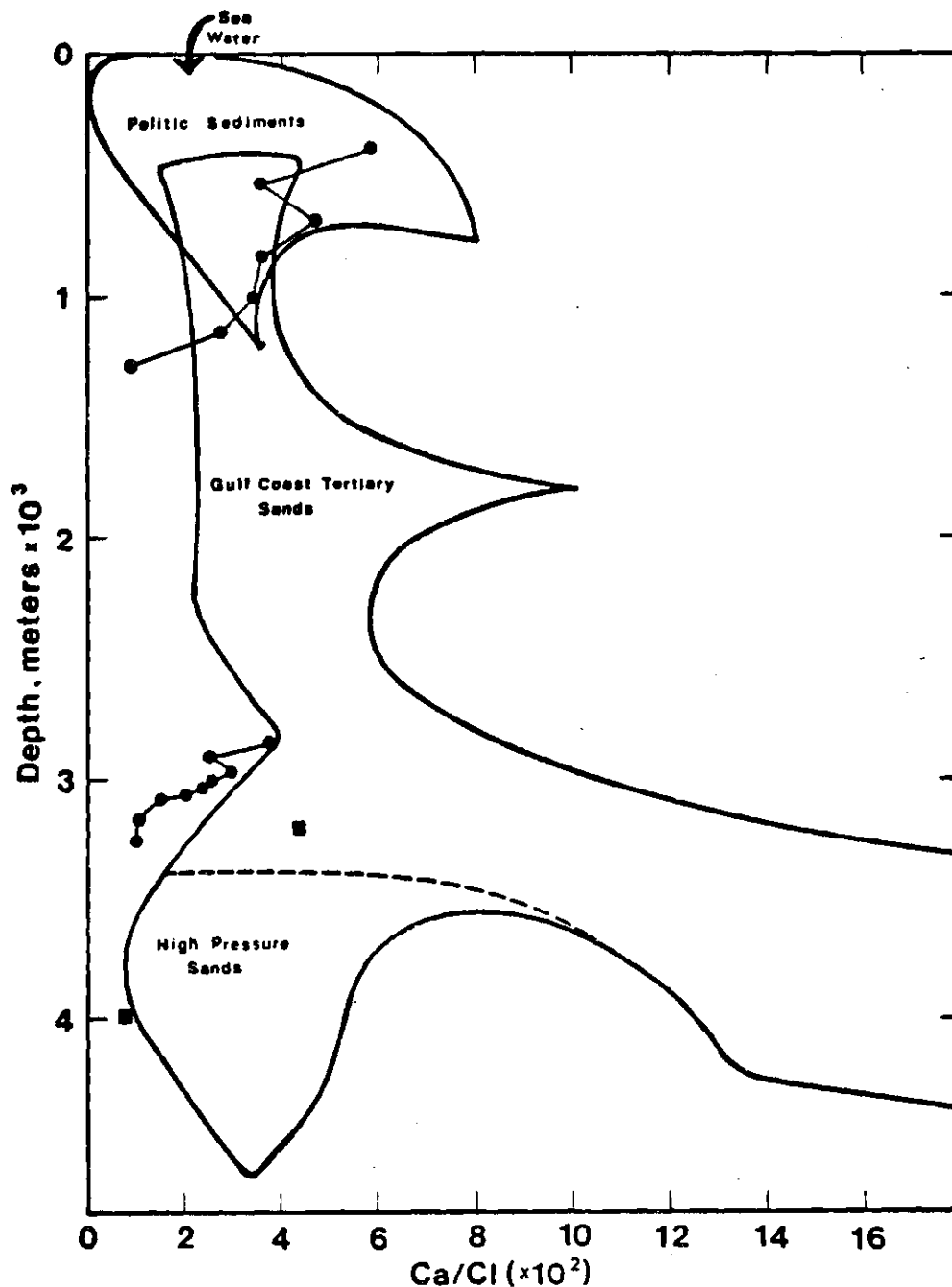


Figure 28e. Interstitial Ca/Cl Variations with Depth in Pelitic Sediments and Gulf Coast Tertiary Sands. (Pelitic sediment data from Deep Sea Drilling Project Reports and Manheim and Bischoff (1968); sandstone data from Schmidt (1971), Dickey, et al., (1972), and Collins (1975); ■ = Deep Gulf Coast shale waters, Russell (1971); ● = This Study.)

general, high interstitial Ca/Cl ratios predominate below 400 m. No definite statement on Ca corrections can be made although, as discussed earlier, there is evidence suggesting a maximum depletion on warming of 20%. The shallow shales of this study are initially higher than sea water in their Ca/Cl ratios. The Ca/Cl drop below 1000 m complements the Na/Cl increase and may be related to exchange ion equilibria. Shallow tertiary sands have Ca/Cl ratios higher than sea water and in normally pressured sands this ratio increases with depth. This can be attributed to the retardation of Ca during reverse osmosis (White, 1965). The deep samples of this study again show a decrease in Ca/Cl with depth from values equivalent to shales at the 1000 m level down to values equivalent with the 1289 sample. This decrease may again be the result of exchange phenomena, however the presence of appreciable authigenic CaCO_3 in sample 3241 indicates that calcite precipitation in a caprock at the top of the high pressure zone may be the more important reaction. The low Ca/Cl ratios of the pressurized sands confirms that inter-layer water release does not result in release of Ca to the pore waters. The shale leach data of Weaver and Beck (1971) and Schmidt (1973), while highly susceptible to CaCO_3 dissolution and absorption of Ca on exchange sites, also shows evidence for Ca loss going into the high pressure zone. The presence of appreciable organic material, providing aqueous carbonate species, as well as the inaccuracy of pH determina-

tions, make calculation of calcite solubility impractical.

The shallow pelitic sediment interstitial SO_4/Cl ratios (Figure 28f) show considerable scatter but values are generally less (often considerably less) than sea water due to the effects of bacterial reduction (Manheim and Sayles, 1974; Geiskies, 1975). Some of the deeper DSDP wells show a reversal at depth back toward increasing SO_4 . The data from this study show considerable scatter with values generally at or above the average sea water SO_4/Cl ratio (Figure 28f). There is a suggestion of a slight systematic rise to around 3000 m followed by a marked rise into the high pressure zone. The SO_4 content of sample 3242 probably continues this trend, as the deficiency in anion charge shown by the chemical analyses of sample 3242 is consistent with an appreciable sulfate content for this sample. Russell (1971) also confirms SO_4 release in the high pressure zone. The increase in shale interstitial SO_4 above the high pressure zone should imply a cessation of the reduction of sulfate. However, the effect of recovery and storage of deep shale cores with reducing interstitial waters would be to promote the oxidation to SO_4 of any reduced species (Beck Pers. Comm.). This raises the possibility that the sulfate analysis performed may in fact be a measure of total dissolved sulfur. The situation can be further complicated by loss of H_2S , if present, during handling. A general increase in dissolved sulfur species with depth could be ascribed to

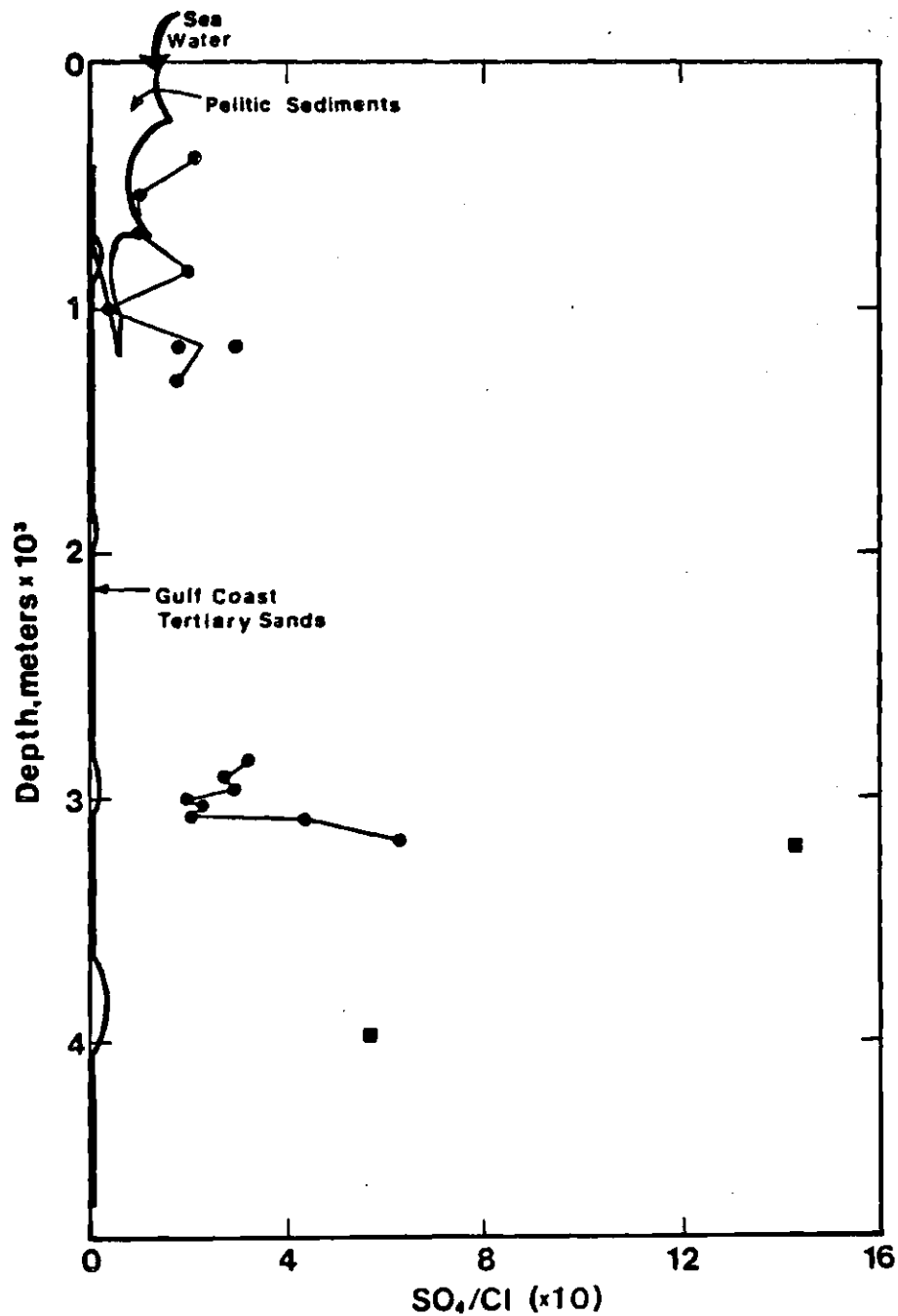


Figure 28f. Interstitial SO_4/Cl Variations with Depth in Pelitic Sediments and Gulf Coast Tertiary Sands. (Pelitic sediment data from Deep Sea Drilling Project Reports and Manheim and Bischoff (1968); sandstone data from Schmidt (1971), Dickey, et al., (1972), and Collins (1975); ■ = Deep Gulf Coast shale waters, Russell (1971); ● = This Study.)

organic decomposition with the increase into the high pressure zone being the result of increased organic reactivity at the temperatures of this depth (Jones, 1975 in Kharaka, et al., 1976) or release and decomposition of organics formerly bound in between clay layers. The removal of some solid sulfur containing compounds by leaching (Table 22) could be due to dissolution and decomposition of organic material. Weaver and Beck (1971) and Schmidt (1973) both show SO_4/Cl increases with depth for leach analyses. The marked depletion in SO_4 relative to chloride shown by Gulf Coast Sands indicates the presence of reducing conditions throughout. The high pressure sands described by Schmidt (1973) show the highest SO_4/Cl sand water ratios indicating that increased sulfur release in the high pressure shales affects the associated sandstone waters.

In the shallow pelitic sediments the HCO_3/Cl ratios show an initial increase of up to an order of magnitude or more. This can be attributed to bacterial attack on organic matter (and accompanying carbonate dissolution phenomena). The shallow pelitic sediment bicarbonate concentrations appear to drop off at depth, returning to near sea water values. The HCO_3/Cl ratios of this study (from Table 1) lie near sea water ratios in the shallow portions of the core (~120 ppm HCO_3) and are considerably higher (695 and 450 ppm HCO_3 at 2906 and 2961 respectively) at depth, falling off to 45 ppm at 3038 m. Unfortunately, HCO_3 analyses deeper

than 3038 m were not obtained in this study leaving doubt as to the relationship of the deep sample HCO_3 data to the high pressure zone. The data of Russell (1971) does not serve to clarify the situation as his extremely high HCO_3/Cl ratios may be influenced by open vessel titration for HCO_3 . The data in this study were obtained by IR analysis of sealed samples. Neither can the leach data of Weaver and Beck (1971) and Schmidt (1973) be of any help here since, as discussed earlier (Table 22), large scale alteration of HCO_3 content is encountered during leaching. The sandstone water data from Schmidt (1973) does give some indication of HCO_3 release in the high pressure zone as high pressure sands show the same increase (but more pronounced) as was seen for SO_4 . All other Gulf Coast Tertiary sands have low HCO_3/Cl ratios. Carbon and sulfur data might be expected to be related, both being involved in organic associations, and therefore increases in HCO_3 in the high pressure sands may also be due to release from shales in the high pressure zone.

A pattern similar to HCO_3 is found with the organic carbon data of this study (Table 1) with shallow values around 50 ppm and deep (~3000 m) values of several hundred parts per million. These analyses probably include a considerable amount of colloidal organic material as well as organic carbon in true solution (Beck and Reuter, 1977). The leach values (Table 5) are also quite high. The SO_4 , HCO_3 and organic carbon data of this study are too limited for

interpretation. All appear to be linked to phenomena at the high pressure zone in both shales and sands. Possible sources include the release of bound organic matter during smectite-illite transformation and the onset of significant organic reactions at around 100°C. The presence of high concentrations of hydrocarbons in geopressurized regions (Jones, 1975 in Kharaka, et al., 1977) may be significant. Complicating factors include the presence of pyrite, siderite and calcite in the samples. The data of this study are not extensive enough to allow the interpretation of the role of these minerals in controlling the water chemistry.

In general then, the major element chemistry of the interstitial waters of recent terrigenous sediments, subject to deep burial, is characterized by processes which result in the maintenance of large scale differences between sands and shales. The extent of these differences is not as great as previous leach data has suggested. Cl contents are low in the shales and high in the sands. This dichotomy may be established during early burial due to the release of more saline waters from the shales into the sands as a result of chemical fractionation within the shale pores. At greater depths the effect of membrane filtration is evident in increasing sandstone Cl contents and perhaps to a lesser extent in the shales. In the high pressure zone Cl again decreases in the shales, probably as a result of interlayer water release during smectite-illite transformations. This

Cl decrease is also evident in the high pressure sands. This would be the result of migration of some high pressure zone shale water into these sands. Changes in the Na content relative to Cl are generally small although the small interstitial Na increases with depth in both sands and shales can result from Na loss from the solid (either exchange positions of Na-feldspar decomposition). K and Mg both decrease in interstitial waters during early burial, probably as a result of uptake by clays (Mg in octahedral positions and/or Mg (as $\text{Mg}(\text{OH})_2$) and K in interlayer positions). Further Mg or K for clay alteration must be primarily derived from decomposition of other minerals as interstitial Mg only decreases slightly below 1000 m and K remains constant up to the high pressure zone. Increased K concentrations in waters of high pressure sands and shales may be the result of initiation of a major decomposition reaction (i. e., K-feldspar decomposition). Ca interstitial variations result from complex interactions with exchange ions, carbonates and organic matter and are therefore difficult to interpret. The deep shale samples, entering the high pressure zone, have low Ca interstitial contents perhaps as a result of the precipitation of CaCO_3 at the top of the high pressure zone. SO_4 , HCO_3 and organic carbon generally increase with depth in the shales and may increase dramatically in the high pressure zone. These three species are interrelated due to the organic-carbonate-sulfide-Eh-pH interdependence. The major effects apparent

in the high pressure zone are: dilution of the previous interstitial waters due to the release of interlayer water, release of K, sulfur species, inorganic carbon and probably organic carbon due to solid-aqueous reactions induced by the smectite \rightarrow illite + H₂O reaction or to the high temperatures associated with it. The presence of a possible carbonate cap above the high pressure zone, due to the contact of chemically different waters, may account for low Ca of interstitial waters at depth.

Limited data were collected on a number of minor interstitial constituents. Among these were Sr, Br, F, B, SiO₂ and some trace metals. The pH was also measured on a few samples. Sr values (Table 3) are approximately equivalent to sea water values in the samples not affected by post-squeezing evaporation, indicating that, at least for these samples (2961 and 3063) CaCO₃ recrystallization does not occur (Sayles and Manheim, 1975). Br and F were analyzed (Table 1) as they were expected to provide evidence for membrane filtration in shales since ionic size (Br > Cl > F) should dictate that membrane reservoir waters have higher Br/Cl and lower F/Cl ratios than sea water. However from previous discussion of Cl data it is apparent that membrane filtration does not produce reservoir solutions in the shales and the Br/Cl and F/Cl are both lower than sea water values, particularly Br/Cl. These low ratios are shale related as can be seen in the fact that the sandiest samples (538 and

1150 II which had no sand lenses removed) have the highest Br contents. The fate of this lost Br is not clear, however consistently higher Br contents in the leach samples (Table 22) relative to the squeezed samples, may indicate a solid sample sink for Br. This would indicate that the relationship from DSDP wells showing Br/Cl ratios remaining constant does not extend to greater depths and would also contradict the conclusion (Rittenhouse, 1967; Collins, 1975) that high salinity, low Br brines can automatically be attributed to salt invasion. The pH in the samples range from 6.5-8.0 (Table 1). Most DSDP analyses of terrigenous sediments have roughly the same range. Decreases in pH relative to sea water (pH = 8.0-8.3) may be the result of the release of CO₂ from organic decomposition. The difficulty of obtaining meaningful pH data due to the effects of temperature re-equilibration and evaporation prior to squeezing does not allow more specific discussion of these data. SiO₂, B and trace metals in interstitial waters will be discussed in the following sections.

5. The Nature of Boron/Silica Variations in Pore Waters and Solids

As suggested in earlier discussion, SiO₂ and boron show related trends which make the examination of these two species together necessary. Pertinent data on silica and boron contents in the samples of this study includes compositions of interstitial waters obtained by squeezing (Table 1)

and water leaching (Table 5), silica removed by Na_2CO_3 leach (Table 14), boron (Table 13) in total solid samples and the $<0.1 \mu\text{m}$ fractions, and certain X-ray diffraction features between 12 and $18^\circ 2\theta$ (CuK) in the $>44 \mu\text{m}$ fraction powder packs which may be attributed to silica compounds.

Silica contents of the interstitial water samples obtained by squeezing and corrected for evaporation (Table 22) are generally <4 ppm, somewhat higher in the shallower samples (up to ~ 10 ppm). Sandstone waters generally have high SiO_2 concentrations (Kharaka, et al., 1977) as a result of high temperature and salinity. DSDP silica values are also generally high, reflecting the importance of amorphous silica in determining aqueous silica content of shallow samples. With depth, in some of the deeper DSDP wells (sites 174, 218, and 241) the silica concentrations drop to values of 10 ppm or lower, reflecting crystallization of amorphous silica. The values obtained in this study as well as from some of the deepest DSDP samples are generally lower than would be expected if equilibrium were controlled by quartz. Some of this discrepancy can be understood when the large scale temperature effect on silica (2.5% increase/ 1°C increase) (Fanning and Pilson, 1971) is considered. However this does not really account for the low silica values as the solubility of silica in equilibrium with quartz at 100°C is much greater than any value from this study even after applying a correction for temperature effects of the magnitude indicated above.

The concentrations of dissolved silica in equilibrium with clay minerals (MacKenzie, et al., 1965; Mackenzie and Garrels, 1967) is consistent with the lower silica values in deeply buried pelitic sediment pore waters. Careful consideration of the equilibrium relationships of silica minerals is necessary in the use of silica concentrations as a temperature indicator (Fournier and Rowe, 1966).

The boron data from the liquids obtained by squeezing (Table 1 corrected for evaporation using Table 22 correction factors) gives the reverse of the silica trend, rising from values less than 1.0 ppm in the shallowest samples to 1.0-3.0 ppm at depth (sea water average = 4.0 ppm). Sayles, et al., (1973a) ascribe approximately the same temperature variations upon squeezing to B as to SiO_2 , suggesting that the two are interrelated. DSDP boron values from waters associated with terrigenous sediments are generally lower in boron than sea water, however depletions are not as extensive as in the deeper samples of this study. Sandstone waters generally contain high boron concentrations, indicating perhaps that the controlling factor in the low boron shale water values is the presence of clay minerals.

The patterns for silica and boron in the leach analysis (Table 5) are similar to the pattern in the waters obtained by squeezing, but the absolute concentrations are around one order of magnitude higher, suggesting that both boron and silica are weakly bound to the solid sample and are

authigenic in origin. A plot of the molar ratio SiO_2/B (Figure 29) shows a trend from high values in the shallow samples to a constant value (~ 0.5 molar ratio) below 1000 m. Both squeeze and leach values show the same trend and approximately the same ratios despite the greatly different concentrations. The absorption of both boron and silica by clay minerals appears to be the most likely mechanism controlling the interstitial water concentrations. The interrelationship of boron and silica interstitial water concentrations and the ready leachability of boron and silica in the solid are consistent with the two stage absorption mechanism of Couch and Grim (1968) which attributes the boron content of illites to the tetrahedral layer where it replaces silica after first being lightly absorbed on clay surfaces.

The boron content of the solid samples (Table 13) shows considerable scatter, probably as a result of the use of an Arc Emission Spectrophotometer to obtain these data. However, it is possible to observe an increase in the boron content with depth for both the $<0.1 \mu\text{m}$ fraction and the bulk sample ($<0.1 \mu\text{m}$ shallow average = 130 ppm B, deep average = 180 ppm B; bulk sample shallow average = 70 ppm B, deep average = 95 ppm B). The higher boron content of the fine fractions is indicative of the association of boron with clays. The increase in boron with depth in the solid samples is probably not due to increasing paleosalinity or increasing illite content with depth, as the paleosalinitys in the wells studied are

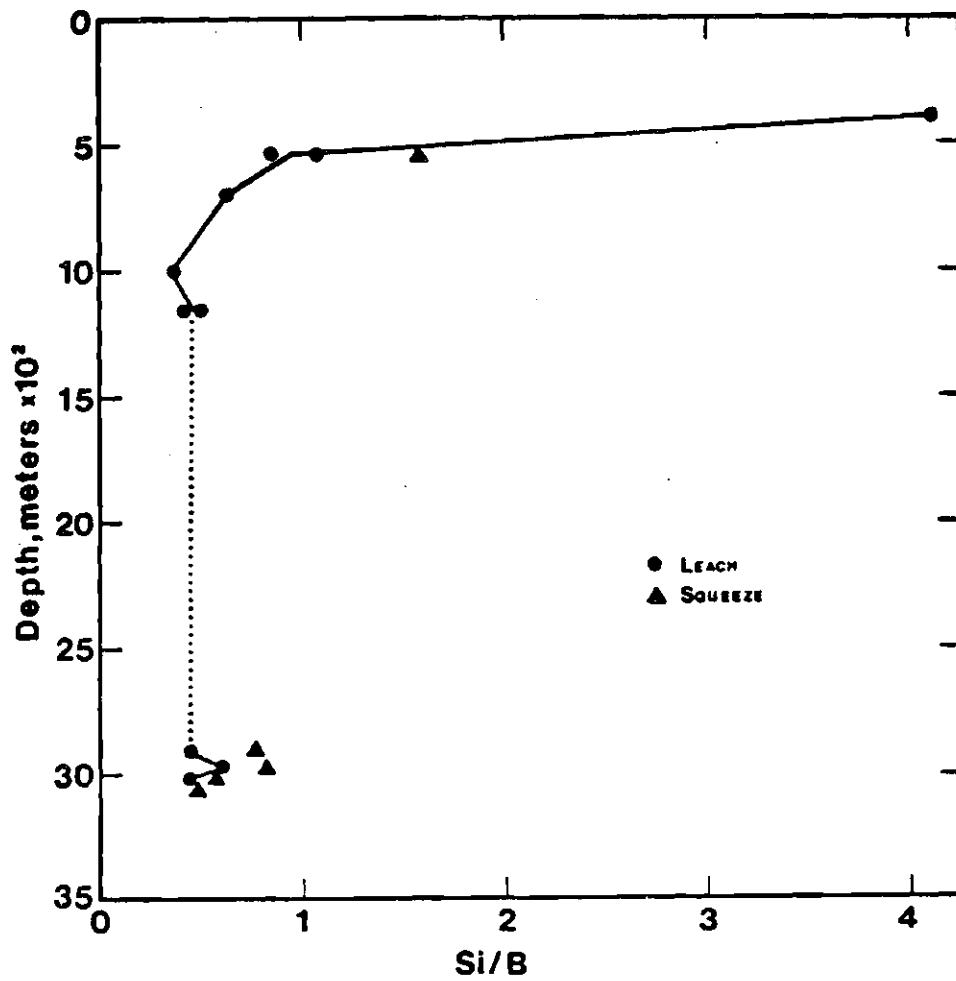


Figure 29. Variation in the Si/B Aqueous Molar Ratio with Depth, Squeezed and Leached Samples.

probably fairly constant and the percentage of 10 A layers in the $<0.1 \mu\text{m}$ fraction (discrete illite and 10 A illite/smectite layers) increases only slightly (~57% to 63% of total $<0.1 \mu\text{m}$ 2:1 clay) with depth. This increase in solid sample boron with depth is possibly the result of a depth dependent diagenetic reaction removing interstitial boron from solution.

The Na_2CO_3 leach for silica will dissolve amorphous silica and possibly weakly absorbed silica from clays while leaving behind quartz. The low values of leachable silica (Figure 30) ($<2\%$ of the solid sample) indicate that little if any amorphous silica is present. That much of the silica leached comes from the clays can be presumed on the basis of the higher proportions of silica leached from the $<0.1 \mu\text{m}$ fractions (Figure 30). In general the trend is to leach greater amounts of silica in the shallower portions (perhaps residual amorphous silica from detrital and biogenic input) and then attain somewhat constant values at depth. In the deeper samples, approaching the high pressure zone, the leachable silica tends to increase again. The offset of the lowermost 3 samples may be related to diagenesis, but it could also result from the fact that these samples are from the second well. As may be seen in Figure 3, there is some indication of faulting between the two wells in a slight downward shift in the fluid pressure from well 2 to well A4 at a depth of ~ 3070 m. This may also be due to uncertainties in the actual depth determinations in the deeper samples.

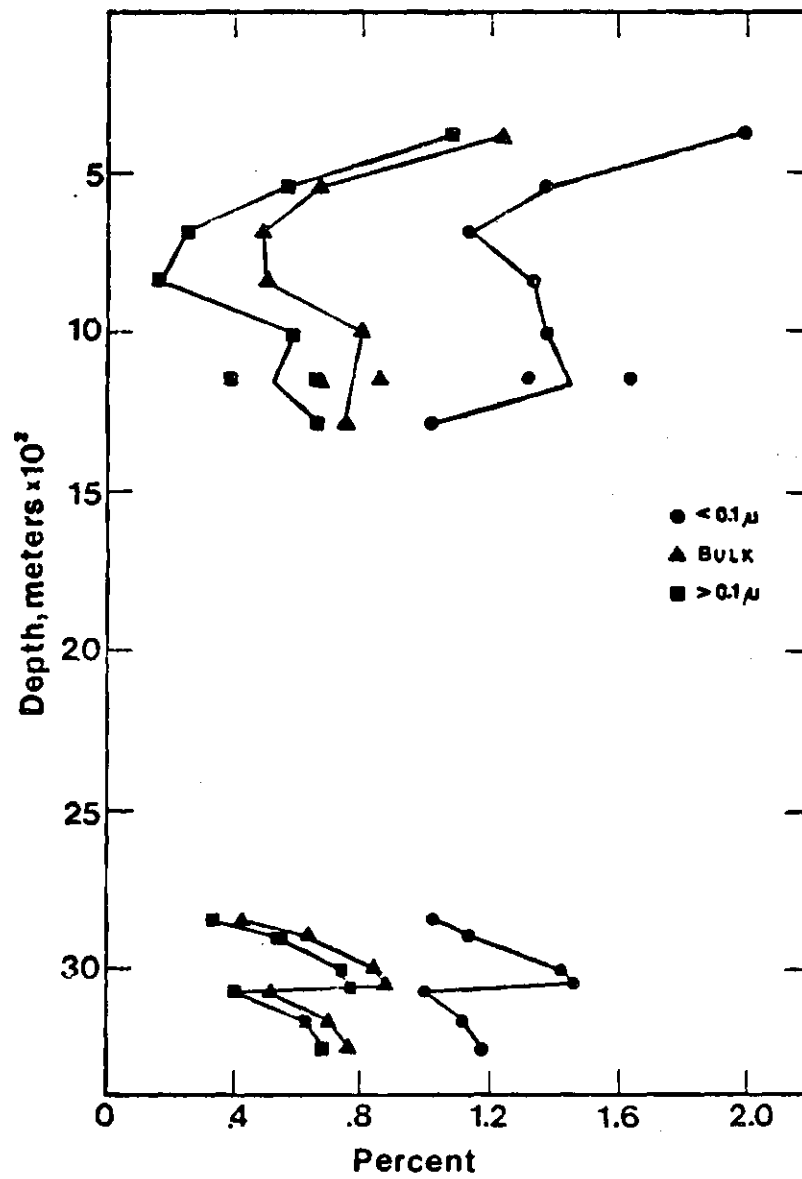


Figure 30. Variation in Na_2CO_3 Soluble Silica with Depth.

Thus this shift in leachable SiO_2 content may be the same increase into the high pressure zone viewed twice. A possible explanation for the increase into the high pressure zone is the release of SiO_2 in the smectite-illite transformation (Hower, et al., 1976), producing poorly crystallized silica phases as an intermediate step in the production of quartz. Some evidence for non-quartz silica structures is seen in the powder pack X-ray diffraction data from the $>44 \mu\text{m}$ fraction where a broad band from 12° - 18° 2θ (CuK) is observed in most samples which has been attributed by Mizutani (1970) to silica compounds undergoing diagenesis.

6. Metals During Burial Diagenesis

Analyses of pore waters for Fe, Cu, Mn, Cr, and Zn were performed (Table 3) where enough material was available (7 samples) after squeeze liquids were allocated for major element analysis. Two of these samples (2906 and 3007) probably underwent evaporation after squeezing and before metal analysis, due to the small (<0.1 ml) aliquot remaining after major element analysis.

Data on the distribution of trace metals in sea water and sediment interstitial waters are presented in Table 25. Average sea water contains low concentrations (≤ 5 ppb) of Cr, Mn, Fe, Co, Cu, and Zn (Brewer, 1975). Order of magnitude increases in trace metal contents of shallowly buried (<4 meter) sediment waters were observed in many of the samples of Brooks, et al., (1968) and Presley, et al., (1972). The

Table 25. Trace Metal Contents of Natural Waters.

	Cr (ppb)	Mn (ppm)	Fe (ppm)	Co (ppb)	Cu (ppb)	Zn (ppm)	
Avg. Sea H ₂ O (1)	0.3	.0002	.002	.05	0.5	.005	
Pelitic Sediment H ₂ O <1 m deep (2)	--	--	.004-.070	<3.0	2.-14.	.004-.15	Range
Pelitic Sediment H ₂ O <4 m deep (3)	--	<.02-3.2	.002-.250	<1.0-4.0	.5-40.	.004-.18	Range
Pelitic Sediment H ₂ O ≤600 m deep (4)	--	.02-9.0	.003-.020	--	6.-20.	.10-.80	Range
This Study	0-300.	.14-1.9	.10-14.2	--	60.-2800.	.20-.60	Range
Sandstone (5) Formation water	10. <10.-34.	1.3 .02-52	7.5 .01-87	5. <5-29	120. 20-490	.80 .03-27.5	Avg. Range
Saline Formation Water (6)	--	.01-.22	.01-3.3	--	2-77	.06-2.3	Range
Metal Rich (7) Oil Field Brines	--	3.-344.	2.-470.	--	--	<2.-575.	Range

(1) Brewer, (1975).

(2) Brooks, et al., (1968), California Borderlands.

(3) Presley, et al., (1972), Scanich Inlet.

(4) Deep Sea Drilling Project V1-35, Presley (1969).

(5) Billings, et al., (1968), Western Canada.

(6) Carpenter and Miller, (1969), Saline Co. Missouri.

(7) Carpenter, et al., (1974), Mississippi Formation Waters.

occurrence of fluids with increased trace metal contents relative to sea water in pelitic sediments buried less than 600 meters has been confirmed in studies of Deep Sea Drilling Project pelitic sediment cores (Presley, 1969; Kaplan and Presley, 1968, 1970; Presley and Kaplan, 1970, 1972; Presley, et al., 1970, 1973, 1974). Maximum concentrations in interstitial waters of shallow pelitic sediment samples range from two orders of magnitude (for Fe, Co, Cu, and Zn) to four orders of magnitude (Mn) above average sea water. The limited samples from this study confirm the increase in trace metal contents in pore waters for depths up to approximately 3000 meters in rapidly accumulating sediments. The lack of aqueous trace metal data from the high pressure zone prohibits discussion of possible trends at greater depths.

Trace metal contents of saline formation waters (Billings, et al., 1968; Carpenter and Miller, 1969; Carpenter, et al., 1974) also show large increases relative to sea water and, in the case of the metal rich Mississippi brines (Carpenter, et al., 1974), relative to pelitic sediment waters.

The increased trace metal content of sediment interstitial waters relative to sea water can possibly be attributed to the formation of bi- and poly-sulfide:metal complexes (Gardner, 1974) and/or organic:metal interaction (Nissenbaum and Swaine, 1976). This would explain the higher metal concentrations in reduced sediments and the presence of aqueous

metals in excess of that expected from solubility calculations (Presley, 1969). The presence of increased metal contents in the samples of this study may thus indicate a reducing environment despite the high SO_4 content of these waters. The generally sulfate-poor, metal-rich sandstone brines probably obtain their high metal contents by some combination of the above methods. Increased temperature and increased salinity with depth will also promote increased trace metals in solution (Krauskopf, 1967). In addition, Carpenter, et al., (1974) propose that the deep formation waters of southern Mississippi obtain their metals from the passage of the brine through thin shales during deep burial. If the shales are acting as sources of metals to the solution during burial then a diagenetic reaction resulting in a bulk sample metal loss from the shales, with depth, must be occurring.

The solid samples in this study were analyzed for Fe, Mn, Zn, Co, Cu, and Cr in the 0.1-2 μm and <0.1 μm fractions. In these fractions the total, reducible (hydroxylamine hydrochloride leach), and oxidizable (H_2O_2 leach) fractions of these metals were determined. Total Mn and Fe were analyzed in all of the 2-44 μm fractions, and total Mn, Zn, Co, and Cu were determined in selected bulk samples. These values are compiled in Tables 16-18. Oxidizable metals in the <0.1 μm and 0.1-2 μm fractions are not tabulated due to a predominance of concentrations below detection limits and a possibility

for contamination of some of the samples (deduced by the presence of some significant concentration differences between $<0.1 \mu\text{m}$ and $0.1\text{-}2 \mu\text{m}$ fraction oxidizable metal contents of single samples). As the oxidizable metals of the finer fractions generally make up $<10\%$ of the total metal concentrations, their discussion can be limited in extent.

The data from the bulk sample Cu, Co, Mn, and Zn analyses (Tables 16-18) and the bulk sample iron data (calculated from the $<44 \mu\text{m}$ size fraction data from Tables 7, 9, 10 and 11) are plotted in Figure 31. Where available, the inclusion of the $>44 \mu\text{m}$ Fe data (Table 12) does not significantly alter the total iron content calculated. The bulk sample metal concentrations show a high degree of scatter that is probably the result of detrital effects. In particular, the sandiest sample (538) is depleted in Cu, Co, Zn, and Fe. Certain elements show similar patterns with depth, particularly Cu, Co, and Zn which correlate quite well. There is a suggestion of a decrease with depth for some of these trace metals in the bulk samples. In the shallowest samples all trace metals have maxima at 692 or 844 meters and generally decrease to 1289 meters while the deep samples have Cu, Co, Mn, and Zn values mostly below the shallow sample trends. The deep sample Mn contents are lower than those of the shallow samples, except at 3242 m where the Mn content rises sharply after gradually increasing from 2851-3164 meters. This jump in Mn content coincides with the high carbonate content

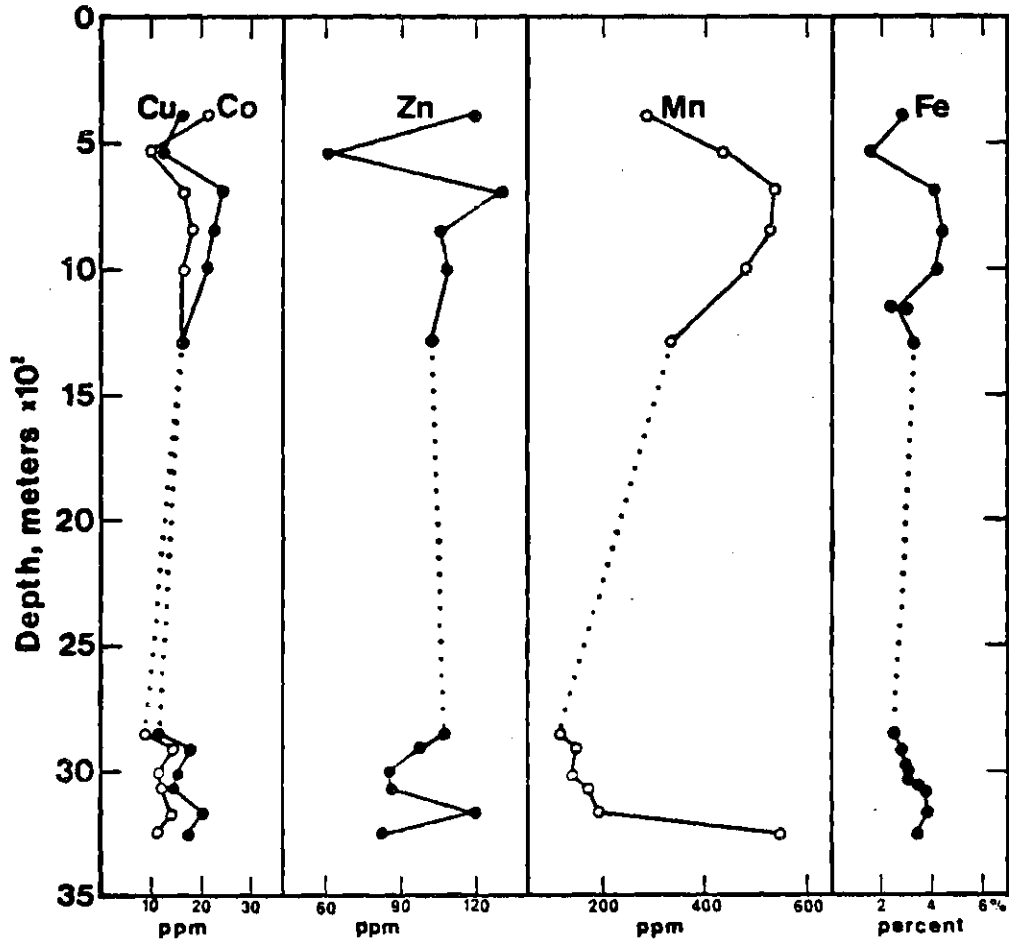


Figure 31. Variation in the Bulk Sample Metal Contents with Depth.

attributed to a high pressure cap and may be the result of diffusion of Mn to the high pressure boundary and precipitation upon contact with the waters of different composition expelled by clay collapse. Diffusion may also account for the metal concentration gradients from 692 to 1289 meters, suggesting that metals are somewhat mobile in the pore waters of shales. The decreases in metal content with depth are not distinct enough to permit these trends to be attributed with certainty to diagenetic loss of metals from the solid. Variations in source and depositional environment cannot be ruled out as possible causes of the observed trends in the bulk sample.

Examination of size fraction trace metal data gives a clearer indication of diagenetic processes operating on these metals. As shown earlier (Figure 18), the iron content shows a depth related decrease in the fine fractions coupled with an increase in the coarser fractions. Similar trends occur in the size fraction data for the other metals. Figures 32 and 33 present the trace metal contents of the $<0.1 \mu\text{m}$ and $0.1-2 \mu\text{m}$ fractions, respectively, with depth. Depth related decreases are observed for Cu, Fe, Zn, and Mn in the $<0.1 \mu\text{m}$ fractions, while Cu, Co, Zn, and Mn show obvious decreases with depth in the $0.1-2 \mu\text{m}$ fractions. As do the bulk samples, the fine fractions provide some evidence for metal content maxima between 692 and 1000 m. The Fe content of the $0.1-2 \mu\text{m}$ fraction is substantially lower than that of the

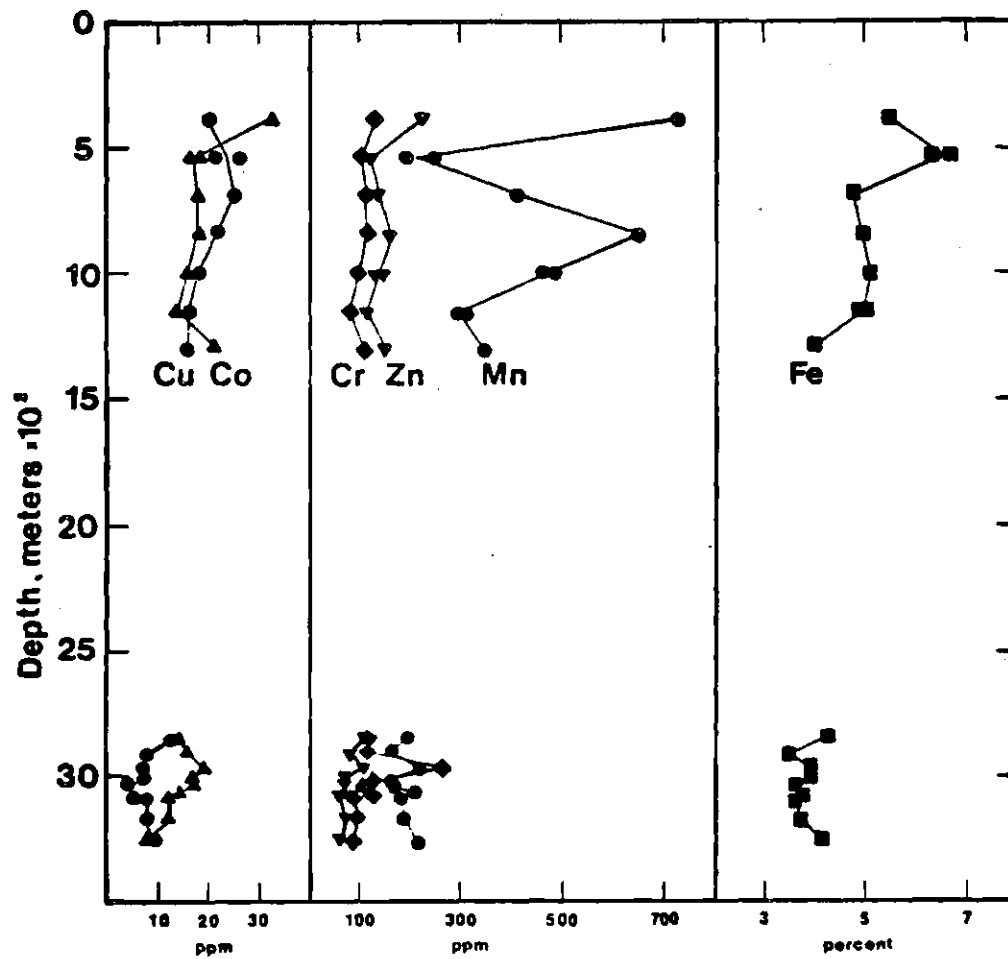


Figure 32. Variation in the $<0.1 \mu\text{m}$ Metal Contents with Depth.

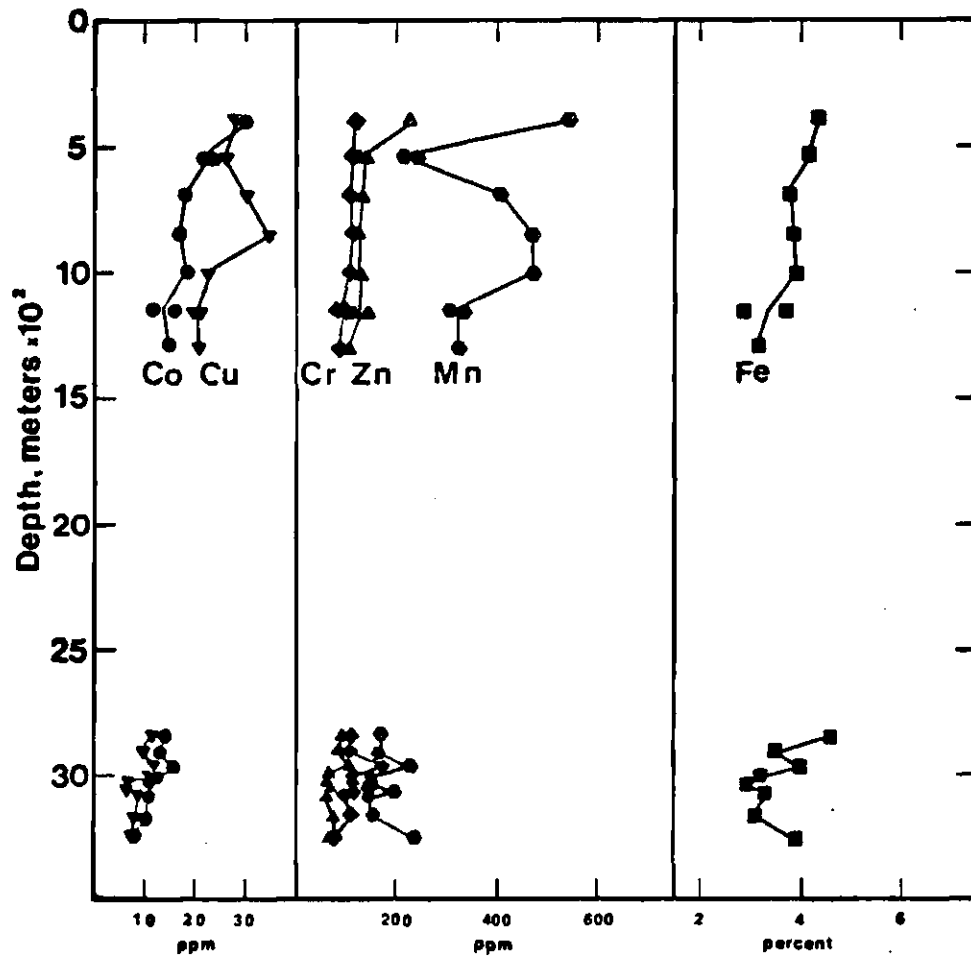


Figure 33. Variation in the 0.1-2 μ m Metal Contents with Depth.

<0.1 μm fraction, particularly in the shallow samples. This would indicate a fine-grained form for the iron of the shallow samples. This is also true, to a lesser extent, for Mn and Zn, while Co and Cr show no distinct size fraction preference. Copper shows the reverse trend, with more Cu being present in the 0.1-2 μm fraction.

The decrease in total iron with depth in the fine fractions is balanced by an increase in the 2-44 μm fraction (Table 17 and Figure 18) and >44 μm fraction (as Fe_2O_3 in Table 12) in order for the Fe in the bulk sample to remain nearly constant with depth (Figure 31). The decreases with depth shown by Mn, Zn, Co, and Cu in the fine fractions are generally larger than the decrease in the bulk samples. The Mn, Zn, Co, and Cu contents of the >2 μm fraction have been calculated by mass balance using data available in Tables 7 and 16-18 and are plotted in Figure 34. Copper, Zn and Mn show depth related increases in the >2 μm fraction and Mn again displays a pronounced maximum at 692 meters. The ratio of the concentration of each metal in the >2 μm fraction to that in the <2 μm fraction shown for Mn, Zn, Cu, and Co in Figure 35, illustrates the pronounced shift of these metals from fine fraction to coarse fraction with depth. Again the Mn content deviates in some of the shallow samples, providing the only ratios appreciably greater than one in the shallow samples. The iron ratio, not plotted here, can be estimated using the Fe contents of the 2-44 μm fractions. This ratio

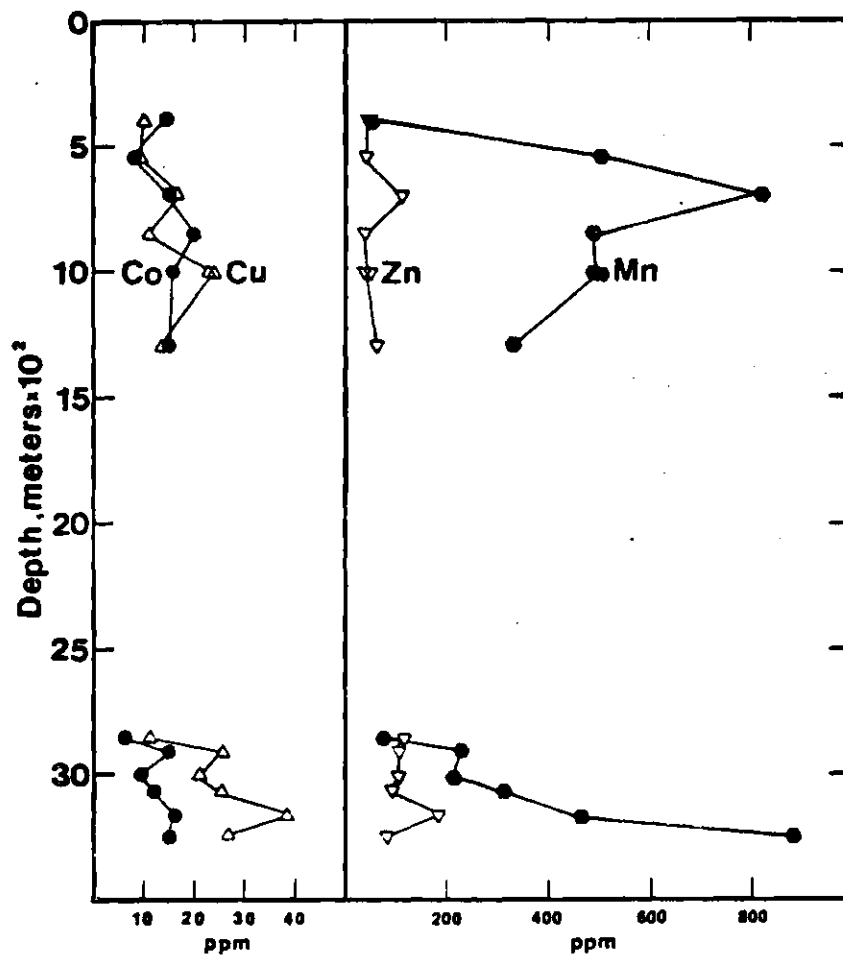


Figure 34. Variation in the >2 μm Metal Contents with Depth.

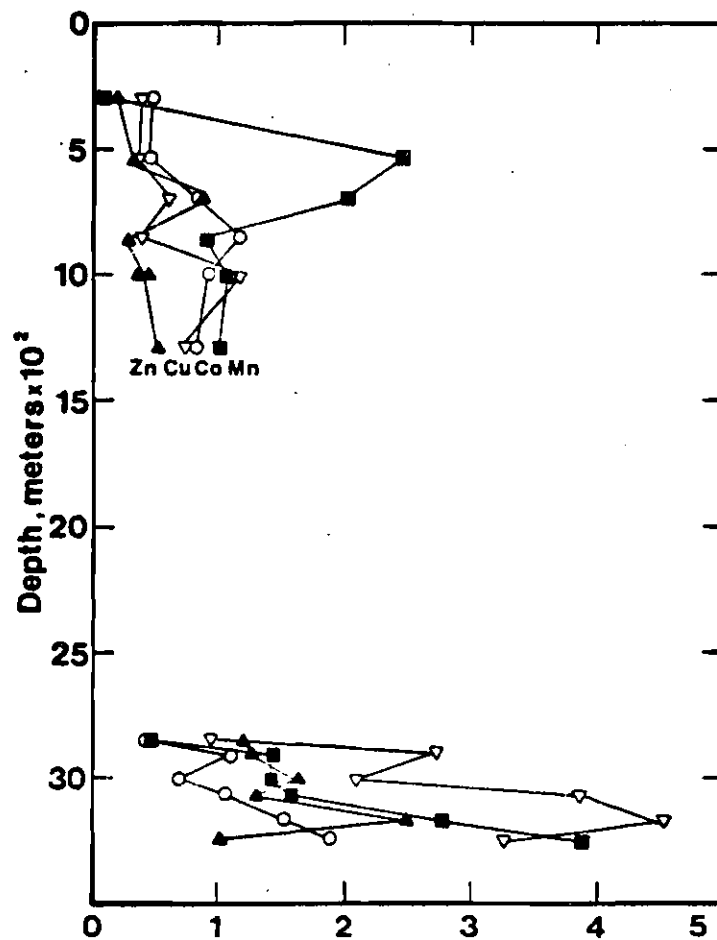


Figure 35. Variation in the $>2 \mu\text{m}/<2 \mu\text{m}$ Metal Ratios with Depth.

also shows a depth related increase of iron in the coarse fraction relative to the fine but with a shallow wedge (at 692-1000 m) where iron contents of the coarse fractions are relatively high.

Thus the distribution of metals in the various size fractions, although showing much scatter, particularly in the shallow samples, provides evidence for a transfer of metals from fine to coarse fractions as depth of burial increases. This is particularly evident in the deep samples, approaching the high pressure zone, where increases in the coarse fraction metal contents, coupled with constant or decreasing fine fraction metal contents, may be a result of diffusion and precipitation, in the coarse fraction, of metals at the high pressure boundary. The region from 538 to 1000 meters is also characterized by maxima in metal contents of the bulk sample and $>2 \mu\text{m}$ fractions, particularly for Mn and Fe (2-44 μm), that may also be due to the diffusion of metals in solution. In the transfer of metals from fine to coarse fractions, migration and diffusion of metals may result in the loss of fine fraction metal from the solid sample that is not balanced by coarse fraction gains in the sample, or in coarse fraction metal increases from addition of metal from outside the immediate sample area. In general, the slight decreases in metal content of bulk samples with depth suggest that some loss of metals to the aqueous system occurs.

The reducible metals in the $<0.1 \mu\text{m}$ and $0.1-2 \mu\text{m}$

fractions are generally less than half of the total metal content of these fractions (Tables 16-18). Reducible Fe makes up less than 10% of the total iron and shows a slight decrease with depth, which parallels the decrease of total iron in the fine fraction. Reducible Cr in the $<0.1 \mu\text{m}$ and $0.1-2 \mu\text{m}$ fractions makes up $<10\%$ of the total Cr in those fractions (except for sample 2961, discussed earlier) and appears to increase significantly in the deeper samples. The $<0.1 \mu\text{m}$ and $0.1-2 \mu\text{m}$ fractions may contain up to 50% of the total Zn, Cu, and Co in the reducible form, however most of the metal decrease with depth is related to the non-reducible fraction. In fact, while reducible Zn and Cu parallel the total metal trends, reducible cobalt actually increases in the deeper samples (particularly in the $<0.1 \mu\text{m}$ fraction). In contrast to the other metals, not only is a significant portion of the fine fraction Mn present in the reducible fraction ($\sim 50\%$), but the decrease in reducible Mn with depth is quite pronounced, with a decrease of about 70% in the reducible Mn with depth accounting for about half of the total Mn decrease in the $<0.1 \mu\text{m}$ and $0.1-2 \mu\text{m}$ fractions.

The reducible fraction probably consists of finely disseminated oxides, carbonates, and metal ions weakly absorbed in exchange positions and on grain surfaces (Presley, 1969). The probable reducing nature of the interstitial waters of this study should have promoted the decomposition of oxides, resulting in low reducible metal contents. The data of

Presley (1969) from the Saanich inlet (<4 meters deep) and the data of Piper (1971) from shallow Framvaren Fjord sediments show higher proportions of acid soluble and reducible and acid soluble metals in the bulk samples than is observed in the fine fractions of this study. This would indicate that either appreciable amounts of the reducible metals are in the coarser fractions or, major portions of the reducible metals are in fact reduced during early burial. In view of the decreasing concentrations with depth for most reducible metals in the fine fractions of the present study (except Co and Cr), the latter seems more likely.

Presley (1969) also found very high contributions being made to the bulk metal content of Saanich inlet sediments by the H_2O_2 oxidizable metals. This fraction would consist primarily of metals in sulfide phases or associated with organic matter susceptible to H_2O_2 oxidation. In the present study, evidence for the presence of pyrite in the $>2 \mu m$ fractions can be seen in X-ray diffraction patterns. However, the oxidizable fractions of the $<2 \mu m$ material appear to be metal poor, particularly in the deeper samples. All oxidizable Fe concentrations in these fine fractions are $<.05\%$ by weight, which corresponds to $<2\%$ of the iron in the fractions. Oxidizable Mn is above detection limits in half of the shallow samples, where it averages ~ 15 ppm in the $0.1-2 \mu m$ and ~ 10 ppm in the $<0.1 \mu m$ fractions. Oxidizable Mn may decrease from 390 to 1289 meters. All analyses of oxidizable Mn in the $<2 \mu m$

fractions of deep samples show ≤ 10 ppm; many of these samples have ≤ 4 ppm oxidizable Mn. Even where oxidizable Mn is relatively most abundant, it is still less than 5% of the total Mn. Oxidizable Zn appears to show the most potential for contamination (mentioned earlier) in these samples. Large deviations between Zn (oxidizable) in the $<0.1 \mu\text{m}$ and $0.1-2 \mu\text{m}$ fractions of some samples necessitate the elimination of some of the Zn data from consideration. These excesses may result from incomplete washing of the sample after the reducing leach, as some of the analyses of oxidizable metals show evidence for contamination by several metals. It is possible to state that most of the oxidizable Zn concentrations are <4 ppm. Again, the oxidizable Zn is only a minor portion ($<5\%$) of the total Zn. Oxidizable Cu and Co are generally <0.6 ppm except for a few samples (mainly shallow) which are <1.2 ppm and one sample (390) which has 1.2 ppm oxidizable Cu and 2.8 ppm oxidizable Co in the $0.1-2 \mu\text{m}$ fraction and 1.2 ppm oxidizable Co in the $<0.1 \mu\text{m}$ fraction. Again these values are small relative to the total content of these metals. All oxidizable Cr values were <2.5 ppm, except for 2961 ($<0.1 \mu\text{m} = 8$ ppm; $0.1-2 \mu\text{m} = 5$ ppm) probably due to drill mud contamination. The $<2 \mu\text{m}$ fractions of this study contain very little metal in an oxidizable form. In the case of Mn, Cr, and Co it is possible to state that the $0.1-2 \mu\text{m}$ fractions have slightly higher amounts of oxidizable metals than the $<0.1 \mu\text{m}$ fraction. The amounts of oxidizable metals should

increase further in the $>2 \mu\text{m}$ fractions as X-ray diffraction detects sulfides in the coarse fractions. The low values in the fine fractions are an indication that the metals associated with the oxidizable portion of organic matter are minimal at moderate depths of burial.

The depth dependent variations in metal contents of the samples can be understood by examining the processes involved in the diagenetic formation of pyrite. The precipitation of iron sulfides, after a reducing environment is provided, is limited by the availability of iron, dissolved sulfate, metabolizable organic matter, and sulfate reducing bacteria (Berner, 1971). The reaction of fine grained monosulfides with H_2S and elemental sulfur produces pyrite at temperatures below 100°C (Rickard, 1969; Berner, 1970). The crystallization of pyrite is generally accompanied by formation of discrete pyrite crystals, microconcretions and layers (Berner, 1971). The source of the iron for pyrite formation would initially be fine grained ferric oxides occurring as coatings on minerals (Berner, 1970), or as iron adsorbed weakly on clays (Carroll, 1958) and organic matter (Nissenbaum and Swaine, 1976). Larger grained minerals, such as iron rich clays (Drever, 1971b; Siever and Kastner, 1972) may also be important contributors. The reduction of aqueous $\text{SO}_4^{=}$ is the primary source of $\text{S}^{=}$ in shallow sediments, although sulfur derived from organic decomposition may also contribute (Berner, 1971).

In this study, Fe loss, primarily from the non-reducible portion of the fine fractions, is balanced by increases in the fine fraction Al_2O_3 content. In addition, the sample with highest Fe content in the fine fraction also has the highest 17 A layer content in the $<0.1 \mu\text{m}$ fraction (538 meters). Therefore Fe loss from the fine fraction is probably the result of loss from structural positions in the montmorillonite. The presence of little reducible iron in the fine fraction is consistent with a structural source for the iron. The trace metals are also marked by similar losses from the non-leachable portions, however Mn, Zn, Cu, and Co all occur in appreciable amounts as reducible metal in the fine fractions as well. In all cases the reducible portion of the metal content is considerably less than the reducible fractions of bulk samples studied by Presley (1969). Only for Mn is an appreciable amount of the fine fraction metal loss associated with the reducible fraction (~50%). This Mn is probably in the form of oxides or carbonates, coating grains of other material or finely disseminated. The oxidizable metals in the fine fractions are all near the lower limits of detection and may decrease with depth.

The diagenetic formation of large crystals or nodules of pyrite is probably responsible for the increase with depth of iron in the coarse fractions. The other metals may also occur in sulfides or carbonates in a similar manner. The samples of this study show two zones where metals are present

to relatively large extent in the coarse fraction. The first of these occurs between 538 and 1000 meters and the metals affected are primarily Mn and Fe. The Fe content of the 2-44 μm fraction (Table 17) is at a maximum between 692 and 1000 meters while Mn $>2 \mu\text{m}$ content is highest relative to the $<2 \mu\text{m}$ content at 538-692 meters (Figure 35). Less obvious increases in coarse fraction Co, Cu, and Zn also occur (Figure 35). This depth range (583-1000 m) encompasses the zone where SO_4/Cl is lowest (Figure 28f) indicating that significant S^- production and sulfide mineral precipitation may have occurred in this region. This zone coincides with a thick sequence of clay and silty clay (Figure 1) and its chemical characteristics may be attributable to the action of anerobic bacteria during deposition and/or burial.

The second zone of enhanced metal content in the coarse fractions includes the deep samples, leading up to the high pressure zone. These samples show consistently increasing metal contents in the coarse fraction with depth, for Fe, Mn, Cu, and Co (Figure 34), while the ratio of the amount of each metal in the coarse fraction to that in the fine fraction increases for these metals and Zn as well (Figure 35). This zone probably results from the disruption of the interstitial water chemistry by release of structural water in the high pressure zone. This water, high in SO_4 and HCO_3 and low in Cl, may promote the precipitation of a carbonate cap which may have been pierced by sample 3242 m. This sample contains

abundant calcite and some dolomite, predominantly in the coarser fractions, which have been recrystallized (as evidenced by the low Sr content of the coarse fraction of this sample (Figure 24)). This carbonate phase appears to act as a dilutant for most of the metals in the $>2 \mu\text{m}$ fraction (Figure 34 and Table 17) with the exception of Mn (and possibly Co) which is apparently included in the carbonate. This may also be true for Mn in the coarse fractions of the shallow samples and it is possible that Mn-carbonate makes up a portion of the fine fraction reducible Mn, which decreases with depth consistent with recrystallization. The other metals, Zn, Cu, and Fe, whose abundances in the coarse fractions of the deep samples peak at 3164, are associated with a coarse fraction sulfide phase which is predominant as microconcretions of pyrite and pyrite replacing forams in this sample. The lack of a significant decrease in the fine fraction metal contents within the zone deep samples indicates that the source for the coarse fraction metal is outside the immediate sample region. Diffusion of metals from above the high pressure zone to precipitate as sulfides upon contact with waters altered by structural water release would account for the observed distribution. The high concentrations of metals in solution and their apparently large mobility would promote the migration of metals from the shales into the sands, which is consistent with the apparent slight metal loss from the shales with depth.

CHAPTER VI

CONCLUSIONS

The analysis of pore waters obtained from sidewall cores of shale layers by pressure extraction provides reliable data on the in situ pore water constituents. The cores of this study are generally free from drill mud contamination after trimming. Evaporation of the cores occurs prior to squeezing but can be corrected for to a satisfactory extent by determination of laboratory and in situ porosities. Extreme caution in storage of cores may minimize evaporation. The chemistry of the solution extracted will vary according to the pressure and temperature of extraction. Pressure effects, related to membrane filtration during sample squeezing, are generally small while temperature effects, resulting from the dependence of exchange equilibria and mineral solubilities on temperature, may be somewhat larger. Examination of leaching techniques of pore water analysis shows that washing samples with dilute solutions results in mineral dissolution and alteration of clay exchange equilibria.

The clay mineralogy of the finer size fractions shows evidence for an increase in 10 A layers in the illite/smectite with depth. The solid sample chemistry and mineralogy of this study is consistent with the reaction, proposed by Hower, et al., (1976), whereby smectite absorbs

K and Al and releases silica to form 10 A layers in the mixed layer clay. However the silica loss from the $<0.1 \mu\text{m}$ fraction is not as great in the samples of this study, as in the data of Hower, et al., (1976), whose samples cover a range extending to greater depth. The Na_2CO_3 leachable silica does show an increase at the high pressure zone that could be due to the formation of poorly crystalline solid from silica released by clays. This would indicate that major silica loss from fine grained clay does not occur until the high pressure zone. In the fine fractions of this study Fe is being removed from the clay to a greater extent than silica. There is also evidence for some Mg loss from the fine fraction with increasing depth. The primary source of K for formation of 10 A layers in the illite/smectite above the high pressure zone is discrete illite which is present in all size fractions and decreases with increasing depth to the high pressure zone. A marked increase in total 10 A layers in the finer fractions of the deeper samples ($\sim 3100 \text{ m}$) indicates the initiation of the major transformation of smectite to illite and coincides generally with the top of the high pressure zone. Additional K sources may be necessary to continue this reaction. Total exchange capacity apparently decreases in the finer fractions with increasing depth, and divalent ions, particularly Ca^{2+} , predominate in exchange positions at depth. There is strong evidence for the transfer of metals from the fine fraction, where they are

associated primarily with the clay minerals, to the coarse fraction, with increasing depth. This may result in slight decreases in the bulk sample metal contents with increasing depth if metal is lost to solution during this transition. Coarse fraction metals associate primarily with sulfides (Fe, Zn, Cu) and carbonates (Mn, Co) and there is evidence that the contact of chemically distinct pore waters at the top of the high pressure zone promotes the transport by diffusion of chemical constituents to the boundary and precipitation of sulfides and carbonates as large crystals or micro-concretions in a caprock above the high pressure zone.

The interstitial waters of rapidly accumulating terrigenous sediments are characterized by large salinity differences between sands and shales. During early burial the shale interstitial waters may lose more saline water into the sand, leaving behind a less saline pore solution. With increased burial, membrane filtration begins to take place, increasing the salinity of the sand waters most noticeably, but perhaps also causing some concentration of shale waters as well. The effluent solution from membrane filtration is apparently removed from the sediment column during compaction. Solid:aqueous reactions are apparently responsible for the observed loss of K, Mg, and Ca and gain in Na (relative to Cl) with increasing depth in the interstitial waters of this study. Clay minerals probably absorb

K and Mg while Ca may replace Na in exchange positions as depth increases. Evidence for release of low salinity inter-layer water as a major cause of the main high pressure zone is present in the low Cl content of the interstitial waters below 3070 meters. This is accompanied by an increase in interstitial K and SO_4 and probably HCO_3 and organic carbon. Trace metals in the pore waters increase with depth.

Low silica contents of the shale pore waters indicates that equilibrium with clay minerals is established at a shallow depth. Silica and boron are associated in a solid phase which readily dissolves on warming (Sayles, et al., 1973a) or leaching, and apparently controls the aqueous Si/B molar ratio at about 0.5 at depths below 600 m. This solid is probably weakly absorbed on clay surfaces and may represent an intermediate stage in the process by which boron is included in the clay structure.

BIBLIOGRAPHY

- Adamson, L. G., Chilingar, G. V., Beeson, C. M., and Armstrong, R. A., 1966, Electrokinetic dewatering, consolidation and stabilization of soils. *Eng. Geol.*, V. 1, p. 291-304.
- Anikouchine, W. A., 1967, Dissolved chemical substances in compacting marine sediments. *Geophys. Res.*, V. 72, p. 505-509.
- Barker, C., 1972, Aquathermal pressuring-role of temperature in development of abnormal pressure zones. *Bull. Am. Assoc. Pet. Geologists*, V. 56, p. 2068-2071.
- Beck, K. C. and Reuter, J. H., 1977, Colloid chemistry of Fe, Al, and organic carbon in natural waters. In preparation.
- Belcher, R. and Wilson, C. L., 1964, New Methods in Analytical Chemistry. 2nd edition. Reinhold Publishing Corp., New York, N. Y., 287p.
- Berner, R. A., 1969, Migration of Fe and S in anerobic sediments during early diagenesis. *Am. Jour. Sci.*, V. 267, p. 19-42.
- Berner, R. A., 1970, Sedimentary pyrite formation. *Am. Jour. Sci.*, V. 268, p. 1-23.
- Berner, R. A., 1971, Principles of Chemical Sedimentology. McGraw-Hill, New York, N. Y., 240p.
- Berner, R. A., 1975, Diagenetic models of dissolved species in the interstitial waters of compacting sediments. *Am. Jour. Sci.*, V. 275, p. 88-96.
- Berry, F. A. F., 1969, Relative factors influencing membrane filtration effects in geologic environments. *Chem. Geol.*, V. 4, p. 295-301.
- Billings, G. K., Hitchon, B., and Shaw, D. R., 1969, Geochemistry and origin of formation waters in the Western Canada Sedimentary Basin. 2) Alkali metals. *Chem. Geol.*, V. 4, p. 211-223.
- Bischoff, J. L., Greer, R. E., and Luistro, A. O., 1970, Composition of interstitial waters of marine sediments: Temperature of squeezing effect. *Science*, V. 167, p. 1245-1246.
- Bischoff, J. L. and Ku, T., 1970, Pore fluids of recent marine sediments: I. Oxidizing sediments of 20°N, continental rise to Mid-Atlantic ridge. *J. Sediment. Petrol.*, V. 40, p. 960-972.

- Brewer, P. G., 1975, Minor elements in sea water. In: Chemical Oceanography. V. 1, 2nd edition. J. P. Riley and G. Skirrow (Editors), Academic Press, New York, N. Y., 606p.
- Broecker, W. S., 1974, Chemical Oceanography. Harcourt Brace Jovanovich Inc., Atlanta, Ga., 214p.
- Brooks, R. R., Presley, B. J., and Kaplan, I. R., 1968, Trace elements in the interstitial waters of marine sediments. Geochim. Cosmochim. Acta, V. 32, p. 397-414.
- Burst, J. F. Jr., 1969, Diagenesis of Gulf Coast clayey sediments and its possible relation to petroleum migration. Bull. Am. Assoc. Pet. Geologists, V. 53, p. 73-93.
- Burst, J. F. Jr., 1976, Argillaceous sediment dewatering. Annual Review Earth Planet. Sci., V. 4, p. 293-318.
- Carpenter, A. B. and Miller, J. C., 1969, Geochemistry of saline subsurface water, Saline county (Missouri). Chem. Geol., V. 4, p. 135-167.
- Carpenter, A. B., Trout, M. L., and Pickett, E. E., 1974, Preliminary report on the origin and chemical evolution of lead and zinc-rich oil field brines in central Mississippi. Econ. Geol., V. 69, p. 1191-1203.
- Carroll, D., 1958, Role of clay minerals in the transportation of iron. Geochim. Cosmochim. Acta, V. 14, p. 1-27.
- Chan, K. M. and Manheim, F. T., 1970, Interstitial water studies on small core samples, Deep Sea Drilling Project, Leg 2. In Peterson, M. N. A., et al., Initial Reports of the Deep Sea Drilling Project, V. 2, p. 367-372.
- Chapman, R. E., 1972a, Clays with abnormal interstitial fluid pressures. Bull. Am. Assoc. Pet. Geologists, V. 56, p. 790-795.
- Chapman, R. E., 1972b, Primary migration of petroleum from clay source rocks. Bull. Am. Assoc. Pet. Geologists, V. 56, p. 2185-2191.
- Chapman, R. E., 1973, Petroleum Geology. American Elsevier Publishing Co., Inc., New York, N. Y., 304p.
- Chester, R. and Hughes, M. J., 1967, A chemical technique for the separation of Ferro-manganese minerals, carbonate minerals and absorbed trace elements from pelagic sediments. Chem. Geol., V. 2, p. 249-262.

- Chilingarian, G. V., Sawabini, C. T., and Rieke, H. H., 1973, Effect of compaction on chemistry of solutions expelled from montmorillonite clay saturated in sea water. *Sedimentology*, V. 20, p. 391-398.
- Collins, A. G., 1975, Geochemistry of Oilfield Waters. Volume 1: Developments in Petroleum Science. Elsevier Scientific Publishing Company, New York, N. Y., 496p.
- Cordell, R. T., 1972, Depths of oil origin and primary migration: a review and critique. *Bull. Am. Assoc. Pet. Geologists*, V. 56, p. 2029-2067.
- Couch, E. L. and Grim, R. E., 1968, Boron fixation by illites. *Clays Clay Minerals*, V. 16, p. 249-256.
- DeSitter, L. V., 1947, Diagenesis of oil field brines. *Bull. Am. Assoc. Pet. Geologists*, V. 31, p. 2030-2040.
- Devine, S. B., Ferrell, R. E., and Billings, G. K., 1972, A quantitative x-ray diffraction technique applied to fine grain sediments of the deep Gulf of Mexico. *J. Sediment. Petrol.*, V. 42, p. 468-475.
- Devine, S. B., Ferrell, R. E. Jr., and Billings, G. K., 1973, Mineral distribution patterns, deep Gulf of Mexico. *Bull. Am. Assoc. Pet. Geologists*, V. 57, p. 28-41.
- Dickey, P. A., Collins, A. G., and Fajardo, I., 1972, Chemical composition of deep formation waters in southwestern Louisiana. *Bull. Am. Assoc. Pet. Geologists*, V. 56, p. 1530-1533.
- Dickinson, G., 1953, Reservoir pressures in Gulf Coast Louisiana. *Bull. Am. Assoc. Pet. Geologists*, V. 37, p. 410-432.
- Drever, J. I., 1971a, Early diagenesis of clay minerals, Rio Ameca Basin, Mexico. *J. Sediment. Petrol.*, V. 41, p. 982-994.
- Drever, J. I., 1971b, Magnesium-iron replacements in clay minerals in anoxic marine sediments. *Science*, V. 172, p. 1334-1336.
- Dunoyer de Segonzac, G., 1964, Les argiles du Cretace superieur dans le Bassin de Doula (Cameroun). *Problèmes de diagenèse: Bull. Serv. Carte Géol. Alsace-Lorraine*, V. 17, p. 237-310.
- Dunoyer de Segonzac, G., 1969, Les mineraux argileux dans la diagenese passage au metamorphisme. *Mem. Serv. Carte Géol. Alsace-Lorraine*, V. 29, 320p.

- Dunoyer de Segonzac, G., 1970, The transformation of clay minerals during diagenesis and low-grade metamorphism: A review. *Sedimentology*, V. 15, p. 281-346.
- Eaton, B. A., 1969, Fracture gradient prediction and its application in oil field operations. *J. Pet. Tech.*, V. 21, p. 1353-1360.
- Ediger, R. D., Peterson, G. E., and Kerber, J. D., 1974, Application of the graphite furnace to saline water analysis. *At. Absorpt. Newsl.*, V. 13, p. 61-64.
- Fanning, K. A. and Pilson, M. E. Q., 1971, Interstitial silica and pH in marine sediment: Some effects of sampling procedures. *Science*, V. 173, p. 1228-1231.
- Foscales, A. E. and Kodama, H., 1974, Diagenesis of clay minerals from lower cretaceous shales of northeastern British Columbia. *Clays Clay Minerals*, V. 22, p. 319-335.
- Fournier, R. O. and Rowe, J. J., 1966, Estimation of underground temperatures from the silica content of water from hot springs and wet steam wells. *Am. Jour. Sci.*, V. 264, p. 685-697.
- Frey, M., 1970, The step from diagenesis to metamorphism in pelitic rocks during Alpine orogenesis. *Sedimentology*, V. 15, p. 261-279.
- Gardner, L. R., 1974, Organic vs. inorganic trace metal complexes in sulfidic marine waters-some speculative calculations based on available stability constants. *Geochim. Cosmochim. Acta*, V. 38, p. 1297-1302.
- Gieskies, J. M., 1974, Interstitial water studies, Leg 25. In Simpson, E. S. W., et al., Initial Reports of the Deep Sea Drilling Project, V. 25, p. 361-394.
- Gieskies, J. M., 1975, Chemistry of interstitial waters of marine sediments. *Annual Review Earth Planet. Sci.*, V. 3, p. 433-453.
- Grim, R. E., 1968, Clay Mineralogy. 2nd edition. McGraw-Hill, New York, N. Y., 596p.
- Hanshaw, B. B. and Coplan, T. B., 1973, Ultrafiltration by a compacted clay membrane - II. Sodium ion exclusion at various ionic strengths. *Geochim. Cosmochim. Acta*, V. 37, p. 2311-2327.
- Hanshaw, B. B. and Zen, E. AN, 1965, Osmotic equilibrium and overthrust faulting. *Bull. Geol. Soc. Amer.*, V. 76, p. 1379-1386.

Helig, D., 1974, Diagenetic alteration of smectite in argillaceous sediments of the Rhinegraben (S. W. Germany). *Sedimentology*, V. 21, p. 463-472.

Giltabrand, R. R., Ferrell, R. E., and Billings, G. K., 1973, Experimental diagenesis of Gulf Coast argillaceous sediment. *Bull. Am. Assoc. Pet. Geologists*, V. 57, p. 338-348.

Holmes, R. S. and Hern, W. E., 1942, Chemical and physical properties of some important alluvial soils of the Mississippi Basin. *U. S. Dep. Agric. Tech. Bull.*, V. 833, 82p.

Horowitz, R. M., Waterman, L. S., Broecker, W. S. and Bopp, R., 1973, Interstitial water studies, Leg 15, new procedures and equipment. In Heezen, B. C., et al., *Initial Reports of the Deep Sea Drilling Project*, V. 20, p. 757-764.

Hottman, C. E. and Johnston, R. K., 1965, Estimation of formation pressures from log derived shale properties. *J. Pet. Tech.*, V. 17, p. 717-722.

Hower, J., Eslinger, E. V., Hower, M. E., and Perry, E. A., 1976, Mechanism of burial metamorphism of argillaceous sediment: 1. Mineralogical and chemical evidence. *Bul. Geol. Soc. Amer.*, V. 87, p. 725-737.

Hulbert, M. H. and Brindle, M. P., 1975, Effects of sample handling on the composition of marine sedimentary pore water. *Bull. Geol. Soc. Amer.*, V. 86, p. 109-110.

Hurd, D. C., 1973, Interactions of biogenic opal, sediment and sea water in the central equatorial Pacific. *Geochim. Cosmochim. Acta*, V. 37, p. 2257-2282.

Kaplan, I. R. and Presley, B. J., 1968, Interstitial water chemistry, Deep Sea Drilling Project, Leg 1. In Ewing, M., et al., *Initial Reports of the Deep Sea Drilling Project*, V. 1, p. 411-414.

Kaplan, I. R. and Presley, B. J., 1970, Interstitial water chemistry; Deep Sea Drilling Project, Leg 2. In Peterson, M. N. A., et al., *Initial Reports of the Deep Sea Drilling Project*, V. 2, p. 373-374.

Kerr, P. F. and Barrington, J., 1961, Clays of deep shale zone Caillou Island La. *Bull. Am. Assoc. Pet. Geologists*, V. 45, p. 1697-1712.

Kharaka, Y. K. and Berry F. A. F., 1973, Simultaneous flow of water and solutes through geologic membranes. I. Experimental investigations. *Geochim. Cosmochim. Acta*, V. 37, p. 2577-2604.

Kharaka, Y. K., Callander, E., and Wallace, R. H. Jr., 1977, Geochemistry of geopressurized geothermal waters from the Frio clay in the Gulf Coast region of Texas. *Geology*, V. 5, p. 241-244.

Klipp, R. W. and Barney III, J. E., 1959, Determination of sulfur traces in naphthas by lamp combustion and spectrophotometry. *Anal. Chem.*, V. 31, p. 596-597.

Krauskopf, K. B., 1967, Introduction to Geochemistry. McGraw-Hill, New York, N. Y., 721p.

Lutz, J. F. and Kemper, M. D., 1959, Intrinsic permeability of clays as effected by clay-water interaction. *Soil Sci.*, V. 88, p. 83-90.

McKelvey, J. G. and Milne, I. H., 1962, Flow of salt solutions through compacted clay. *Clays Clay Miner.*, Proc. Natl. Conf. Clays Clay Miner., V. 11, p. 248-259.

Mackenzie, F. T. and Garrels, R. M., 1965, Silicates: Reactivity with sea water. *Science*, V. 150, p. 57-58.

Mackenzie, F. T., Garrels, R. M., Bricker, O. P., and Bickley, F., 1967, Silica in sea water: Control by silica minerals. *Science*, V. 155, p. 1404-1405.

Magara, K., 1968, Compaction and migration of fluids in Miocene mud stone, Nagakoa Plain, Japan. *Bull. Am. Assoc. Pet. Geologists*, V. 52, p. 2466-2501.

Magara, K., 1974a, Compaction, ion filtration and osmosis in shale and their significance in primary migration. *Bull. Am. Assoc. Pet. Geologists*, V. 58, p. 283-290.

Magara, K., 1974b, Aquathermal fluid migration. *Bull. Am. Assoc. Pet. Geologists*, V. 58, p. 2513-2521.

Magara, K., 1975a, Reevaluation of montmorillonite dehydration as cause of abnormal pressure and hydrocarbon migration. *Bull. Am. Assoc. Pet. Geologists*, V. 59, p. 292-302.

Magara, K., 1975b, Importance of aquathermal pressuring effects in Gulf Coast. *Bull. Am. Assoc. Pet. Geologists*, V. 59, p. 2037-2045.

Mangelsdorf, P. C. Jr., Manheim, F. T., and Gieskes, J. M. T. M., 1970, Role of gravity, temperature gradients, and ion-exchange media in the formation of fossil brines. *Bull. Am. Assoc. Pet. Geologists*, V. 54, p. 617-626.

Mangelsdorf, P. C. Jr., Wilson, T. R. S., and Daniell, E., 1969, Potassium enrichments in interstitial waters of recent marine sediments. *Science*, V. 165, p. 171-174.

Manheim, F. T., 1966, A hydraulic squeezer for obtaining interstitial water from consolidated and unconsolidated sediments. *U. S. Geol. Surv. Prof. Paper*, 550-C, p. 256-261.

Manheim, F. T., 1970, The diffusion of ions in unconsolidated sediments. *Earth Planet. Sci. Lett.*, V. 9, p. 307-309.

Manheim, F. T., 1974, Comparative studies on extraction of sediment interstitial waters: Discussion and comment on the current state of interstitial water studies. *Clays Clay Minerals*, V. 22, p. 337-343.

Manheim, F. T. and Bischoff, J. L., 1969, Geochemistry of pore waters from Shell Oil Company drill holes on the continental slope of the northern Gulf of Mexico. *Chem. Geol.*, V. 4, p. 63-82.

Manheim, F. T., Chan, K. M., and Sayles, F. L., 1970, Interstitial water studies on small core samples, Deep Sea Drilling Project, Leg 5. In *McManus, D. A., et al., Initial Reports of the Deep Sea Drilling Project*, V. 5, p. 501-512.

Manheim, F. T. and Sayles, F. L., 1974, Composition and origin of interstitial waters of marine sediments, based on deep sea drill cores. In: *The Sea*. V. 5, E. D. Goldberg (Editor), Interscience Publishers, New York, N. Y., 895p.

Manheim, F. T., Sayles, F. L., and Friedman, I., 1968, Interstitial water studies on small core samples, Deep Sea Drilling Project, Leg 1. In *Ewing, M., et al., Initial Reports of the Deep Sea Drilling Project*, V. 1, p. 403-410.

Manheim, F. T., Sayles, F. L., and Waterman, L. S., 1973, Interstitial water studies on small core samples, Deep Sea Drilling Project, Leg 10. In *Bryant, W., et al., Initial Reports of the Deep Sea Drilling Project*, V. 10, p. 615-624.

Manheim, F. T., Waterman, L. S., and Sayles, F. L., 1974, Interstitial water studies on small core samples, Leg 22. In *von der Borch, C. C., et al., Initial Reports of the Deep Sea Drilling Project*, V. 22, p. 657-662.

Marshall, C. E., 1948, The electro chemical properties of mineral membranes. VIII. The theory of selective membrane behavior. *J. Phys. Coll. Chem.*, V. 52, p. 1284-1295.

- Martin, R. I., 1955, Fundamentals of Electric Logging. The Petroleum Publishing Co., Tulsa, Okla., 68p.
- Milne, I. H., McKelvey, J. G., and Trump, R. P., 1964, Semi-permeability of bentonite membranes to brines. *Bull. Am. Asso., Pet. Geologists*, V. 48, p. 103-105.
- Mizutani, S., 1970, Silica minerals in the early stage of diagenesis. *Sedimentology*, V. 15, p. 419-436.
- Mokady, R. S. and Low, P. F., 1968, Simultaneous transport of water and salt through clays-I. Transport mechanisms. *Soil Sci.*, V. 105, p. 112-131.
- Murthy, A. S. P. and Ferrell, R. E. Jr., 1972, Comparative chemical composition of sediment interstitial waters. *Clays Clay Minerals*, V. 20, p. 317-321.
- Nissenbaum, A. and Swaine, D. J., 1976, Organic matter-metal interactions in recent sediments: the role of humic substances. *Geochim. Cosmochim. Acta*, V. 40, p. 809-816.
- Parnham, W. E., 1966, Lateral variations of clay mineral assemblages in modern and ancient sediments. *Proc. Int. Clay Conf.*, V. 2, p. 135-146.
- Perry, E. A. and Hower, J., 1970, Burial diagenesis in Gulf Coast pelitic sediments. *Clays Clay Minerals*, V. 18, p. 165-177.
- Pinsak, A. P. and Murray, H. H., 1959, Regional clay mineral patterns in the Gulf of Mexico. *Clays Clay Miner.*, *Proc. Natl. Conf. Clays Clay Miner.*, V. 7, p. 162-177.
- Piper, D. Z., 1971, The distribution of Co, Cr, Cu, Fe, Mn, Ni and Zn in Framvaren, a Norwegian anoxic Fjord. *Geochim. Cosmochim. Acta*, V. 35, p. 531-550.
- Powers, M. C., 1967, Fluid release mechanisms in compacting marine and mud rocks and their importance in oil exploration. *Bull. Am. Assoc. Pet. Geologists*, V. 51, p. 1240-1254.
- Presley, B. J., 1969, Chemistry of interstitial water from marine sediments. Ph. D. Thesis, University of California at Los Angeles, 225p.
- Presley, B. J., 1971, Appendix: Techniques for analyzing interstitial water samples. Part I: Determination of selected minor and major inorganic constituents. In Winterer, E. L., et al., *Initial Reports of the Deep Sea Drilling Project*, V. 7, p. 1749-1755.

Presley, R. J., Brooks, R. R., and Kappel, H. M., 1967, A simple squeezer for removal of interstitial water from ocean sediment. *J. Marine Res.*, V. 25, p. 355-357.

Presley, B. J., Goldhaber, M. B., and Kaplan, R. I., 1970, Interstitial water chemistry Deep Sea Drilling Project, Leg 5. In McManus, D. A., et al., *Initial Reports of the Deep Sea Drilling Project*, V. 5, p. 513-522.

Presley, B. J. and Kaplan, I. R., 1970, Interstitial water chemistry: Deep Sea Drilling Project, Leg 4. In Bader, R. G., et al., *Initial Reports of the Deep Sea Drilling Project*, V. 4, p. 415-430.

Presley, B. J. and Kaplan, I. R., 1972, Interstitial water chemistry: Deep Sea Drilling Project, Leg 11. In Hollister, C. D., et al., *Initial Reports of the Deep Sea Drilling Project*, V. 11, p. 1009-1012.

Presley, B. J., Kolodny, Y., Nissenbaum, A., and Kaplan, I. R., 1972, Early diagenesis in a reducing Fjord, Saanich Inlet, British Columbia-II. Trace element distribution in interstitial water and sediment. *Geochim. Cosmochim. Acta*, V. 36, p. 1073-1090.

Presley, B. J., Petrowski, C., and Kaplan, I. R., 1973, Interstitial water chemistry, Deep Sea Drilling Project, Leg 10. In Bryant, W., et al., *Initial Reports of the Deep Sea Drilling Project*, V. 10, p. 613-614.

Presley, B. J., Trefry, J., Armstrong, D., and Nuzzo, M., 1974, Appendix IV: Interstitial water chemistry: Deep Sea Drilling Project, Legs 21 and 22. In von der Borch, C. C., et al., *Initial Reports of the Deep Sea Drilling Project*, V. 22, p. 861-864.

Reynolds, R. C., 1965, The concentration of boron in Precambrian seas. *Geochim. Cosmochim. Acta*, V. 29, p. 1-16.

Reynolds, J. C. Jr. and Hower, J., 1970, The nature of interlayering in mixed layer illite montmorillonites. *Clays Clay Minerals*, V. 18, p. 25-36.

Rickard, D. T., 1969, The chemistry of iron sulphide formation at low temperatures. *Stockholm Contr. Geology*, V. 20, p. 67-95.

Rieke III, H. H. and Chilingarian, G. V., 1974, Compaction of Argillaceous Sediments. V16: Developments in Sedimentology. Elsevier Scientific Publishing Company, New York, N. Y., 424p.

Rieke III, H. H., Chilingar, G. V., and Adamson, L. G., 1966, Notes on the application of electrokinetic phenomena in soil stabilization. Proc. Int. Clay Conf., V. 1, p. 381-389.

Rittenhouse, G., 1967, Bromine in oil-field waters and its use in determining possibilities of origin of these waters. Bull. Am. Assoc. Pet. Geologists, V. 51, p. 2430-2440.

Rosenbaum, M. S., 1976, Effect of compaction on the pore fluid chemistry of montmorillonite. Clays Clay Minerals, V. 24, p. 118-121.

Russell, K. L., 1970, Geochemistry and hamyrolisis of clay minerals, Rio Ameca, Mexico. Geochim. Cosmochim. Acta, V. 34, p. 893-907.

Russell, K. L., 1971, Fresher interstitial waters from normal marine shales. A. G. U. Fall Meeting, San Francisco, Cal., 1971.

Russell, K. L. and Fallgatter, W. S., 1972, Interstitial water chemistry in experimentally heated sediments. G. S. A. 85th Annual Meeting, Minneapolis, Minn., Nov., 1972.

Sayles, F. L. and Manheim, F. T., 1975, Interstitial solutions and diagenesis in deeply buried marine sediments: results from the Deep Sea Drilling Project. Geochim. Cosmochim. Acta, V. 39, p. 103-127.

Sayles, F. L., Manheim, F. T., and Chan, K. M., 1970, Interstitial water studies on small core samples, Leg 4. In Bader, R. G., et al., Initial Reports of the Deep Sea Drilling Project, V. 4, p. 401-414.

Sayles, F. L., Manheim, F. T., and Waterman, L. W., 1972, Interstitial water studies on small core samples, Leg 11. In Hollister, C. D., et al., Initial Reports of the Deep Sea Drilling Project, V. 11, p. 997-1008.

Sayles, F. L., Manheim, F. T., and Waterman, L. S., 1973a, Interstitial water studies on small core samples, Leg 15. In Heezen, B. C., et al., Initial Reports of the Deep Sea Drilling Project, V. 20, p. 783-805.

Sayles, F. L., Wilson, T. R. S., Home, D. N., and Mangelsdorf, P. C. Jr., 1973b, An in situ sampler for marine sediment pore waters: Evidence for potassium depletion and calcium enrichment. Science, V. 181, p. 154-156.

Schlumberger Well Surveying Co., 1958, Introduction to Schlumberger Well Logging. Schlumberger Document #8, 176p.

Schlumberger Well Surveying Co., 1972, Log Interpretation Charts.

Schmidt, G. W., 1973, Interstitial water composition and geochemistry of deep Gulf Coast shales and sandstones. Bull. Am. Assoc. Pet. Geologists, V. 57, p. 321-337.

Segar, D. A. and Gonzales, J. G., 1972, Evaluation of atomic absorption with a heated graphite atomizer for the direct determination of trace transition metals in sea water. Anal. Chim. Acta, V. 58, p. 7-14.

Serruya, C., Picard, L., and Chilingarian, G. V., 1967, Possible role of electrical currents and potentials during diagenesis (electrodiagenesis). J. Sediment. Petrol., V. 37, p. 695-698.

Shishkina, O. V., 1968, Methods of investigating marine and ocean mud waters. In: G. V. Bogomolov, et al., (Editors), Pore Solutions and Methods of Their Study (A Symposium). Izd Nauka i Tekhnika, Minsk, p. 167-176.

Sholkovitz, E., 1973, Interstitial water chemistry of the Santa Barbara Basin sediments. Geochim. Cosmochim. Acta, V. 37, p. 2043-2075.

Siever, R., Beck, K. C., and Berner, R. A., 1965, Composition of interstitial waters of modern sediments. J. Geol., V. 73, p. 39-73.

Siever, R. and Kastner, M., 1972, Shale petrology by electron microprobe: pyrite-chlorite relations. J. Sediment. Petrol., V. 42, p. 350-355.

Spears, D. A., 1973, Relationship between exchangeable cations and paleosalinity. Geochim. Cosmochim. Acta, V. 37, p. 77-86.

Strickland, J. D. H. and Parsons, T. R., 1968, A practical handbook of seawater analysis. Bull. Fish. Res. Board Can., 167, 311p.

Stumm, W. and Morgan, J. J., 1970, Aquatic Chemistry. Wiley-Interscience, Div. of John Wiley and Sons, New York, N. Y., 583p.

Van Everdingen, R. O., 1968, Mobility of main ion species in reverse osmosis and the modification of subsurface brines. Can. J. Earth Sci., V. 5, p. 1253-1260.

Van Moort, J. C., 1971, A comparative study of the diagenesis alteration of clay minerals in Mesozoic shales from Papau, New

Guinea and Tertiary shales from La. USA. *Clays Clay Minerals*, V. 19, p. 1-20.

Von Engelhardt, W. and Gaida, K. H., 1963, Concentration changes of pore solutions during the compaction of clay sediments. *J. Sediment. Petrol.*, V. 33, p. 919-930.

Warner, T. B., 1971, Electrode determination of fluoride in ill-characterized natural waters. *Water Res.*, V. 5, p. 459-465.

Waterman, L. S., Sayles, F. L., and Manheim, F. T., 1973, Appendix II: Interstitial water studies on small core samples, Legs 16, 17 and 18. In Kulm, L. D., et al., Initial Reports of the Deep Sea Drilling Project, V. 14, p. 1001-1012.

Weaver, C. E. and Beck, K. C., 1971, Clay-water diagenesis during burial: How mud becomes gneiss. *Geol. Soc. Amer. Spec. Paper* 134, 96p.

Weaver, C. E. and Wampler, J. M., 1970, K, Ar, illite burial. *Bull. Geol. Soc. Amer.* V. 81, p. 3423-3436.

White, D. E., 1965, Saline waters of sedimentary rocks. In: *Fluids in Subsurface Environments*. A Young and J. E. Galley (Editors), *Am. Assoc. Pet. Geologists*, Mem. 4, p. 342-366.

White, S. M., 1975, Interstitial water studies, Leg 31. In Karig, D. E., et al., Initial Reports of the Deep Sea Drilling Project, V. 31, p. 639-654.

Wyllie, M. R. J., 1949, A quantitative analysis of the electrochemical component of the SP curve. *J. Pet. Tech.*, V. 19, p. 479-487.

Wyllie, M. R. J., 1951, An investigation of the electrokinetic component of the self-potential curve. *Trans. A. I. M. E.* 192, p. 1-15.